Resilience Assessment of the Built Environment of a Virtual City

(Article begins on next page)

04 August 2020

Doctoral Dissertation
Doctoral Program in Structural Engineering (30th Cycle)

Resilience Assessment of the Built Environment of a Virtual City

Ali Zamani Noori
******

Supervisor
Prof. Gian Paolo Cimellaro

Doctoral Examination Committee:
Prof. Bozidar Stojadinovic, Referee, ETH Zürich
Prof. Sean Wilkinson, Referee, Newcastle University
Prof. Anastasios Sextos, Examination Committee, University of Bristol
Prof. Giuseppe Lacidogna, Examination Committee, Politecnico di Torino
Prof. Giuseppe Marano, Examination Committee, Politecnico di Torino

Politecnico di Torino
April 26, 2019

I hereby declare that, the contents and organization of this dissertation constitute my own original work and does not compromise in any way the rights of third parties, including those relating to the security of personal data.

………………………………......
Ali Zamani Noori
Turin, April 26, 2019

Summary

The prediction of physical impacts on the built environment caused by natural disasters has always been a challenge for urban planners and decision makers. Damage assessment is a complex problem due to the strong correlation and interdependencies among buildings portfolio and different infrastructures of a community. Several parameters, such as buildings' spatially distribution, uncertainties in mechanical and geometrical parameters, different hazard intensities, etc. should be addressed by simulation models.

This dissertation aims at developing a quantitative model to assess damages occurred to the built environment after a seismic event. A virtual city was designed based on the city of Turin in Italy as a testbed to validate the developed methodology. The structural design parameters of each building were determined according to the seismic design codes associated to the buildings' year of construction, while the average mechanical, geometrical, and construction parameters were identified through a typological approach for each building. The dynamic structural response of each single building was evaluated by performing large scale simulations considering the buildings' spatial distribution across the city. Uncertainties related to geometric and mechanical parameters for each building were explicitly taken into account performing Monte Carlo Simulations. Fragility curves were developed for each building and the virtual city is accordingly mapped into different hazard zones. Results show that the level of the damage is directly proportional to the building's year of construction. The main share of damaged buildings belongs to masonry buildings which were mostly designed according to old design codes where either there was no seismic design procedure or less seismic design requirements.

Furthermore, the social direct losses in terms of causalities were estimated and the number of injured for each neighborhood was calculated. Results show that the expected number of casualties inside masonry buildings is about four

times more than the one referred to concrete buildings. This is due to the fact that in the virtual city masonry buildings are more vulnerable than concrete buildings.

The proposed simulation model was then extended to simulate the interdependency between buildings and the hospital network within the virtual city. The ability of the hospital network to provide care to all injured arriving at the Emergency Departments was investigated, and then two different solutions were proposed in order to make the city able to manage the post-earthquake scenario. The described method helps to estimate the capacity of cities' emergency network and provides an efficient and simple tool for evaluating the first order response of the healthcare facilities of a city under an emergency.

Finally, a new indicator-based approach for computing community resilience was presented. The methodology is a deterministic approach based on the structure of PEOPLES framework for assessing resilience. The interdependency among the resilience variables was taken into account by introducing an interdependence matrix approach. The methodology was applied to the virtual city and the resilience of the physical infrastructure under an earthquake scenario was computed. In order to enhance the community resilience, two different strategies including 'increasing system robustness' and 'reducing the recovery time' were studied. Results show that 'increasing system robustness' strategy is more efficient than the 'reducing recovery time' one in improving the resilience of the virtual city.

The work is considered a promising attempt to evaluate the earthquake-induced damage to the building stock for a variety of possible earthquake scenarios while reducing the computational effort. In addition, the resilience quantification model with its graphical representation can support decision-makers to explore how the community responds to a disaster and to identify where exactly resources should be spent to efficiently improve the resilience.

Acknowledgment

Lastly, I would like to express sincere appreciation to my family for their unconditional love and their incredible support throughout my doctoral studies. No amount of words can express my gratitude for all they have done for me.

The detailed contribution of the PhD candidate in the development of each chapter is outlined below:

Chapter 3:
- development of a physical model to obtain tri-linear backbone curve through MATLAB algorithms;
- modeling uncertainties associated with geometrical and mechanical parameters of each building;
- development of a mathematical model to estimate the inter-story drift according to top floor displacement as sum of the elastic and the post-elastic contributions;
- using SAP2000 Application Programming Interface (API) to perform non-linear dynamic analysis automatically;
- contribution in collecting data for building inventory of the virtual city;
- performing nonlinear dynamic analyses for entire city under fixed seismic scenarios.

Chapter 4:
- development of fragility curves for the building's portfolio of the virtual city;
- human casualty assessment for the virtual city based on HAZUS methodology.

Chapter 5:
- estimation of patient distribution for each neighborhood of virtual city;
- assessment of the number of patients for each hospital;
- evaluation of the patient arrival rate for a given seismic scenario;
- assessment of the patient's waiting time using a meta-model developed by Cimellaro et al. 2016a;
- assessment of hospital network functionality;
- development of strategies to improve resilience of the hospital network through two different approaches ("emergency management with an operative center" and "increase the emergency network capacity").

Chapter 6:
- contribution in collecting community resilience indicators and allocating them to the PEOPLES framework components;
- development of the interdependence matrix approach and aggregation methodology;
- contribution in developing the open source tool;

- evaluation of virtual city's resilience for the physical infrastructure dimension;
- performing parametric analyses to investigate the influence of different strategies in improving virtual city's resilience.

I would like to dedicate this thesis to my loving parents

Contents

List of Tables

List of Figures

Chapter 1

Introduction

1.1 Problem definition

The devastating effects have recently demonstrated that risk management is a paramount issue for seismically active areas. The prediction of physical damage and modeling impacts of an earthquake on the built environment is always a challenge to political or community organizations. Damage assessment for an urban area is more complicated than doing so for an individual building due to the interactions and interdependencies that exist between different entities of a community.

To reduce seismic risk efficiently, an informed decision-making process with the aid of reliable and quantitative assessment models is required. A building portfolio can be thought of as a system of interconnected building components spatially distributed in a large area. Given the large number of buildings within an urban area, the simulation models should be able to capture the correlation between building parameters and also to include the large uncertainties involved in assessing the demands and capacities of buildings. The influence of these parameters is apparent when estimating large infrequent losses for an urban area since they tend to dominate overall functionality of community after the earthquake.

The primary focus of this dissertation is to develop a methodology to evaluate the seismic vulnerability of buildings portfolio of a large-scale city. Significant efforts have been made previously to evaluate the earthquake-induced damage to building stock subjected to seismic hazards. Generally, the simulation models are based on statistical (*data-driven*) and deterministic approaches (*physics-driven*). In the first case, the building damage assessment is based on statistical data collected from previous seismic events. Thus, the accuracy of the data-driven methods is dependent on the data availability. On the contrary, physics-driven methods are based on physical models that are used to predict the structural damage through nonlinear static or dynamic analyses. Nonlinear static analysis

does not take into account the dynamic characteristics of an earthquake since the seismic excitation is considered as a monotonically increasing function. Nonlinear time history analysis provides an accurate evaluation of building damage, while for a large number of buildings in a city it requires a huge computational effort.

Many recent research studies use the nonlinear dynamic analyses to evaluate the structural response. The probability of damage is then estimated through development of fragility curves. Looking at available models in literature, the simulation models assess the structural seismic damage classifying the buildings into groups (typological approach). Usually, buildings are grouped based on building archetype, number of story, seismic design level. Although these approaches provide a rapid and simplified estimate, their estimation might be inconsistent with expected results specifically for estimating losses for a city-scale community. Indeed, response of individual building is significantly dependent on various parameters such as building geometry, structural characteristics, construction elements, etc. Therefore, a computational framework for the analysis of large-scale city models considering buildings specific characteristics is required. In addition, the spatial distribution of buildings should be considered to address the correlations and interdependencies between community entities.

The accuracy of simulation models strictly depends on availability of the building data. Most of the structural parameters are of random nature, and consequently, uncertainty exists in the behavior of the structural members. On the other hand, for the large number of buildings in a city, it is not possible to collect in detail all the buildings data. Therefore, simulation models should be able to model the uncertainties associated with construction elements, mechanical, and geometrical parameters for each single building.

Beside the vulnerability assessment, community stakeholders and decision makers are usually more interested to see how their community will respond to a perturbation and to monitor the functionality of the built environment after a disaster. Several community resilience frameworks have been developed to compute the resilience providing guidelines (qualitative measures) or tools (quantitative measures). Although many attempts have been made to consolidate research on community resilience, no accepted method exists so far and there are still difficulties in developing concrete assessment approaches and reliable indicators. Development of a deterministic approach, adaptable to communities of different types and sizes, capable to capture the interdependencies between community entities, and finally to measure the total community resilience, is still a challenge.

1.2 Objectives

This dissertation first aims to develop a consistent, quantitative and realistic earthquake-induced damage assessment model for building portfolios. The proposed method is intended for city developers and community decision makers interested in vulnerability assessment and risk management. The methodology is

intended to be generic, such that it can be adapted to the characteristics of any building portfolio of a selected city. The model development followed from a review of existing methodologies with offering following features:

- Identify the capacity curve and development of fragility curve for each single building within a city by performing nonlinear dynamic analysis. This leads to accurately estimate the level of damage for each individual building without losing accuracy and consistency with the expected results;
- Inclusion of uncertainties associated with construction elements, mechanical and geometrical parameters for each single building performing Monte Carlo Simulations (MCS);
- Inclusion of the correlations between buildings spatial distribution, level of damage, and hazard intensity.
- Reducing computational effort by developing an appropriate mathematical model of a building capacity curve to estimate the potential seismic vulnerability of building stock.

The second objective of the dissertation is to develop an indicator-based approach for computing community resilience. In this regard, the methodology offers the following advantages:

- Provide a dynamic resilience measure to quantify the functionality of community entities and enable to aggregate the multitude functions to obtain the final community resilience;
- Inclusion of interdependencies between different dimensions of a community by development of an interdependence matrix approach.

A virtual city is designed based on the built environment of Torino, Italy. The application of the proposed framework is illustrated by assessing the seismic vulnerability of the virtual city. Moreover, the functionality of hospital network of the virtual city as an example of correlation between community entities is explored.

1.3 Outline

The core goal of this research is to develop a simulation model to assess the physical damage and to estimate losses associated with the impacts of an earthquake to a community at city scale. Existing earthquake-induced simulation methodologies to predict the physical damage to built environment due to earthquake are presented in Chapter 2. Moreover, existing community resilience frameworks and quantification methods are explored.

Chapter 3 presents a new approach to predict the potential damage of an earthquake scenario on the built environment. A virtual city consisting of different buildings categories based on typical Italian building portfolio is developed. Large scale simulation models are performed to evaluate the seismic effects at

increasing intensities. This model is the basis for further detailed work and necessary components for next chapters in dissertation.

Fragility functions to assess the probability of having different levels of damage for each single building are developed and accordingly the city is mapped into different seismic-impacted zones. Consequently, indoor casualties including the number of injured and their severities are computed indicating the social economic loss (Chapter 4). This chapter is a building for a model used in Chapter 5.

Chapter 5 includes application of a new methodology to estimate the capacity of a hospital network in the virtual city to withstand the emergency. The ability of healthcare facilities in the virtual city to deliver the emergency services to patients (estimated in Chapter 4) after an earthquake scenario is assessed.

Chapter 6 proposes an indicator-based approach for quantifying urban community resilience and to compute the serviceability function including interdependencies between different community's infrastructures based on PEOPLES framework. The methodology is applied to the virtual city as a testbed.

The thesis outline and the linkage between different chapters are shown in Figure 1.
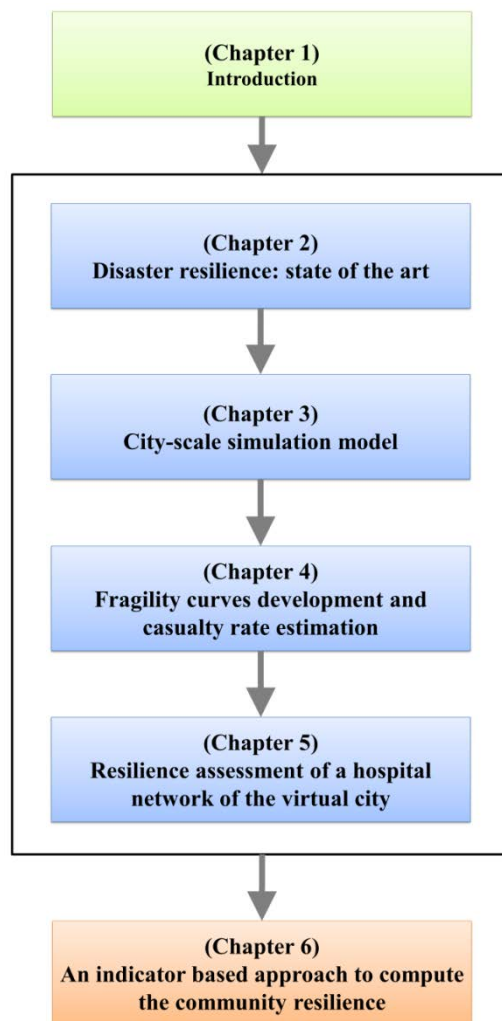
Figure 1. Research outline.

Chapter 2

Disaster resilience: state of the art

Over the past two decades, several studies have been conducted to address the resilience of communities, systems and networks. In this chapter, a review of existing methodologies available in literature, along with a discussion of their respective advantages and disadvantages, is given. First, resilience definitions and its mathematical formulation are presented. Then, an overview of existing community resilience frameworks and modelling methodologies to assess the physical impacts of natural disasters on urban areas (specifically earthquake events) are presented and their limitations are discussed. While this literature review is by no means exhaustive, it is intended to highlight areas in existing simulation methodologies that may benefit from additional work. These are then investigated in the development of city-scale seismic simulation model proposed in this dissertation. Finally, a brief overview of available resilience quantification methods along with a discussion of their limitation is given and then used in development of community resilience quantification methodology proposed in this work.

2.1 Resilience definition

Natural disasters and man-made hazards have been responsible of several life losses as well as disruption of business network in communities over the last three decades. According to International disaster dataset, despite substantial progress in science and technology, communities are still vulnerable and risk of damage due to disasters is increasing. Recent experiences show clearly that not all threats can be averted because of inherent uncertainties associated with natural and man-made disasters. This caused the shift in attention from vulnerability and risk assessment to the topic of resilience engineering (Stumpp, 2013).

The concept of resilience is multi-dimensional, and therefore involves various subjects of different disciplines such as economics, environmental planning, social, ecology, political science, engineering and etc. Different definitions for

resilience are available in the literature. Haimes (1998) defined resilience as the ability of a system to return to its optimal condition in a short period of time. Gunderson et al. (2002) defined the resilience as the speed to return to the initial condition after a perturbation.

The community resilience concept mainly in the context of seismic response and recovery has been studied by Chang and Shinozuka (2004). The term resilience was defined by Allenby and Fink (2005) as "the ability of a system to remain in a practical state and to degrade gracefully in the face of internal and outside changes". Manyena (2006) evaluated the available definition of resilience in literature and suggested the resilience as the "intrinsic capacity of a system, community or society predisposed to a shock or stress to adapt and survive by changing its non-essential attributes and rebuilding itself". DHS-RSC (2008) proposed the resilience definition in scale of system, infrastructure and government as the ability to resist, absorb, adopt or recover from an adverse occurrence. Later on, Wagner and Breil (2013) defined resilience as the ability to "withstand stress, survive, adapt and bounce back from a crisis or disaster and rapidly move on".

In engineering, resilience is the ability to withstand stress, survive, adapt, and bounce back from a crisis or disaster and rapidly move on. It can also be defined as "the ability of social units (e.g. organizations, communities) to mitigate hazards, contain the effects of disasters when they occur, and carry out recovery activities in ways to minimize social disruption and mitigate the effectors of further earthquakes" (Cutter et al. 2014).

2.2 Resilience formulation

The absence of a concise and methodical approach makes it extremely difficult to evaluate resilience. Since the adoption of the Hyogo framework in (Manyena 2006), strategies involved in hazard planning and disaster risk reduction have experienced a paradigm shift from a vulnerability assessment approach to a resilience-based approach (Mayunga 2007). The Resilience can be applied either on a deterministic approach (scenario basis) or a probabilistic approach (including uncertainties). In the probabilistic approach, different random variables such as response measure, disaster intensity measure, performance serviceability measure, and recovery time and function can affect the expected value of the resilience index.

There are several formulations in literature to how resilience is defined. Bruneau et al. (2003) defined resilience as "the ability of a system to reduce the chances of a shock, to absorb such a shock if it occurs (abrupt reduction of performance) and to recover quickly after a shock (re-establish normal performance)". According to Bruneau et al. (2003), the resilience of a system depends on its serviceability performance. The serviceability performance (Q) ranges from 0 % to 100 %, where 100% and 0% imply full availability and non-availability of services, respectively. The occurrence of a disaster at time t_0 causes damage to the system and this produces an instant drop in the system's

serviceability (ΔQ). Afterward, the system is restored to its initial state over the recovery period (t_0-t_1). The loss in resilience is considered equivalent to the service degradation of the system over the recovery period. This concept is mathematically defined as:

$$LOR = \int_{t0}^{t1} [100 - Q(t)] dt \qquad (1)$$

where *LOR* is the loss-of-resilience measure, t_0 is the time at which a disastrous event occurs, t_1 is the time at which the system recovers to 100% of its initial serviceability, $Q(t)$ is the serviceability of the system at a given time *t*.

The recovery time (t_1-t_0) and the recovery path are two key components that can affect the resilience index value. The recovery phase (time and path) depends on many variables such as resources, system preparedness, restoration plans and etc. Different types of restoration shapes such as linear, exponential, step function, trigonometric and random function have been proposed on literature. Kafali and Grigoriu (2005) proposed an exponential shape for a system representing a system with high initial speed recovery. However, due to system complexity, most common resilience estimation model, such as HAZUS (2014), adopt a simple linear trend to evaluate the recovery phase. The linear trend is generally used when there is not enough available data regarding the system resources and recovery plans (Whitman et al., 1997).

The definition provided by Bruneau et al. (2003) has been later improved by Cimellaro et al. (2010). They defined resilience as "a function indicating the capability to sustain a level of functionality or performance for a given building, bridge, lifeline network, or community, over a period defined as the control time (T_C) that is usually decided by owners, or society (usually is the life cycle, life span of the system etc.)". Thus, resilience can be defined analytically as the area under the serviceability performance curve *Q(t)* of a system, normalized accordingly to the considered control time (T_C):

$$R = \int_{t_1}^{t_r} \frac{Q(t)}{T_C} dt \qquad (2)$$

where *R* is the resilience index; *Q(t)* is the system functionality at time *t*; t_1 is the moment when the disturbance occurs and the system functionality drops from its initial value q_0 to q_1; t_r is the moment when the initial serviceability is completely recovered and equal to q_r; T_C is the control time. Figure 2 shows the performance curve derived using Equation (2). The serviceability *Q(t)* ranges between 0% and 100% to indicate the complete absence of functionality of the service and its complete effectiveness, respectively. Resilience graphically is identified as area underneath serviceability function of a system. In this thesis, the definition provided by Cimellaro et al. (2010) is followed to evaluate the community resilience.
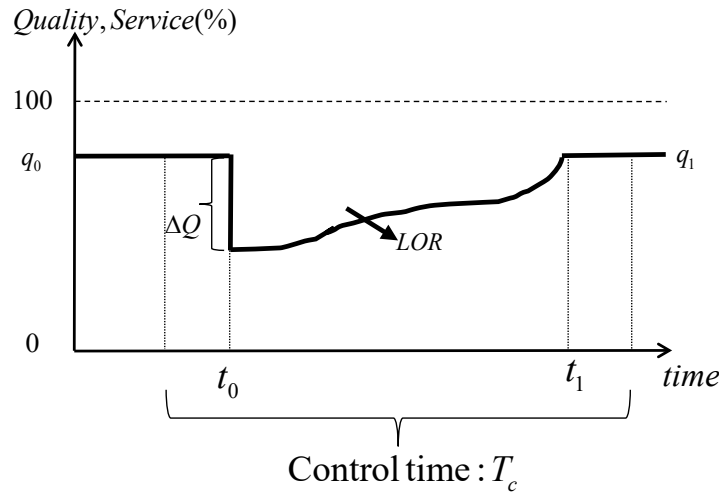
Figure 2. Example of a serviceability function and resilience evaluation.

2.3 Resilience frameworks

By looking at available resilience definitions in literature, resilience can be considered as a desired outcome or, in a broader way, as a process leading to a desired outcome. Reducing resilience to an outcome does not take into account the performance of the process itself, or the effort to reach a certain result, while the second approach is comprised of a series of events, actions, or changes to enhance the community resilience against an extreme event. Under this definition, resilience includes activities such as community preparedness, code adoption and enforcement, and hazard mitigation.

Several frameworks are currently available in literature to address different dimensions of community resilience. Resilience frameworks are grouped according to the spatial dimension as city, state and country scale. A brief description for some existing resilience framework is given below and their features and applicability are evaluated.

2.3.1 NIST framework

National Institute of Standards and Technology (NIST 2015) is a city scale resilience framework based on comprehensive list of community parameters. It summarizes the available guidance, tools, and metrics to address the community resilience against different type of hazard considering different hazard intensities. The framework addresses process and activities leading to desired level of resilience outcomes for both prior and after disaster events. The first includes the community preparedness and adaption capacity to changing conditions. The second is defined as the ability of a community to withstand and recover rapidly from disruptions.

The framework presents three different metrics to compute the total community resilience including recovery time, economic metrics, and social metrics. The recovery time is used to estimate the restoration time for the buildings and community infrastructure after a disaster. Economic metric

represents the business network, income, tax, and sustained growth of a community. Finally, social metric reflects the human needs such as safety and security, survival, and sense of belonging to community. However, these metrics are defined in terms of guidelines without a specific description to how use and apply them in practice. In addition, there is not a systematic methodology to quantify the community resilience and to model interdependencies exist between different dimensions of the community. The framework is not limited intrinsically, but it has been developed specifically for cities across United States.

2.3.2 SPUR Framework

San Francisco Planning and Urban Research Association (SPUR) Framework is a community resilience framework at the city level specific to city of San Francisco (SPUR 2009). The main aim of this framework is to make resilient the city of San Francisco by applying seismic mitigation policies and strategies. The framework focuses on the city demands in three different phases prior, during, and after the earthquake. Different disaster plans are defined establishing performance goals associated to an expected earthquake scenario. The performance goals are set for each group of infrastructures such as hospital network, emergency housing, critical response buildings, etc. Then, a target recovery time is defined for each group to guaranty the community functionality at an accepted level after the earthquake.

However, the framework does not provide a direct performance metric for economic and social dimensions which can have an important impact during the recovery period. In addition, the framework is only limited to earthquakes and does not include other natural and man-made hazards.

2.3.3 UNISDR

The United Nations International Strategy for Disaster Reduction (UNISDR) is a city level framework to evaluate the community resilience against natural disasters (UNISDR 2011). The methodology is based on scorecards in form of checklists to measure the current level of cities, identify priorities for investment and action, and to track the status of the city over the recovery time. However, the framework does not offer a theoretical approach which clearly explains how to apply these methods in practice. Additional information is required to assess the performance of critical networks and their interdependencies. Furthermore there is not any specific metric tool to assess the recovery time considering all community dimensions such as social and economical aspects.

2.3.4 Oregon resilience plan

The Oregon resilience plan is a state resilience framework which was built upon the SPUR framework in 2013 (OSSPAC 2013). The framework identifies policy options and provides recommendations to increase the community

resilience in terms of lives losses, households displaced, buildings damaged, and commerce flowing during and after a Cascadia earthquake and tsunami. The framework also suggests policy directions to protect critical infrastructures such as transportation, energy, information and communication, water and wastewater systems specific to coastal communities. The framework determines the likely impacts of magnitude 9.0 Cascadia earthquake and tsunami and proposes a method to estimate the recovery time after such a hazard event. It also describes an acceptable time frame for each critical network to fulfill the expected resilience performance goals.

The Oregon resilience plan with respect to the SPUR framework provides a methodology to evaluate resilience of economic dimension, but still it lacks in quantifying the social aspects. Furthermore, the methodology is limited to earthquake and tsunami hazard type.

2.3.5 HAZUS methodology

Hazus methodology (Hazus 2014) is a national framework level developed by Federal Emergency Management Agency's (FEMA). It contains several models to estimate potential losses due to earthquakes, hurricanes, and floods. Although the methodology can be extended to other nations but the current version of framework covers only the regions in United States.

The models are based on Geographic Information Systems (GIS) technology to evaluate the physical, social, and economic impacts of disasters. The performance level and recovery times are explicitly estimated or normalized in terms of economic losses while the economic outputs are not tabulated or illustrated as a function of time. Only the losses that can be avoided through mitigation strategies can be estimated while the costs for these mitigation actions are not included in analysis, thus, the return on investments cannot be calculated properly. Furthermore, all the losses are considered independently and the interaction between different community dimensions is neglected.

2.3.6 PEOPLES framework

The PEOPLES framework is a multidimensional resilience framework that can be applied in communities in different size from city level to country level. The framework is not hazard specific and is able to identify the different resilience characteristics of a community both in time and space. The framework was proposed by Cimellaro et al. (2016a) to model possible responses of a community considering the interdependency between the different community layers. The acronym PEOPLES stands for seven community dimensions including:

1. Population and demographics: it includes parameters that describe the social-economic composition of the community. This dimension measures the social vulnerability that could hinder the functionality of the emergency and

recovery systems (e.g. population density, age distribution, presence and integration of minorities and socio-economic status);

2. Environment and ecosystem: it estimates the capability of the environment and of the ecosystem to get back to its pre-hazard conditions. It includes water, air and soil assessments as well as a measure of the biodiversity and the sustainability relations;

3. Organized government services: it covers the services that the government guarantees before and after an extreme event. A great importance is given to the mitigation and recovery processes, which include the preparedness to hazards and all disaster risk reduction measures;

4. Physical infrastructure: it considers the buildings and facilities that are the prevalent interests of civil engineers and traditional resilience analysis. Particularly, two different aspects are analyzed in this dimension: facilities, which includes housing and services which are not crucial for the emergency response, and lifelines, which instead consists of the services that are of vital importance for the management of critical situations;

5. Lifestyle and community competence: this dimension takes into account the capability of a community to face problems by means of political partnerships. This includes both the abilities of a community (i.e. the skills of their components) and its perceptions (i.e. the judgments and feelings that a community has on itself);

6. Economic development: it describes the economic situation of the community. It can be easily divided in two terms, a static component, which measures the present economic condition, and a dynamic one, which instead takes into account the development and economic growth of the community;

7. Social-cultural capital: this last dimension contains an evaluation of the community's attitude to react to disasters and to return to the pre-event conditions. It includes a lot of subcategories that measure the people's commitment in the community and the social-cultural heritage.

The framework provides new ways through which decision makers can take actions under emergencies. However, the framework does not introduce a specific technique to quantify the community resilience and even to model interdependencies between different dimensions in practice. Furthermore, there is not any specific metric tool to evaluate the physical impacts on community and to estimate the recovery time for different community dimensions such as social and economical aspects. Some improvements should be envisioned to allow the framework in quantifying total community resilience.

2.4 Resilience of the built environment

Community resilience strictly depends on the performance of the built environment following a disaster. The functionality of the built environment, including building stock and critical infrastructures as well as their supports to

economic, social and public institutions, is essential for immediate response and recovery after a disaster. A resilient built environment is "designed, located, built, operated and maintained in a way that maximizes the ability of built assets, associated support systems (physical and institutional) and the people that reside or work within the built assets, to withstand, recover, and mitigate for, the impacts of extreme natural and human induced hazards" (Bosher 2008).

Recent disasters have shown the high vulnerability of the built environment against natural disasters and the need of making cities more resilient (Kreimer et al. 2003, Godschalk 2003, Dubbeling et al. 2009, UN-ISDR 2010, Albrito 2012). Traditional engineering approaches and standards focus on the performance of each individual building or facility. While, the process to make resilient a built environment is quite complex due to several interactions and interdependencies exist between the community dimensions (Malalgoda et al. 2014). As an example, the performance of a hospital network of a city depends not only on hospital building performance, but also involves several interactions and interdependencies with critical infrastructures. It is clear that hospitals cannot remain functional without power and water, even if they have no structural damage after a disaster.

Mannakkara and Wilkinson (2013) identified different factors which increase the risk of disasters of a built environment. Inadequate or insufficient consideration of natural hazards and their intensities, neglecting building codes and regulation, constructions and design processes, and illegal occupancy are some of the examples which can increase the risk of disasters in a community. The entities of a built environment must be designed in a way to be able to reduce the loss of functionality after a disaster and speed up the recovery.

After natural disasters such as Northridge earthquake, Indian Ocean tsunami, Hurricanes Katrina and Sandy, Haiti earthquake, etc., several studies have been conducted to evaluate the effects of natural hazards to the built environment (NIST 2006, Van de Lindt et al. 2007, Kuligowski et al. 2014, Dashti et al., 2014, Maranghides and McNamara 2016). Post-disaster reports in literature confirm that the losses due to natural disasters are increasing more rapidly than the growth in population. On the other hand, the percentage of population living in urban areas is rapidly increasing since the cities are becoming centers of economic activities. According to United Nations, about 2/3 of the population will live in urban areas by 2050. This rapid urbanization causes higher level of interdependencies between community entities that makes cities more vulnerable against natural events (Malalgoda et al. 2013a).

Earthquake is one of the most destructive events, especially when it strikes a populated urban area with high volume of buildings and complex infrastructures. Despite recent advancement in earthquake engineering, the regional economic loss due to earthquake still remains very high. Recently, the attention in research has been shifted toward developing robust earthquake loss prediction models using large-scale simulations. The European RISK-UE project (2006) focused in assessment of direct and indirect losses to physical infrastructures following an earthquake scenario. It led to propose a series of "Plans of Action" to increase the

preparedness and awareness of urban communities against seismic hazard (Mouroux and Le Brun 2006).

Hori (2006) studied the earthquake effects to an urban environment using an Integrated Earthquake Simulation (IES). The input data was collected into a Geographic Information System (GIS) and then converted in suitable numerical models. IES analyses were organized in parallel computational processes implemented using a super computer. The methodology requires high computational resources that always are not easily available for community decision makers.

The Mid-America Earthquake (MAE) Center proposed a comprehensive framework for risk management and regional loss assessment (Steelman and Hajjar, 2008). The methodology was applied to the city of Memphis, Tennessee as a Testbed and seismic vulnerability of the building stock as well as the expected damage to direct economic loss were evaluated. The building inventory damage and fragility curves were estimated by applying vulnerability formulations specific to the construction of Mid-America. The structural response and the probabilities of damage states were predicted through nonlinear time history analyses using constitutive modeling of uni-axial SDOF. The available fragility curves in literature were used to assess the vulnerability of group of buildings categorized according to building height, occupancy, and structure type. For the structure types that the fragility curves were not available, a fragility set was obtained from the parameterized fragility method to incorporate the expected characteristics for the local ground motion in the study region. Two main adjustments were made to the parameterized fragility method including modification of elastic damping ratio and uncertainty parameters. The uncertainties associated with models were considered using alternate fragilities changing structure types and then weighting the obtained results to account for likelihood of alternate structure types. HAZUS Technical Manual (FEMA, 2006) was used to model the uncertainty terms. The demand uncertainty was obtained as a result of the regression correlation of the hazard parameter with the structural response of the SDOF model and they were combined by a square root of sum of squares (SRSS) method with demand uncertainties arising from variability in response to ground motion records. In addition, open-source software MAEViz was introduced as a risk assessment tool to support decision makers providing more transparent and flexible analysis framework methodology and algorithms. Some of the tool's components should be synthesized and analyzed within the GIS environment.

A European SYNER-G research project proposed an innovative methodological framework for the systemic seismic vulnerability assessment of buildings and critical infrastructures of urban or regional areas including their interactions and interdependencies. The methodology has been applied to the city of Thessaloniki in Greece modeling building stock, transportation, water, and power networks. Fragility curves for each group of buildings based on the inventory of city have been developed (Pitilakis et al. 2014). A connectivity analysis has been performed to calculate the specific interdependencies between different systems. Then, the overall performance of each system has been

evaluated in term of average losses. The methodology is based on the results of a single event and it allows identifying the most critical elements within a system to control the performance of the network. However, it evaluates the vulnerability of building stock through development of fragility curves specific to group of buildings classified based on the height of the building and year of construction, while, there are several uncertainties, such as material characteristics, structural element design parameters, building geometry and occupancy type, that can affect the vulnerability assessment of each individual building.

The Center of Excellence for Risk-Based Community Resilience Planning (Ellingwood et al. 2016) developed a multidisciplinary computational framework including the interdependencies between buildings and community networks. The methodology has been applied to a virtual community testbed "Centerville". The city was designed envisioning a typical medium city scale of Midwestern United State including specific building inventory. The linkage of physical infrastructure and the systems has been modeled and the impact of extreme events has been estimated through different physics-based models. The methodology allows issues of scalability in community infrastructure modeling and provides useful information for community stakeholders to evaluate the interrelationships between physical and social infrastructure systems.

Seismic risk assessment involves three variables including physical system vulnerability, earthquake hazard, and the level of exposure to hazard. The level of vulnerability is the only variable that can be controlled, intervened and improved to reduce the physical damages and losses in an urban community (Vicente et al., 2008). Coburn (1992) described how the majority of losses due to a natural disaster, such as an earthquake, is associated to the building stock damages. Due to large number of buildings in an urban area, large-scale simulation models are required to predict the seismic response of building stock. The simulation models are generally based on statistical (*data-driven*) or deterministic approaches (*physics-driven*).

In the data-driven method, the building damage assessment is based on statistical data collected from previous seismic events. Therefore, the accuracy of the data-driven methods is dependent on the available data. One widely used data-driven method is the Damage Probability Matrix (DPM) which predicts the level of damage for different seismic intensities and buildings typologies (Whitman 1973). The concept of DPM was widely adopted into the ATC-13 report (Rojahn and Sharpe 1985) to evaluate the earthquake damage data for California that includes the DPMs for 78 different facility types. Later, Dolce et al. (2006) applied a modified version of it to the city of Potenza, Italy, while Eleftheriadou et al. (2013) extended the DPM-based methodology to the building stock in Southern Europe.

The physics-driven methods are based on physical models that are used to predict the structural damage through nonlinear static or dynamic analyses. In case of nonlinear static approach, Capacity Spectrum Method, CSM (Freeman 1998) or N2 method (Fajfar and Gašperšič 1996) may be used. El Ezz et al. (2014) adopted the CSM to assess the seismic damage of Quebec City, Canada.

The building inventory of the city was prepared based on construction material, structural type, height, and seismic design level. Each building type was modeled as equivalent Single Degree of Freedom (SDOF).

Nonlinear static analysis of buildings does not take into account the dynamic characteristics of an earthquake since the seismic excitation is considered as a monotonically increasing function. To overcome this limitation, nonlinear time history analysis may be used. Korkmaz (2009) proposed a combined probabilistic seismic safety approach performing nonlinear time history analyses. This method was applied to unreinforced masonry low-rise buildings to estimate the regional seismic vulnerability of Pakistan.

Tang et al. (2011) assessed the collapse resistance of Reinforced Concrete (RC) frame structures representative of the Chinese school stock. A parametric study was conducted by performing Incremental Dynamic Analyses (IDA) (Vamvatsikos et al. 2002) for all the configurations of RC frames designed according to the 2001 Chinese Code (GB 2001). The final collapse resistance of the analyzed RC buildings was evaluated through the Collapse Margin Ratio (CMR) according to ATC-63 (ATC 2009).

HAZUS (FEMA 2012c (book lu)) provided a methodology to estimate the regional earthquake losses to physical systems based on an extensive US national database. The buildings are considered as SDOF systems and the responses are evaluated through pushover analysis using the capacity spectrum method. The methodology cannot estimate accurately the economic loss for building components at different stories. Moreover, using the capacity spectrum method, the influence of the ground motion characteristics cannot be easily considered.

Lu et al (2014) proposed a GPU/CPU cooperative computing method to predict the seismic damage on buildings in urban areas. The buildings response is reproduced through multi-story shear models using nonlinear time-history analysis. The benchmark cases demonstrate a more effective performance-to-price ratio of the proposed approach, despite the need for specific hardware architectures to support GPU computing.

Xiong et al. (2015) have described a 3D urban polygonal model to solve two major challenges in urban seismic simulation: data acquisition and high-fidelity visualization. The automatic generation of 3D-GIS data of buildings is described to achieve the integrated earthquake simulation-based at the urban scale. Later on, Zehe et al. (2015) proposed the architecture for a cloud-based urban systems simulation platform which specifically aims at making large-scale simulations available to typical users.

Zeng et al. (2016) proposed a methodology to estimate the regional earthquake loss for an urban area based on the FEMA P-58. The methodology is an extended version of HAZUS (FEMA 2012c (book lu) allowing the detail prediction of economic loss at each story of building. The response of each building at each story level is evaluated by performing nonlinear time-history analyses of a series of nonlinear MDOF models. The building data for structural and non-structural components are obtained from building design drawings and

field investigation. The vulnerability of building stock is then evaluated based on fragility curves adopted from FEMA P-58.

In the context of regional seismic damage simulation, Lu et al. (2017) proposed a shear model for Multi Degree of Freedom (MDOF) systems and a shear-flexure model for tall buildings. Inter-story nonlinear properties were simulated through a tri-linear backbone curve and a single-parameter hysteretic model was proposed to take into account the dynamic degradation of the mechanical properties. All the parameters related to the MDOF models were determined based on the Chinese design codes and the statistical data were gathered from the available results of experimental and analytical studies.

While there are a number of detailed studies found in the literature for large-scale seismic simulation, a numerical solution enables to limit computational efforts without losing accuracy and consistency is still lacking. The available simulation models assess the seismic vulnerability of the city through pre-established fragility and capacity functions by classifying the buildings into different groups (typological approach). Usually, buildings are grouped based on building archetype, number of story, building occupancy, and seismic design level. Although these approaches provide a rapid and simplified estimate, their results might be inconsistent with the expected outcomes. Indeed, response of individual building is significantly dependent on various parameters such as building geometry, structural characteristics, construction elements, etc. Given the large number of buildings within a an urban area, building simulation model has to be able to accurately capture the main nonlinear properties of a single building while reducing the computational time required to assess the damage.

In addition, the large amount of data that are required to model the building stock may not be available or accessible, especially for medium or large-scale cities. Thus, the simulation models should be able to model the uncertainties associated to mechanical and geometrical parameters of an individual building. Finally, the simulation models should be able to include visualization capability to facilitate and support decision making process.

2.5 Resilience quantification

Assessment and measurement of resilience is still at the preliminary stage of development and is a challenge yet for communities due to its complexity. Measuring resilience is among the most difficult tasks due to the intricacy involved in the process.

Several solutions for measuring resilience are available in literature. Chang and Shinozuka (2004) introduced a measurement framework to quantitatively assess the disaster resilience of communities. They proposed a series of resilience measures in a probabilistic context based on the work by Bruneau et al (2003). The proposed framework has been implemented in a case study of the Memphis water system under an earthquake event. However, social and economic aspects were not clearly integrated within the framework.

Ouyang et al. (2012) proposed a multi-stage framework to analyze infrastructure resilience establishing an expected annual resilience metric by defining a series of resilience-based improvement strategies for each stage. Furthermore, Ayyub (2015) defined other resilience metrics with clear relationships to the most relevant definition of the reliability and risk notions. The framework meets logically consistent requirements drawn from the measure theory considering the recovery phase based on spatial and temporal considerations.

Kwasinski et al. (2016) proposed a hierarchical framework for assessing resilience at the community level. The model is represented through community dimensions and their relationships with community services, systems, and resources. Several challenges that can influence a comprehensive community resilience assessment methodology have been identified. However, natural resources, as an important element in the resilience planning process, have not been considered in the proposed framework.

Gilbert and Ayyub (2016) proposed microeconomic models and metrics to quantify the economic resilience of engineering systems. These metrics provide a sound basis for the development of effective decision-making tools for multi-hazard environments and lead to significant savings through risk reduction and expeditious recovery. Later on, Liu et al. (2017) introduced a method that combines dynamic modeling with resilience analysis. Interdependent critical infrastructures have been analyzed using the framework by performing a numerical analysis of the resilience conditions in terms of design, operation, and control for a given failure scenario.

Cimellaro et al. (2016b) proposed a resilience index for water distribution networks which is the product of three parameters. This index has been used to compare different restoration plans in a small town in the South region of Italy. Kammouh et al. (2017a) have introduced a quantitative method to assess the resilience at the state level based on the Hyogo Framework for Action (UNISDR 2007). The approach introduced was an evolution of the risk assessment concept. The resilience of 37 countries has been evaluated and a resilience score between 0 and 100 has been assigned to each of them (Kammouh et al. 2018).

Didier et al. (2018) presented a compositional demand/supply disaster resilience quantification framework (Re-CoDeS) based on demand and supply layers, defined locally for civil infrastructure and community components linked by a system service model. The methodology is a bottom-up approach classifying the different component and system resilience configurations with respect to their post-disaster behavior. System lack of resilience was defined as the main resilience measure computed by the aggregation of the lack of resilience of the components identifying the aggregated demand and the aggregated consumption.

By looking at the available measurement tools, it is possible to distinguish some features that separate them. Some measurements schemes are purely qualitative in their approach, and others are quantitative. In general, the resilience measurement approaches can be classified in to four different groups. The first group is composed of schemes based on scorecards to evaluate the performance of

the system. Scorecards are in checklist forms which identify a series of qualitative questions about the presence or absence of resilience items and actions. Each question is associated with a score and the total resilience of the system is measured by summation of all scores.

The second group is based on indicators or indices to quantitatively measure the system resilience. The indices are representative of system characteristics and can be statistically evaluated. The overall system resilience is computed by aggregation of each single index. The third group is based on the combination of scorecards and indices providing tools for resilience assessment (such as guidance, surveys, procedures, or data). Finally, the last group is composed of approaches which use mathematical models to simulate the interactions and relationships within the system. The models can be used to measure the resilience of different dimension of the system (such as physical, social, economic, etc.) through performing computational simulation (Renscher et al. 2010).

The measurement scheme also can be classified into top-down or bottom-up approach. For example, PEOPLES framework is a top-down approach that starts with the big picture (i.e. resilience) and then breaks down into smaller segments. Each subsystem is then refined in yet greater detail, sometimes in many additional subsystem levels, until the entire specification is reduced to base elements (Cimellaro et al. 2016).

Another top-down measurement tool is the Baseline Resilience Indicator for communities (BRIC) (Cutter et al. 2014). This tool same as PEOPLES framework is quantitative but it focuses more on the inherent resilience of communities. BRIC is practically oriented towards the fieldwork unlike the PEOPLES framework whose application is still within the research field. San Francisco Planning and Urban Research Association framework (SPUR) (SPUR 2009) is a qualitative framework that measures the capability to recover from earthquakes. The framework considers the restoration of buildings, infrastructures, and services to assess the resilience of the physical infrastructure. Examples of other top-down approaches are: the Hyogo Framework for Action (HFA) (UNISDR 2005); the UK Department for International Development (DFID) Interagency Group (Twigg 2009b); ResilUS (Miles and Chang 2011); etc.

There also exist bottom-up approaches which are mainly designed to help communities predict and plan for resilience. These bottom-up measurement tools take an all-hazards approach in their assessment. They are generally qualitative types of assessments that the community does itself, or it works with local stakeholders to derive its assessment. Some bottom-up approaches include: the Conjoint Community Resiliency Assessment Measure (CCRAM) (Cohen et al. 2013); the Communities Advancing Resilience Toolkit (CART) (Pfefferbaum et al. 2011); the Community Resilient System (White et al. 2015); etc. A more exhaustive list of resilience measurement tools classified according to several characteristics can be found in (Cutter 2016). Several other works have been carried out to define and quantify the resilience of communities but mostly with a focus on engineering systems (Woods 2017; Park et al. 2013; Hosseini et al. 2016; Jovanović et al. 2016; etc.).

By looking at the available resilience measurement tools, there is no single or widely accepted method to quantify the community resilience (Cutter et al. 2014). Even though much efforts has already been made to boost research on community resilience indicator (Cutter et al. 2010; Norris et al. 2008; Twigg 2009a), there is still no acceptable method for the evaluation of community resilience (Abeling et al. 2014). Although the use of indicators is perceived as an important instrument to measure the resilience of a system, developing a standardized set of resilience indicators is clearly challenging for such a dynamic, constantly reshaping and context-dependent concept.

To add the state of the art, this dissertation primary focuses on development of a quantitative framework to assess the damage to buildings portfolio of a city-scale community given a seismic scenario (Chapter 3). The applicability of the proposed model is verified by applying in a large-scale virtual city and the effectiveness of the methodology in modeling correlation between built environment entities is shown (Chapter 4 and Chapter 5). Furthermore, a community-level resilience model is proposed to quantify the resilience of community using the structure of PEOPLES framework (Chapter 6).

Chapter 3

City-scale simulation model

Nowadays, computer-based simulation is the most useful and feasible methodology for reproducing the behavior of a system under an external perturbation. In the context of seismic simulation for building stock, the structural behavior must be reproduced through appropriate mathematical models to simulate the real behavior of the structure. Given the large number of buildings in a city, this requires complex numerical models and an excessive computational effort. Thus, a simple and efficient mathematical algorithm capable to provide performance reliability with low cost computational effort is needed.

To add to the state of the art in evaluation of earthquake-induced damage to built environment, this chapter proposes a modeling methodology to assess the seismic vulnerability of building stock of large-scale cities for a variety of possible earthquake scenarios. The building seismic damage is evaluated through performing nonlinear dynamic analysis for each individual building subjected to a given seismic input. First, the mathematical simulation model and the methodology to develop backbone curves for each single building are presented. Then, a model to include the uncertainties associated with geometry and mechanical properties for each individual building using Monte Carlo Simulation (MCS) is proposed. Furthermore, an automated tool is developed to perform simulation analysis, extract all the buildings response parameters, perform post-processing analyses, and to estimate and visualize the level of damage for each building. At the end, a virtual city based on the built environment of Turin (Italy) is designed and the applicability of the developed methodology is validated.

3.1 Nonlinear model

A large component to an urban environment is residential buildings. When a catastrophic event such as an earthquake occurs in a built environment, the consequential structural damage may cause high losses (casualties, repair costs, and repair time). Thus, a concise and methodical approach is needed to estimate

the fragility of the building stock. Nonlinear MDOF model is able to satisfactorily capture the nonlinear properties of multi-story buildings, predict the Engineering Demand Parameters (EDPs), and assess a reasonable level of damage. In the proposed approach, the global capacity of a building is simulated through a tri-linear backbone curve (Figure 3).
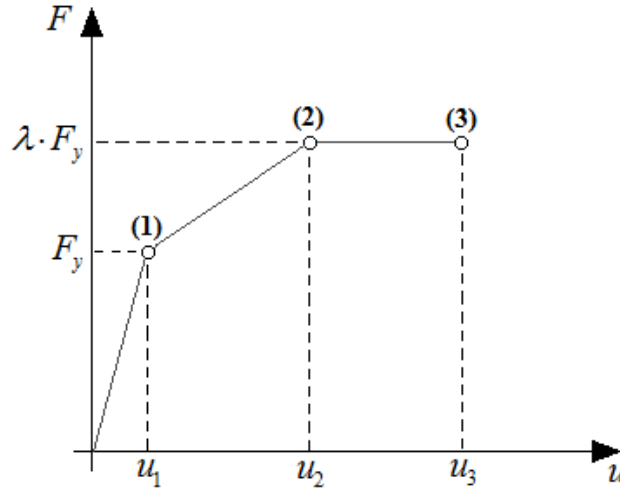
Figure 3. Trilinear backbone curve.

The first point of the trilinear backbone curve (1) indicates the yield point ($\lambda \cdot F_y - u_1$) corresponding to the formation of the first plastic hinge in the weakest base column. After the yield point, the stiffness is significantly reduced until the next point (2), for which the maximum shear base capacity ($\lambda \cdot F_y$) is reached. The ultimate point (3) corresponds to the collapse of the building (complete damage). The evaluation of the shear base and top displacement parameters for each point is discussed in the following subsections.

The three main points of the curve are evaluated using a nonlinear static approach for a MDOF system. To achieve this goal, a MATLAB algorithm has been developed considering the uncertainties on the geometric and mechanical parameters used in the analyses. Variation of the parameters within an acceptable range is considered through an MCS obtaining a set of tri-linear backbone curves for each building. The ranges of the main building's parameters are selected according to the level of knowledge of the building. In addition, the deterioration of the mechanical properties (such as strength and elastic modulus of concrete) is taken into account through the aging equation proposed by Euro code 2 (EC2, 2004) according to the year of construction. Once the Matlab algorithm evaluates the tri-linear backbone curve at each step of MCS, the SAP2000 API is used to apply to all the buildings the data set obtained by the algorithm.

This automated procedure is capable of reducing the computational time and analyze the dynamic responses dispersion caused by the data uncertainty. Therefore, the median response and associated dispersion for each building within the virtual city can be estimated. This approach is suitable to allow a decision-maker the ability to explore how their community responds to a disruptive event

21

and quantify the mean performance of buildings and their uncertainty in the dynamic response after a hazard.

Assimilating the dynamic nonlinear response of a structural system to a unique backbone curve leads to analyze the building as a nonlinear equivalent Single Degree Of Freedom (SDOF) model. Considering an SDOF system allows for a reduction in the computational effort needed to assess the response of a large number of structures. Finally, due to limited amount of detailed building information about its dynamic behavior, the hysteresis is considered according to the Takeda model (Takeda et al. 1970) implemented in SAP2000.

3.1.1 Elastic parameters

Generally, the geometry of a residential building is mostly regular in plan and elevation, therefore the mass and stiffness can be assumed to be mostly uniformly distributed. In these cases, the evaluation of the response of MDOF system with a nonlinear static procedure is close to the real response of the structure.

Thus, a nonlinear static analysis (pushover) is performed to assess the base shear and top displacement values corresponding to the formation of the first plastic hinge at the base level (yield point). In order to consider all Degrees Of Freedom (DOFs), the stiffness matrix of the structure is evaluated considering the building as a bending type system. Since the load patterns are applied in two main directions of the buildings, the modal characteristics are derived by considering the stiffness matrix in the two directions for a 2D system. Thereafter, the static condensation procedures are performed to reduce the number of DOFs to the translational DOFs. Moreover, the model assumes that the mass of each story is concentrated in the center of the mass on its elevation and represented by a mass point (Figure 4).
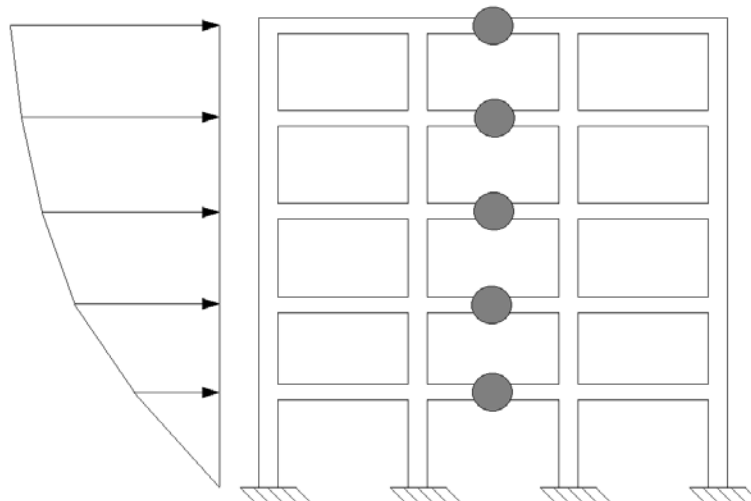
Figure 4. Concept of nonlinear MDOF system.

Equations (3) and (4) summarizes the global stiffness and mass matrices of a MDOF model, respectively.

$$K = \begin{bmatrix} k_{11} & k_{12} & \cdots & k_{1dof} \\ k_{21} & k_{22} & \cdots & k_{2dof} \\ \vdots & \vdots & \vdots & \vdots \\ k_{dof1} & k_{dof2} & \cdots & k_{dofdof} \end{bmatrix} \tag{3}$$

$$M = \begin{bmatrix} m_1 & 0 & \cdots & 0 \\ 0 & m_2 & \cdots & 0 \\ \vdots & \vdots & \vdots & \vdots \\ 0 & 0 & \cdots & m_{dof} \end{bmatrix} \tag{4}$$

where *dof* represents the total number of DOFs. The yielding base shear force is assessed by applying a monotonic load pattern on the building proportional to a given modal shape. A multi-modal approach is carried out to consider all the modal shape contributions, especially for buildings that have geometric irregularities:

$$\Phi_{tot} = \sum_{i=1}^{dof} \{\Phi_i\} \cdot g_i \tag{5}$$

where Φ_{tot} is the modal shape considering all modal contributions (Φ_i). The modal participation factors are represented by the term g_i.

3.1.2 Post-elastic parameters

Once the structure reaches the yield point, the stiffness is significantly reduced until point (2) for which the maximum shear base capacity is reached. Thus the top shear base remains constant and the top displacement increases (perfectly plastic behavior) until the ultimate value. The maximum shear base capacity is estimated through the kinematic approach of the limit analysis (Greenberg-Prager theorem). The implemented Matlab code is capable to identify the local or global collapse mechanism of the considered building. As illustrative example, a general global collapse mechanism of a frame subjected to a distribution of horizontal forces is shown (Figure 5).
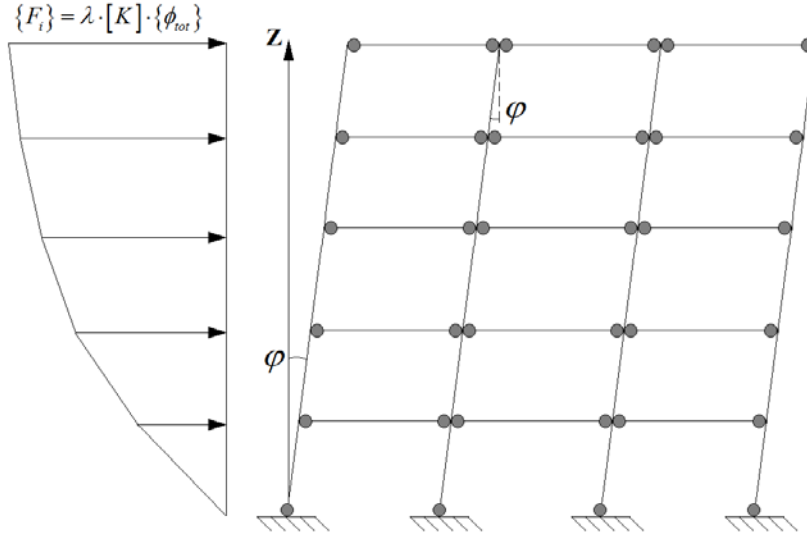
Figure 5. Global collapse mechanism.

This approach leads to take into account the strength contribution of all the structural elements (beams and columns). According to the kinematic theorem of the limit analysis, the global over-strength factor (λ) is assessed by the ratio between the internal and external work of the structural system with equal columns and beams dimensions:

$$\lambda = \frac{n_c \cdot M_{y,c} + 2 \cdot n_{span} \cdot dof \cdot M_{y,b}}{\sum_{i=1}^{dof} \{F_i\} \cdot \{z_i\}} \tag{6}$$

where $M_{y,c}$ and $M_{y,b}$ are the yielding bending moment for the columns and beams, respectively. The parameters n_c represents the number of columns, n_{span} indicates the number of spans in the considered direction, and dof is the number of master DOFs which corresponds to the story number of the building. The external work is given by the denominator expression and it is due to the horizontal load patterns $\{F_i\}$ multiplied by the distance between the considered story and the base at each elevation level $\{z_i\}$.

One of the limitations of this procedure consists of the load pattern's shape. In fact, the monotonic horizontal force distribution does not change its shape due to the progressive formation of the plastic hinges in the columns (non-adaptive approach). Once the shear base capacity is determined, the top displacements corresponding to points (2) and (3) of the tri-linear backbone curve (u_2 and u_3 in Figure 3) have to be assessed. Since the shear base capacity is previously evaluated, the definition of reduction factor (R_μ) can be used to calculate the displacement u_2. The reduction factor accounts for ductility, over-strength, redundancy, and damping of a structural system:

$$R_\mu(T, \mu, \xi) = \frac{F_{EL}(T, \xi)}{\lambda \cdot F_y(T, \mu, \xi)} \tag{7}$$

where $\lambda \cdot F_y$ is the maximum shear capacity and F_{EL} represents the equivalent elastic shear force. As mentioned previously, the reduction factors depend on

24

ductility (μ), over-strength (λ), damping (ξ) and elastic building characteristics (such as period, T). Several mathematical formulations have been proposed for evaluating the reduction factor. One of the most used expressions is based on the equal energy rule (short period systems, $T<0.5$ s) or equal displacement rule (long period systems, $T>0.5$ s):

$$\begin{cases} R_\mu = \sqrt{2 \cdot \mu - 1} \quad (T < 0.5s) \\ R_\mu = \mu \quad (T > 0.5s) \end{cases} \tag{8}$$

The ductility parameters are expressed as a ratio between the ultimate displacement and the displacement for which the maximum shear capacity occurs. According to the proposed tri-linear backbone curve, the ductility is given by the ratio between displacements u_2 and u_3. Furthermore, the ultimate top displacement is evaluated based on the equal energy theorem (Figure 6).
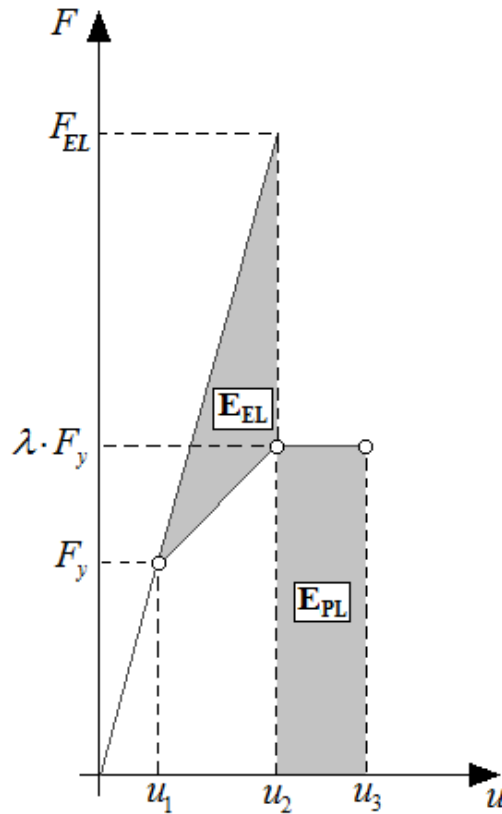
Figure 6. Equivalent elastic energy (E_{EL}) and elasto-plastic energy (E_{PL}) of the system.

According to the Figure 6, the energy balance between the equivalent elastic energy (E_{EL}) and elasto-plastic energy (E_{PL}) is reported in Equation (9):

$$\left(u_2 - u_1\right) \cdot \frac{\left(R_\mu - 1\right)}{2} = \left(u_3 - u_2\right) \tag{9}$$

In the proposed approach, the two unknown displacement values are evaluated through an iterative procedure. The reduction factor value is fixed and then the displacement u_2 is assessed:

25

$$u_2 = \frac{R_{\mu, fixed} \cdot \lambda \cdot F_y}{k} \qquad (10)$$

where k is the stiffness of the system. According to Equation (9), the ultimate top displacement u_3 is evaluated and then the reduction factor is calculated by using Equation (8). This iterative procedure continues until the corresponding calculated reduction factor converges for given initial approximation (Figure 7).
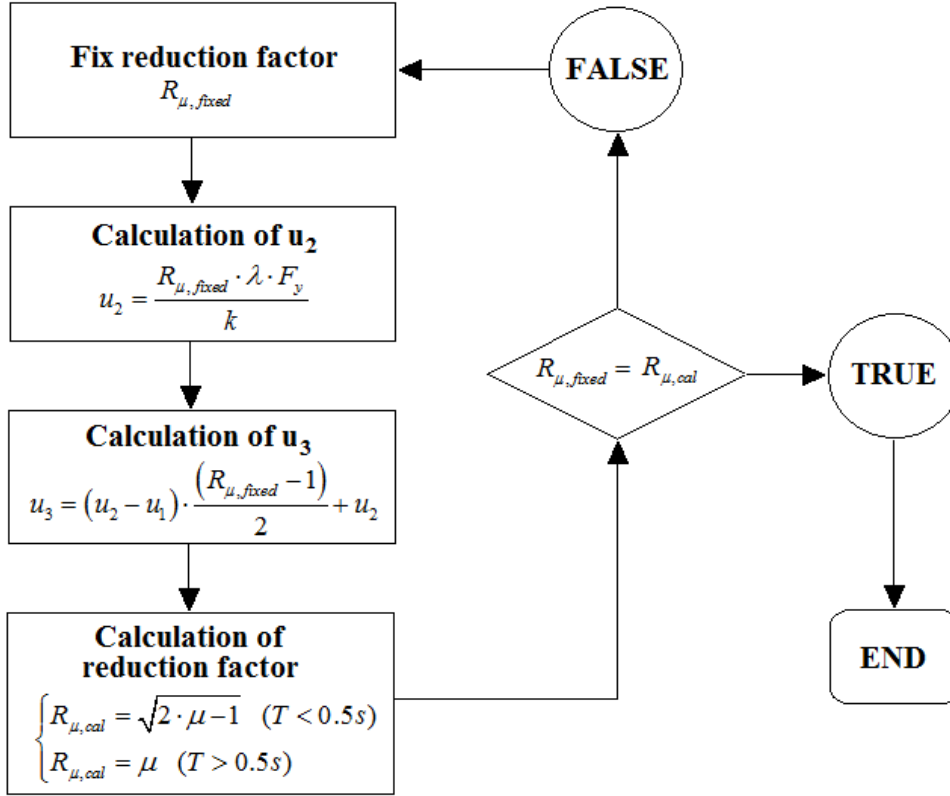
Figure 7. Iterative procedure to evaluate the reduction factor.

3.2 Analysis implementation and simulation

The proposed approach is capable of applying nonlinear time history analyses to a large number of buildings. The dynamic response of the structural system in a built environment takes into account a considerable amount of parameters. The building inventory, containing all the information (such as material, geometry and mechanical properties) has been developed and allocated on an external server. All this data are accessible by a MATLAB code organized in several functions that manage the seismic input definition, MCS for evaluation of the nonlinear parameters, and SAP2000 API actions.

Due to the large number of variables and the time requested for processing, parallel algorithms running on multiple processors are developed with MATLAB. The global behavior of each building has been modeled by using multi-linear plastic link element available in SAP2000. The mechanical characteristics have been defined automatically according to the obtained backbone curves from MCS. Figure 11 depicts the schematic model used for simulating the global shear

26

capacity of each building. The equivalent damping coefficient has been assessed according to the Rayleigh formulation considering the first and second building's period as control periods.
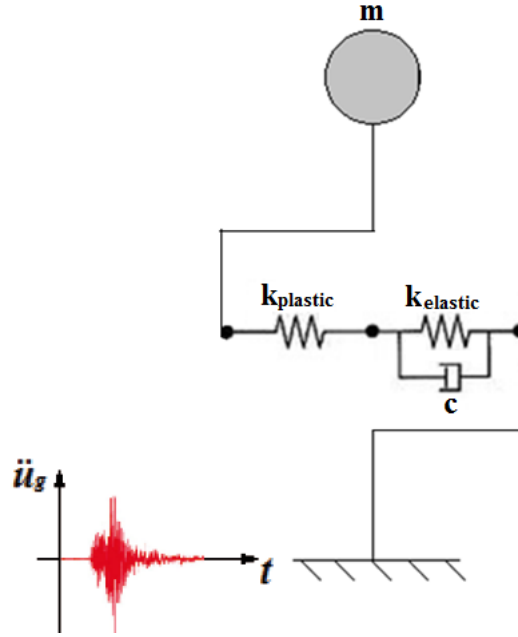
Figure 8. Multi-linear plastic model.

The displacements response of a SDOF system tends to provide a global response parameter which is not representative of the experienced damage. An approximated model has been proposed to convert the global response of an equivalent SDOF system to the response of the associated MDOF system.

Given a generic building, its global capacity curve has been estimated based on the pushover analysis. The seismic action has been assimilated to a lateral invariant force distribution ($\{F\}$) proportional to the equivalent modal shape of the structure which takes into account all the modes of vibration through their modal participation factors. Based on the elasticity theory, the displacements of each story of the building can be assessed:

$$\{u_e\} = \alpha \cdot \{\Phi_{eq}\} = \alpha \cdot \{F\} \cdot [K_{BT_R}]^{-1} \tag{11}$$

where $[K_{BT_R}]$ represents the stiffness matrix of the structure, while $\{u_e\}$ is the vector containing the lateral displacements of each story. When the first plastic hinge occurs in the weakest vertical frame member, the direct proportionality between the stiffness matrix and the lateral force distribution is not valid.

The maximum shear capacity has been derived based on the limit analysis. Therefore, the kinematic configuration associated with the collapse of the building is known. It has been assumed that the lateral displacement distribution after the global yield point is directly proportional to the displacement pattern represented by the collapse mechanism. This displacement pattern refers to the plastic contribution ($\{u_p\}$). Based on these assumptions, the lateral displacement

27

distribution which identifies the response of the MDOF system ($\{u_{MDOF}\}$), can be evaluated as sum of the elastic and the plastic contributions. Figure 9 shows an illustrative example of the estimation of the lateral absolute displacement of each story based on the calculated top displacement.
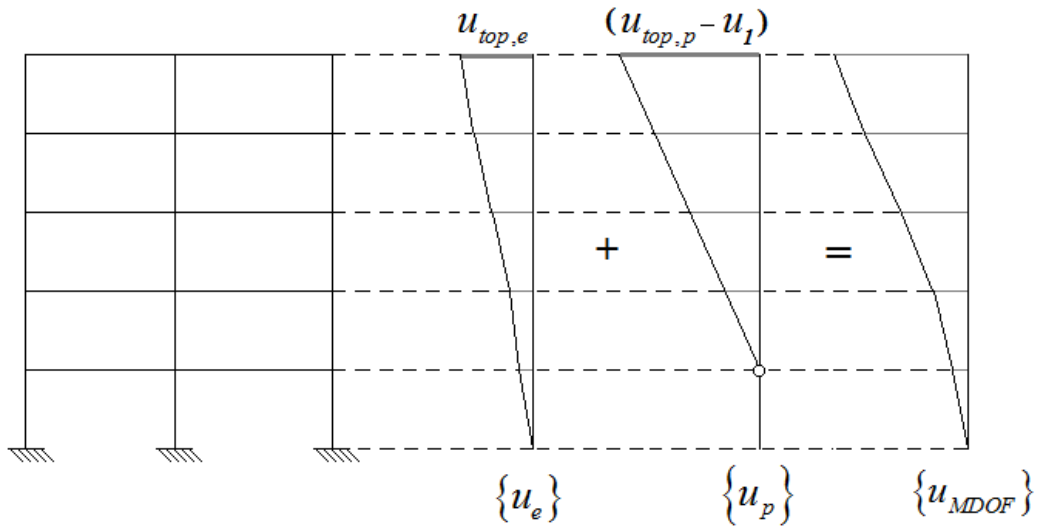
Figure 9. Elastic and plastic displacements distributions.

3.2.1 Software architecture

The analysis flow is controlled through an interactive graphical user interface (GUI) that allows for selection of an earthquake scenario in the virtual city (magnitude and epicenter location). Furthermore, the acceleration time history can be selected and processed in both North-South (NS) and East-West (EW) directions. In order to take into account the de-amplification of the seismic excitation with the epicenter distance, the shear wave velocity in the upper most 30 m (V_{S30}) for the city of Turin is included in the database. The V_{S30} map has been obtained via USGS website (USGS 2013) at the link (http://earthquake.usgs.gov/hazards/apps/vs30/). The Boore-Atkinson (Boore and Atkinson 2008) attenuation law is used to estimate the attenuation of the time history's peaks. A Matlab function is provided for calculating distances between the selected epicenter and the center of the mass of each building. Moreover, the equivalent shear wave velocity is assessed according to the V_{S30} map, and considered in the attenuation model.

The main Matlab function controls the building's data flow, and then the MCSs are carried out to evaluate the backbone curves for each building, considering the epistemic uncertainties in the input model parameters.

3.2.2 SAP2000 API

The SAP2000 Application Programming Interface (API) is a programming tool that offers efficient access to the analysis and design technology of the SAP2000 structural analysis software. A direct interaction with third-party applications is allowed during run-time analysis. The API software library

provides access to a collection of objects and functions capable of remotely controlling the data exchange and setting data in SAP2000. Both pre- and post-processing procedures are managed by a Matlab language code which mainly provides the two-way data exchange. This procedure is capable of significantly reducing the time needed for data exchange, especially for large data models. This automated post-processing analysis allows us to extract all the response parameters needed to estimate the level of damage for each building. The Figure 10 depicts the typical data flow for pre-processing, processing, and post-processing using the SAP2000 API.

Once the Matlab functions assess the nonlinear parameters (tri-linear backbone curves) and the processed seismic input, they are transferred to SAP2000 through API tool. Due to the limited amount of detailed building information, the hysteresis is considered according to the Takeda model. Thus, the nonlinear time history analyses are performed in the SAP2000 environment and the derived output is remotely controlled by Matlab. Figure 11 shows in detail the software data flow used in the simulations.
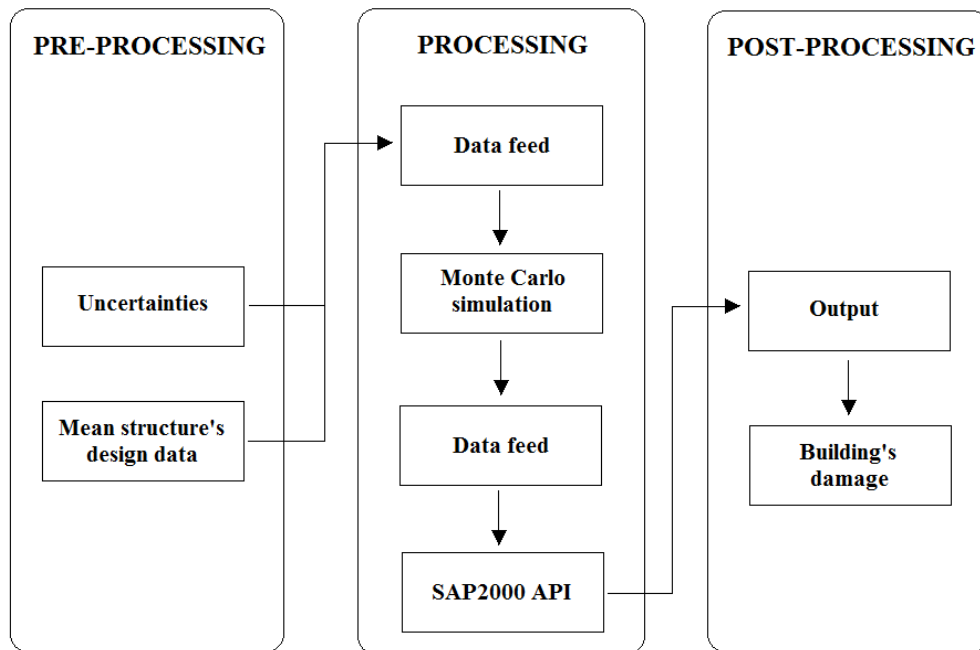
Figure 10. Model data flow: pre-processing, processing, and post-processing.
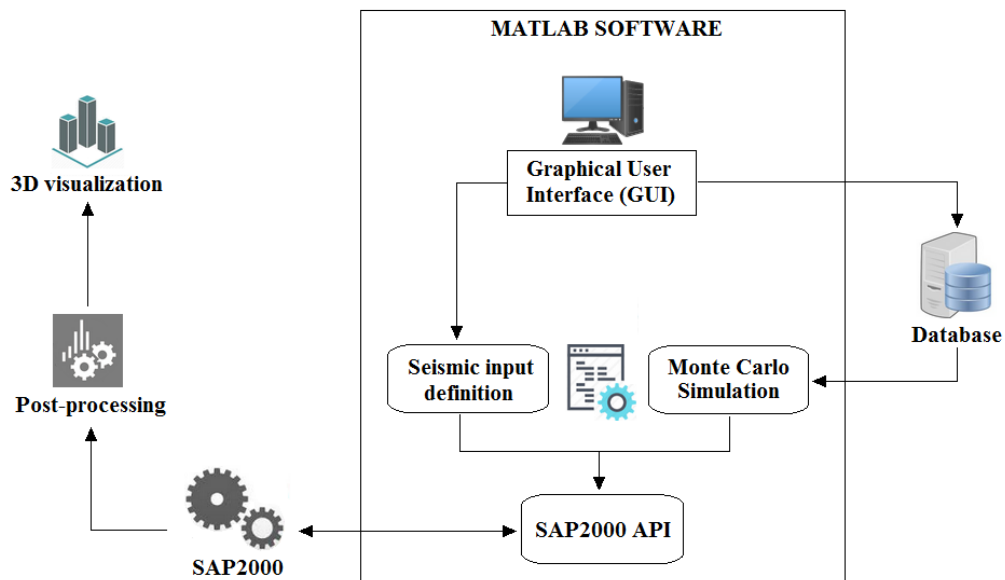
Figure 11. Software data flow.

According to the maximum drift, the structural damage is assessed for each building and the associated level of damage is evaluated (slight, moderate, extensive, and complete) based on. A 3D visualization tool is also provided which shows the dynamic response of the building within the virtual city. This visualization tool can be helpful for monitoring and evacuation management in smart cities.

3.3 Methodology validation

Validation of a computational framework, in term of whether the results are credible, is always a challenge. As a potential technique, the methodology can be validated with comparing the results for an individual building. In this section, the validation of the described simulation model is presented. Two RC buildings are assumed as two case studies to verify the simulation model. The first case study (Figure 12a) is a five story RC building with a square plan, while the second case study (Figure 12b) is a seven story RC building with a rectangular plan. Both case studies have a span length of 4.40 m in the x direction and 6.00 m in y direction, representative of most residential buildings in virtual city. The story height for both buildings is considered as 3.00 m.
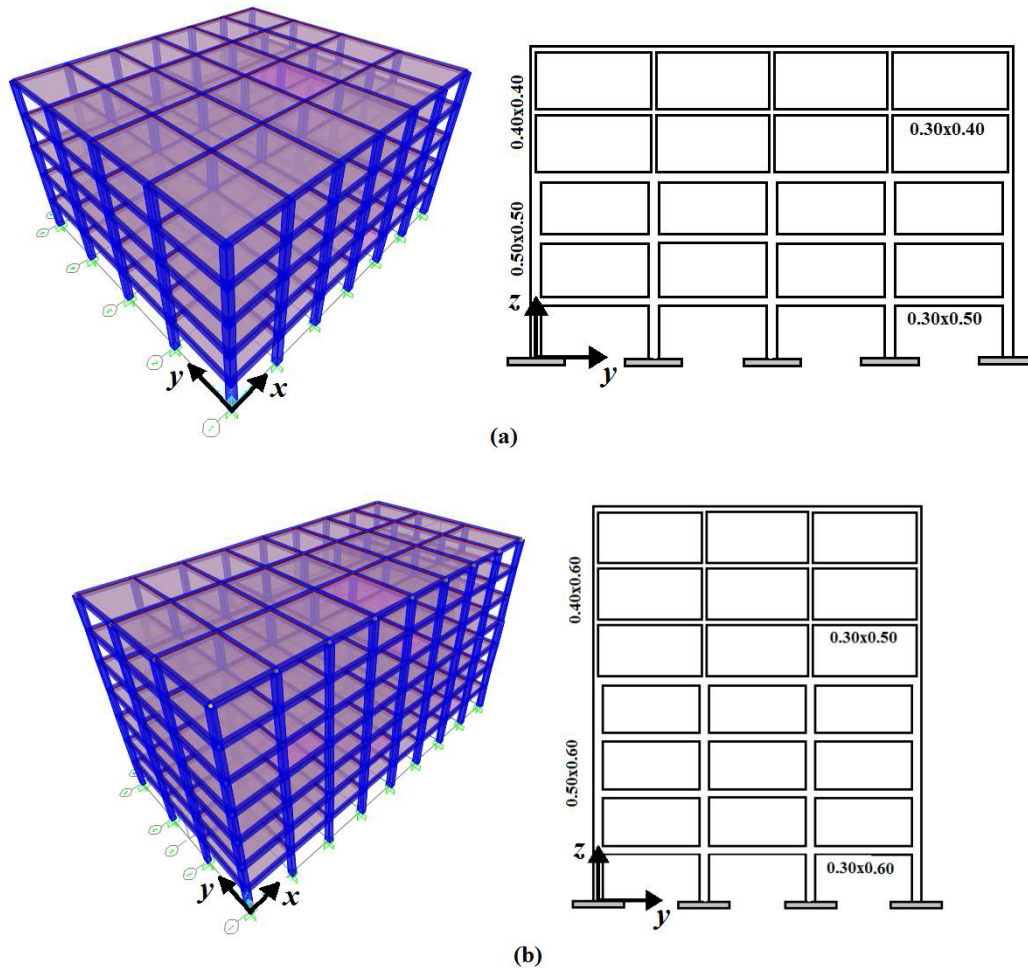
Figure 12. five story RC building(a) and seven story building (b) case studies.

The structural members have been designed according to the Italian seismic regulations (NTC18, 2018). A symmetric reinforcement has been considered for both beams and columns sections. A strength class C30/37 has been adopted for the concrete, while the B450C strength class has been considered for the steel reinforcement bars. Reinforcement ratios of 2.5 % and 1.8 % have been considered to design columns and beams, respectively.

The software SAP2000 (CSI, 2018) has been used to model the case study buildings. Concentrated plasticity model (FEMA 356 type P-M2-M3 for columns and M2-M3 for beams) has been chosen to account for the nonlinearity in the structural components. A 5% damping ratio has been assumed according to Rayleigh formulation. The mechanical and geometrical parameters have been considered as random variables and the associated mean and dispersion values have been assumed. MCS have been performed by assuming a number of iterative steps equal to 100, and then the median backbone curves have been assessed for both horizontal directions. A comparison between the capacity curves obtained through the pushover analysis performed in SAP2000 and the estimated median backbone curves, for x and y directions, are shown in Figure 13 and Figure 14, respectively.
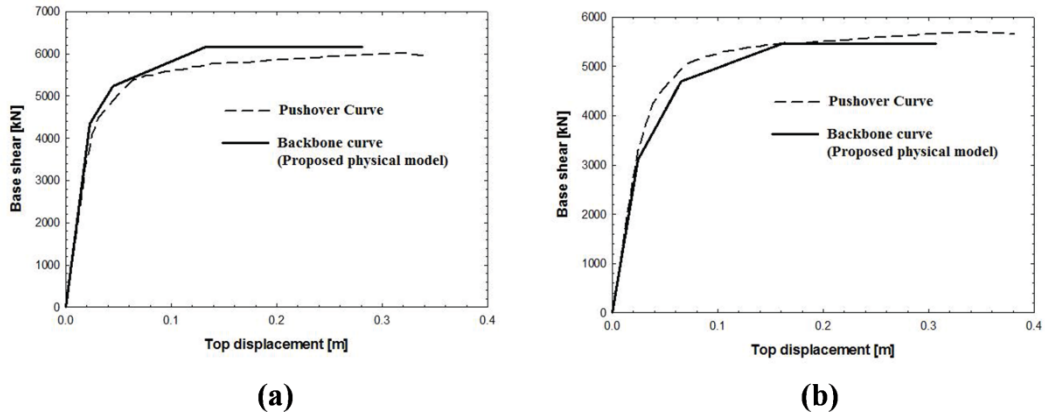
Figure 13. Comparison between capacity curves for case study; *x* (a) and *y* (b) directions.
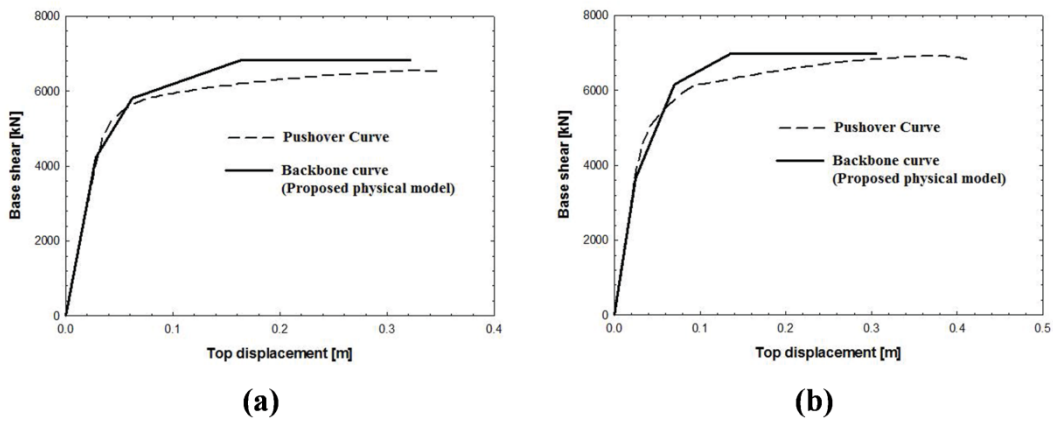
Figure 14. Comparison between capacity curves for second case study; *x* (a) and *y* (b) directions.

For both case studies, the median backbone curves provide comparable and reliable results. Moreover, collapse top displacements associated with the median backbone curves are always lower than those ones obtained through the pushover analysis. In addition, the estimated maximum shear capacity tends to be equal or, in some cases, greater than the expected one. This is due to the application of the kinematic theorem of the limit analysis, which provides an upper bound limit of the structural capacity in terms of force. This in turn leads to assume a stiffer behavior with respect to the real one.

3.4 Virtual city: building database

The virtual city has been designed based on the buildings stock for the city of Turin, Italy. The virtual city has the area of 120.1 km2 with the total population of 908,000. Four building sectors that provide essential functions to a community, including housing (residential building, hotel, shelter, etc.), education (school, university, library, etc.), business (shopping center, retail store, heavy industry, etc.), and public services (hospital, police station, church, airport, etc.) are considered. Table 1 lists in detail the building sectors supporting the physical,

economical, and social dimensions of the virtual city. In total, the virtual city has 30,122 buildings.

The plan dimensions of each building have been gathered through CADMAPPER file for the entire city of Turin. In addition, the numbers of stories have been obtained by the shape-file of "Carta Tecnica Comunale (CTC)" of the city of Turin, available at the website http://www.comune.torino.it/geoportale/. The building inventory of the city is based on the building typology concept already used in many European countries at national and regional levels. However, the lack of information about some buildings makes it difficult to have perfect knowledge of any individual building. For this reason, some building's attributes (e.g. year of construction, type of deck) have been assigned based on known data for the entire city. Six different categories of construction year have been utilized according to the main changing from standard Italian codes (Table 2).

Table 1. Buildings stocks and the map of the virtual city.
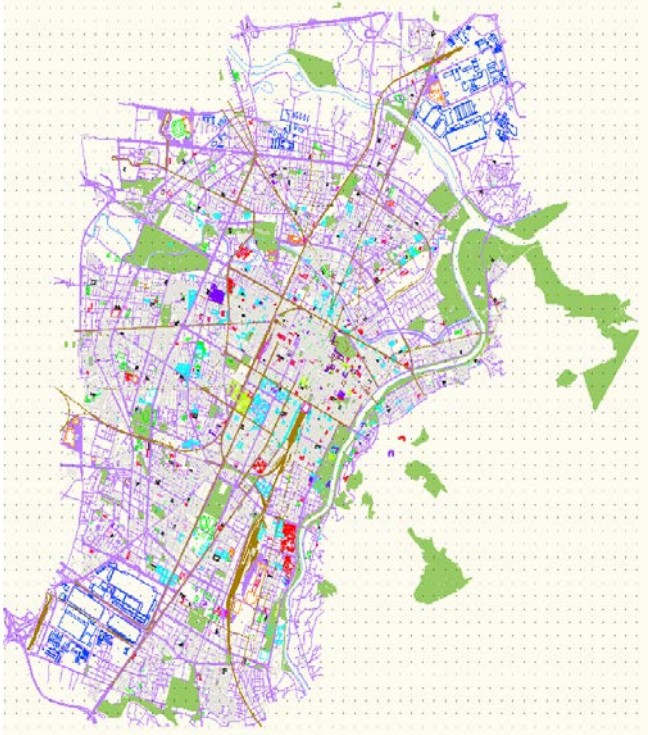
Physical Infrastructure	Building	Residential	23420	
		Mobile Home	62	
	Hospital		17	
	Fire Station		3	
	Police Station		60	
	Educational	Elementary School	157	
		Middle School	105	
		High School	97	
		University	70	
Social Infrastructure	Hotel		31	
	Historical Building		951	
	Castel and Palace		18	
	Church		176	
	Sport		265	
	Cinema		48	
	Museum		156	
	Theater		38	
	Library		15	
Economic. Infrast.	Industrial Build.	Light	321	
		Heavy	108	
	Commercial	Retail store	25	
		Malls	12	

Table 2. Different categories for the building's year of construction.
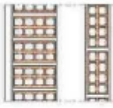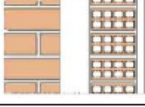
I	II	III	IV	V	VI
< 1916	1916-1937	1938-1974	1975-1996	1996-2008	> 2008

The numbers of buildings for each year of construction category have been assigned according to the Italian census Institute based on the city of Turin.

Corrado et al. (2012) provided typical Italian building construction elements depending on the year of construction. Classification of building construction elements (e.g. deck, wall, etc.) plays a key role in the assessment of mass. Seven different typical deck and three typical external walls have been selected and distributed based on their year of construction (Figure 15).

DESCRIPTION		YEAR
	Vault ceiling with solid bricks	< 1900
	Ceiling with wood beams and hollow bricks	< 1900
	Ceiling with reinforced concrete	1900 - 1930
	Vault ceiling with bricks and steel beams	< 1930
	Vault ceiling with hollow bricks and steel beams	1910 - 1940
	Ceiling with reinforced brick-concrete slab	> 1930
	Ceiling with reinforced brick-concrete slab, low insulation	> 1976

(a)

DESCRIPTION		YEAR
	Solid brick masonry (25 cm)	1900 - 1950
	Hollow wall brick masonry (30 cm)	> 1930
	Hollow wall brick masonry with solid and hollow bricks (40 cm)	1930 - 1975

(b)

Figure 15. Typical Italian building's decks (a) and walls (b) used for residential occupancy in different years (Corrado et al. 2012).

All the buildings have been divided into two groups based on material: concrete and masonry. Considering limited information in the building attribute data, an accurate determination of the nonlinear structural parameters is rather challenging. The major objectives of this work are to provide a simplified and accurate method for assessing the dynamic response of residential buildings in a generic built environment. For this purpose, the geometric characteristics of the structural elements (e.g. columns and beam sizes) have been defined in order to

respect all the technical standards for a given year of construction and for a given seismic hazard scenario (medium or high level).

3.5 Case study: Norcia earthquake scenario

Seismic scenario has been identified within the virtual city and the structural damage to the buildings has been assessed in order to test the proposed simulation approach. The seismic input definition has been set in terms of epicenter location, magnitude, and time history recorded in the epicenter. The epicenter distance associated with the center of gravity of the downtown is 9 km. The horizontal acceleration time histories in both X and Y directions recorded during the Central Italy earthquake (6.5 M_w, 2016/10/30) in the station of Norcia (NRC) have been assumed as representative of the seismic accelerations recorded at the epicenter. Figure 16 depicts the North-South c component of the acceleration time history recorded in the station of Norcia. A PGA value of 0.37 g has been recorded.
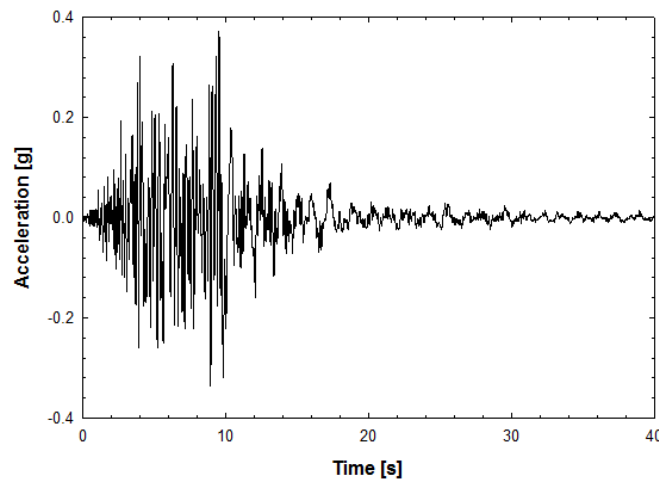
Figure 16. North-south component of time history acceleration applied to the virtual city at X direction, Norcia Earthquake.

A simplified procedure has been proposed to estimate the geometrical attenuation at any building location within the virtual city. The geometrical attenuation of the seismic excitation has been estimated through the Boore-Atkinson (Boore and Atkinson 2008) attenuation law. For this purpose, the shear wave velocity in the upper most 30 m (V_{S30}) for the city of Turin has been considered to model the soil characteristics. The V_{S30} map has been obtained via USGS website (USGS 2013) at the link http://earthquake.usgs.gov/hazards/apps/vs30/ and saved in the database. Equivalent shear wave velocity in the uppermost 30 m ($V_{s30,eq}$) has been evaluated at each building location. A set of scale factors have been calculated which identify the peak's attenuation of the acceleration time history at each building location. Then, horizontal acceleration time histories in both horizontal directions have to be selected to be representative of the typical site hazard. The acceleration time histories at each building location have been evaluated by multiplying the accelerations recorded in the epicenter by the associated scale factors which

considered the geometrical attenuation. As first order evaluation of the damage assessment of the virtual city has been provided by consider the geometrical attenuation only.

Figure 17 shows the 2D map of PGA values calculated by taking into account the geometrical attenuation. The location of the considered epicenter is shown as a red star at the south- west of the virtual city.
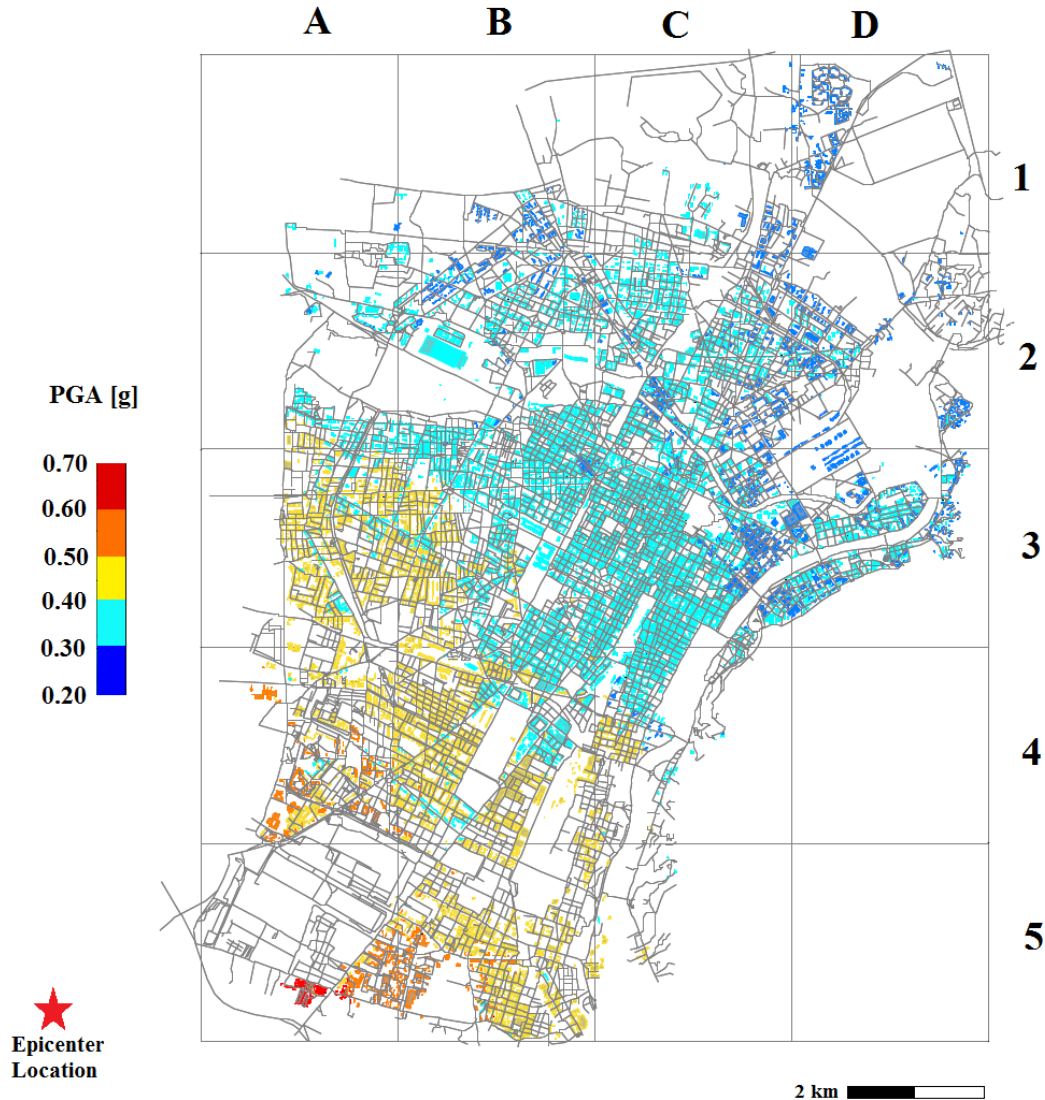
Figure 17. PGA map applied as seismic scenario.

The physical building modeling has been obtained through the dedicated algorithm and the dynamic characteristics of the built environment have been set on SAP2000 environment. A number of 100 iterations has been set to perform MCS and assess the median backbone curve for each building. Ground displacements time histories have been derived and applied at the base of each building model. Time history analysis has been performed and the dynamic building response of the virtual city has been estimated. The outputs have been automatically saved in terms of maximum absolute top displacement of each

multi-linear plastic element. The results have been arranged into tabular file by specifying the file name and the format.

The top displacement of each element have been derived and used for defining the related maximum inter-story drift according to the proposed seismic response model. Thus, the building damage levels have been derived based on the threshold of inter-story drifts proposed by Ghobarah (2004). Figure 18 illustrates the 2D visualization of the damage level for the entire virtual city under the considered seismic scenario. It shows that the downtown of the virtual city (C4) is more vulnerable zone since it consists of mostly old masonry buildings.
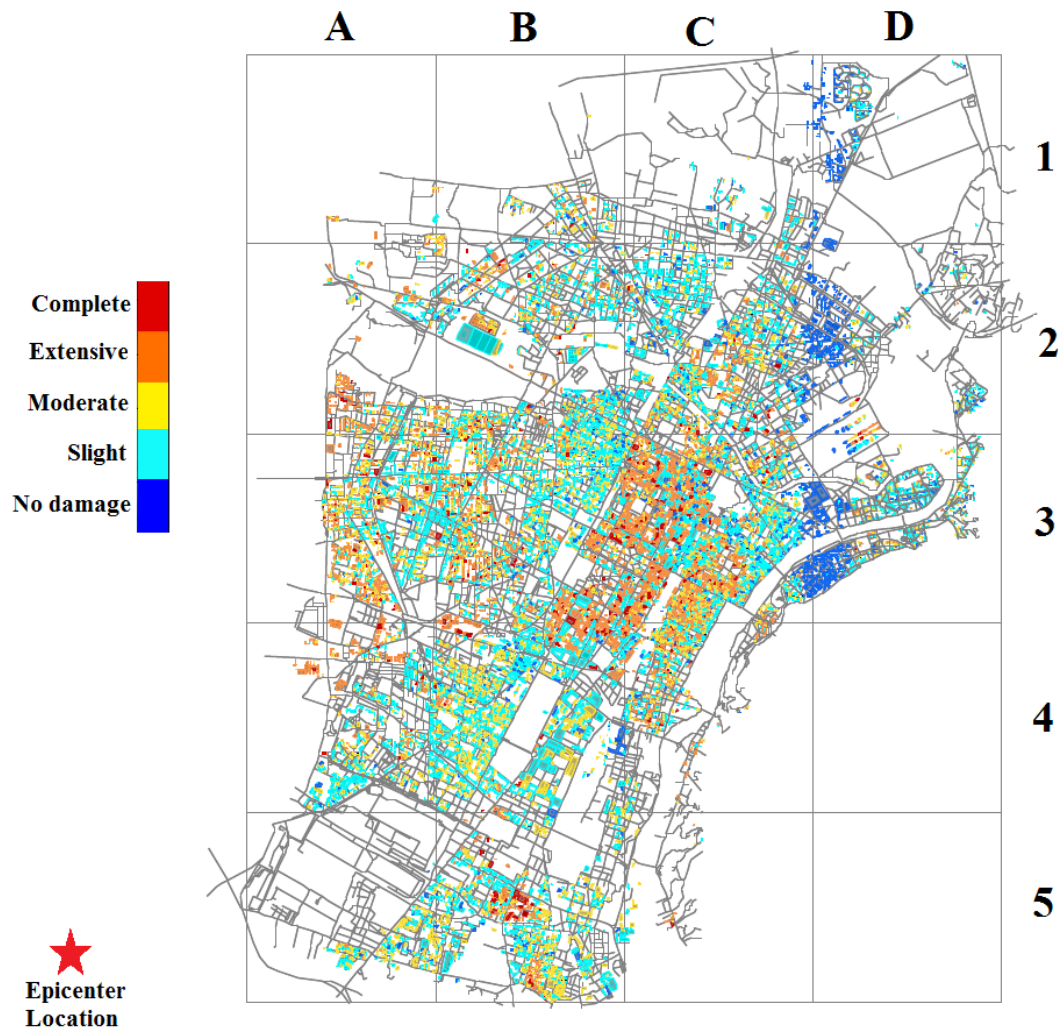
Figure 18. 2D visualization of the damage level to the buildings within the virtual city.

The total percentages of buildings associated with each damage state has been calculated and reported in Figure 19. Most part of the buildings has experienced Slight DS (about 38 %), while 30 % and 22 % of the buildings have a Moderate and Extensive DSs, respectively. Only 3 % of the buildings are collapsed, whereas the remaining part is undamaged (about 9 %). The distribution of damaged buildings based on the level of damage (DS) and the year of constructions is shown in Figure 20. It shows that the most part of the buildings built before 1916 have experienced extensive and moderate DSs, while the newest buildings mostly

have the slight damage. It is due to this fact that newest building were designed according to design codes with more stringent seismic design requirements.
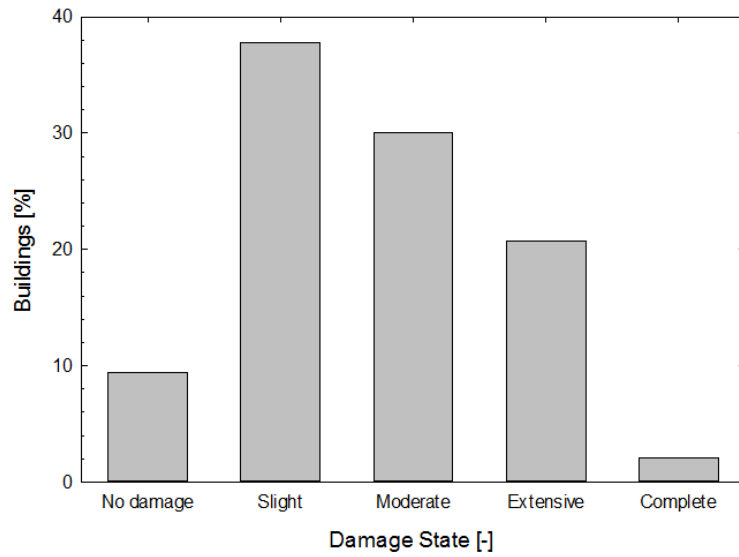
Figure 19. Buildings' damage distribution within the virtual city.
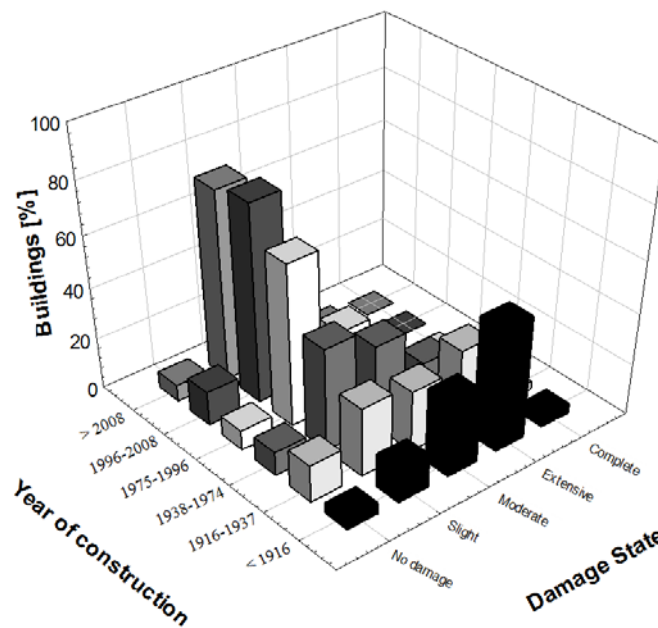
Figure 20. Buildings percentage distribution within the virtual city based on year of constructions and building damage states.

At the end, a 3D visualization of the virtual city' response, in terms of top displacements at different time steps, is shown in Figure 21 for a part of the city.
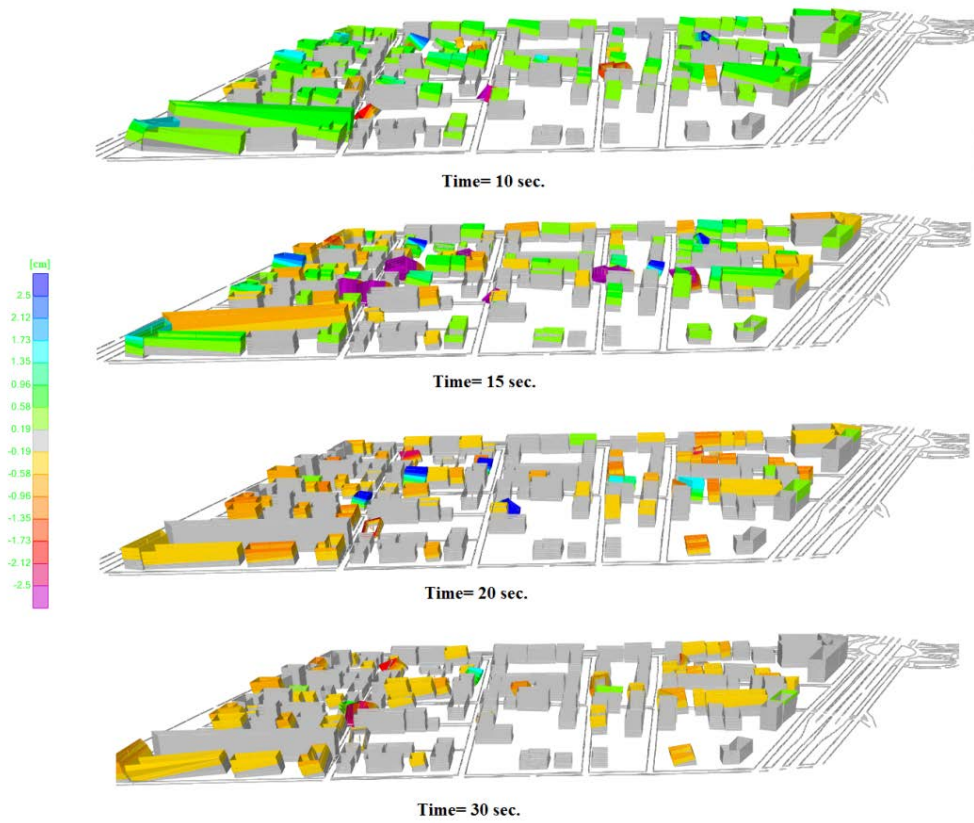
Figure 21. Displacement contours at four different time steps.

In this chapter, a new simulation model to assess the vulnerability of buildings portfolio was presented. The methodology starts with a mathematical simulation to obtain the capacity curve for each individual building. Tri-linear backbone curve representing the building's global behavior is estimated accounting for the uncertainties associated with building geometrical and structural design parameters. Then, the level of damage for each single building is evaluated by performing nonlinear dynamic analysis for a given earthquake scenario. The methodology was applied to a developed virtual city. This model is a basis for further work described later in Chapter 4 for social loss estimation in terms of casualty rate.

Chapter 4

Social loss estimation

The devastating consequences of earthquakes during recent decades demonstrated that risk management is a critical issue for seismically active regions. Estimation of potential losses for the built environment of a community is more complex than for a single site. Between entities of the built environment there are always strong correlations and interconnections that make it difficult to assess the functionality of a community with respect to an individual building. The influence of interconnection between buildings is more apparent when assessing large infrequent losses for a building portfolio within a community. Such losses tend to dominate repair time and cost of whole community after a seismic event. Thus, resilience of the built environment can only be estimated accurately if the interconnection and correlations between the building performances are included in model.

This chapter aims to develop a quantitative earthquake risk assessment model for buildings portfolio considering the buildings spatial distribution within the virtual city. The primary focus is to develop fragility curves for each individual building within the built environment performing large scale simulations, and accordingly to assess the level of the damage for each hazard level. Furthermore, HAZUS methodology (NIBS 2012) is applied to the residential buildings to estimate the direct social losses in term of casualties. The number of injured and their corresponding severities are computed for each neighborhood of the virtual city.

4.1 Ground motion selection

The performances of the building portfolio depend on different parameters such as buildings spatially distribution, seismic source, structural design parameters, similarities in site effect and etc. For example, for the built environment in which the entities are close proximity to each other will experience similar earthquake excitation due to shared site conditions and distance

between sites (Baker and Cornell 2006; Thompson et al. 2010). Neglecting this correlation in ground motion intensity can lead to underestimate large rare losses and to overestimate small frequent losses (Jayaram and Baker 2010; Park et al. 2007).

Estimation of the geological, geotechnical and geophysical characteristics of the considered virtual city is beyond the scope of this research. The soil response parameters have been described in terms of PGA at any soil surface sites within the virtual city. The PGA spatial distribution have been assessed by computing the macrozoning information of a moderate seismic hazard site located in Italy and considering an equivalent soil amplification factor based on the shear wave velocity in the upper most 30 m (V_{s30}) map obtained via USGS website (USGS, 2013) at the link http://earthquake.usgs.gov/hazards/apps/vs30/. A moderate Italian seismic hazard site (Soveria Mannelli, Lat: 39.0833, Long: 16.3667) have been assumed as representative of the seismic hazard of the virtual city.

Macro-zoning data, in terms of PGA have been collected with reference to three Hazard Levels (HLs) which is representative of the seismic intensity that may occurs in the reference site (http://esse1-gis.mi.ingv.it/). The selected HLs are associated to different performance levels which are Damage Control (DC), Life Safety (LS), and Collapse Prevention (CP). HLs are quantitative defined through the probability that the considered hazard parameter is exceeded in a certain time interval. Table 3 lists the macro-zoning values of PGA at the reference site for each HL which is expressed through its exceedance probability in 50 years according to NTC08 (2008) for a rigid soil.

Table 3. Performance levels and associated PGA values.

Performance Level	DC	LS	CP
Hazard Level	63%	10%	5%
PGA [g]	0.13	0.32	0.40

Seismogenic characteristics of the considered site have been also assessed according to the de-aggregation study of the site (available at the link: http://esse1-gis.mi.ingv.it/). De-aggregation study provides the maximum and minimum values of magnitude and source-to-site distance representative of the seismic site hazard. Table 4 lists the moment magnitude and source-to-site distance assumed for each HL based on the de-aggregation study of the reference site.

Table 4. De-aggregation values in terms of magnitude-epicenter distance parameters.

Hazard Level	63%	10%	5%
Moment magnitude M_w [-]	4.0 – 6.0	4.5 - 7.0	5.0 - 7.5
Epicenter distance R_{epi} [km]	0 - 40	0 - 30	0 - 30

A set of seven real ground motions in both horizontal directions for each HL have been selected and assumed as representative of the seismic input. A seismic energy-based GMSM has been used to select the set of motions to be used in the nonlinear dynamic analyses (Marasco and Cimellaro 2018). The GMSM procedure emerges from comparing a set of horizontal ground motions at various ranges of frequency with the target frequency content. The selected records are compatible with the seismic site in terms of the spectral acceleration at the period of reference and seismgenic parameters.

Numerical results showed that the selected group of ground motion records causes an identical elastic seismic action and approximately equal plastic dissipation on the structure. This in turn leads to significantly affect the structural response estimation and the structural damage prediction. The adopted GMSM approach is able to reduce the scatter of the structural response parameters around the corresponding mean values and enhance the accuracy in preserving the median demand. In addition, the comparisons with other methods showed the accuracy of the estimated median EDPs for every hazard scenario.

Given the three HLs, the associated horizontal design spectra for each soil category (NTC09 2008) have been defined and assumed as target spectra. The software OPENSIGNAL (Cimellaro and Marasco 2015) have been used to obtain the design spectra by considering the reference site of Soveria Mannelli (Lat: 39.0833 , Long: 16.3667). PGA has been assumed as IM parameter, while the period range 0-0.8 s has been considered for spectrum compatibility process.

The selection procedure has been also based on the research of records characterized by seismogenic parameters compatible with the de-aggregation values (Table 4). The selection of the records representative of the seismic scenario within the virtual city has been performed through OPENSIGNAL (Cimellaro and Marasco 2015). Table 5 to Table 7 presents the main characteristics of the selected record for each HL.

Table 5. Selected records representative of the hazard level with exceedance probability of 63 % in 50 years.

63 % in 50 years				
Record ID	**Description**	**Event date**	**M_w**	**R_{epi} [km]**
1	Northern California	1975/08/01	5.2	10.4
2	Imperial Valley (aftershok)	1979/08/06	5.0	12.6
3	Anza, Horse Canyon	1980/02/25	5.2	12.7
4	Mammoth Lakes (aftershok)	1980/05/25	4.8	11.6
5	Coalinga (aftershock)	1983/05/02	5.1	13.1
6	Northridge (aftershok)	1994/01/17	5.1	21.5
7	Anza	2001/10/30	4.9	24.7

Table 6. Selected records representative of the hazard level with exceedance probability of 10 % in 50 years.

10 % in 50 years				
Record ID	**Description**	**Event date**	**M_w**	**R_{epi} [km]**
1	Mammoth Lakes	1980/05/25	6.1	10.9
2	Coalinga	1983/05/02	6.2	10.0
3	Whittier Narrows	1978/10/01	6.0	15.3
4	Biga	1983/07/05	6.1	17.7
5	Umbria Marche	1997/09/26	6.0	27.0
6	Northwest China	1997/01/21	6.1	19.1
7	Taiwan (aftershock)	1999/09/21	6.2	10.1

Table 7. Selected records representative of the hazard level with exceedance probability of 5 % in 50 years.

5 % in 50 years				
Record ID	**Description**	**Event date**	**M_w**	**R_{epi} [km]**
1	Parkfield	1966/06/28	6.2	32.6
2	Imperial Valley	1979/08/06	6.5	27.6
3	Mammoth Lakes	1980/05/25	5.9	18.5
4	Coalinga	1983/05/02	6.2	16.2
5	Chalfant Valley	1986/07/21	6.2	14.3
6	Loma Prieta	1989/10/17	6.9	27.2
7	Norcia	2016/10/30	6.5	5.4

4.2 Fragility curves

The type and extent of damage that a structural component may experiences is uncertain. ATC21 (2017) observed that the nonlinear building response, defined through an EDP, at a given earthquake scenario is lognormally distributed and the best approximation of the building's dynamic response is the median of the lognormal distribution (θ). The median parameter is substantially equal to the geometric mean of the building' response which is represented by the selected EDP (Equation (12))

$$\theta = \exp\left[\frac{\sum_{i=1}^{n}\ln(EDP_i)}{n}\right] \tag{12}$$

The building' response parameters are considered as random variables and n represents the total number of the random samples EDP_i. These observations are valid for a given seismic scenario which is identified through a specific Intensity Measure (IM) parameter. According to FEMA P-58 (2012) provisions, the measure of dispersion of the building's response (β) at a given earthquake

43

scenario, is represented by the standard deviation of the lognormal distribution (Equation (13))

$$\beta = \sqrt{\left[\frac{\sum_{i=1}^{n}\left(\ln(EDP_i / \theta)\right)^2}{n-1}\right]^2} \qquad (13)$$

Assuming different seismic scenario described through a set of IMs, the fragility functions associated with the buildings may be derived. Fragility function is defined as a probabilistic relationship between the frequency of exceeding a certain damage level and the measure of the earthquake excitation. It is worth mentioning that the damage level is described through the chosen EDP, whereas the selected IM define the earthquake excitation.

Fragility functions are derived based on the statistical analysis of damage recorded in past earthquakes, simulated in analytical or numerical methodologies, expert judgment elicitations, or on a combination of these methodologies (Maio and Tsionis 2015).

Analytical approach defines a direct relationship between the structural response and the damage effects (Rossetto et al. 2013). Numerical models are adopted to predict the structural response allowing taking into account detailed mechanical and geometrical characteristics. Empirical approaches are based on the statistical analysis of the post-earthquake damage observation data which are interdependent with the macroseismic intensity. Expert judgments are required in assessing the seismic vulnerability of buildings in case the available data are poor. Hybrid approaches combine post-earthquake damage statistics with analytical methodologies. These approaches may be useful to estimate the building stock vulnerability of a large scale environment in case the collected damage data is not adequate and the use of simulation requires a high computational effort. Then, a combination of analytical simulations, post-earthquake surveys, and expert judgments may result an efficient approach. Kappos et al. (1998) generated fragility functions of the typical Greek building stock through a combination of statistical and nonlinear dynamic analyses for all the existing RC building typologies.

An analytical approach has been adopted to assess the fragility functions of the buildings located within the virtual city. The derived fragility functions are associated with the four considered DSs which are: slight, moderate, extensive, and complete. Inter-story drift has been assumed as EDP while the associated thresholds have been considered according to Ghobarah (2004).

The dynamic response of the buildings has been obtained through direct integration time history analysis in SAP2000. The seismic scenario has been defined through a set of motions selected and modified to be representative of the site seismic intensity, according the "*approach 2*" explained in section 3.2. The outputs have been automatically saved in terms of maximum absolute top displacement of each multi-linear plastic element that simulates the building. The results have been arranged into tabular file by specifying the file name and the

format. The top displacement of each element have been derived and used for defining the related maximum inter-story drift according to the proposed seismic response model. Finally, the fragility curves have been derived and the median θ and dispersion β parameters identifying all the four considered DSs have been assessed.

A database containing all the median and dispersion parameters associated with the slight, moderate, extensive, and complete DS has been created for both horizontal directions of the buildings within the virtual city. The median PGA of each DS is a parameter representative of the seismic vulnerability of a given building as the IM.

The 2D visualization of the median PGA values associated with the slight DS, Median DS, Extensive DS, and Complete DS are presented in Figure 22, Figure 23, Figure 24, and Figure 25, respectively. The results show that the downtown of the virtual city (*C3*) that is mostly composed of old masonry buildings is the most vulnerable zone. The spatial distribution of the building archetypes (Figure 26) and year of construction (Figure 27) confirm that the vulnerability distribution is higher in the zones where the old buildings are located since they were not designed according to high seismic design requirements. In addition, the masonry buildings represent the most vulnerable part of the building stock of the virtual city. In the virtual city, masonry buildings were mostly designed according to old design codes where either there was no seismic design procedure or less seismic design requirements. The result confirms that the main share of damaged to the city belongs to masonry buildings rather than concrete structures.
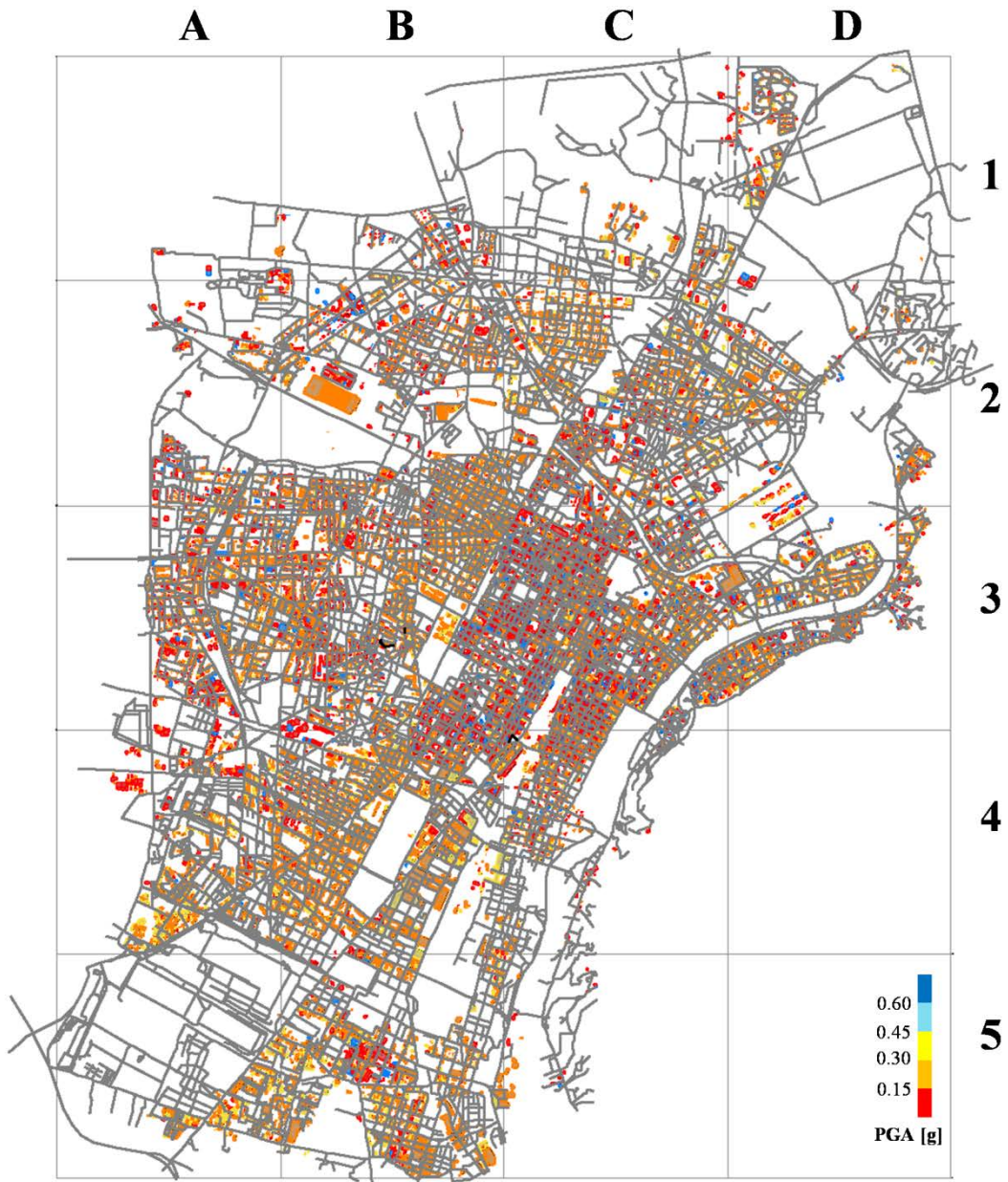
Figure 22. 2D visualization of the median PGA associated with Slight Damage State.
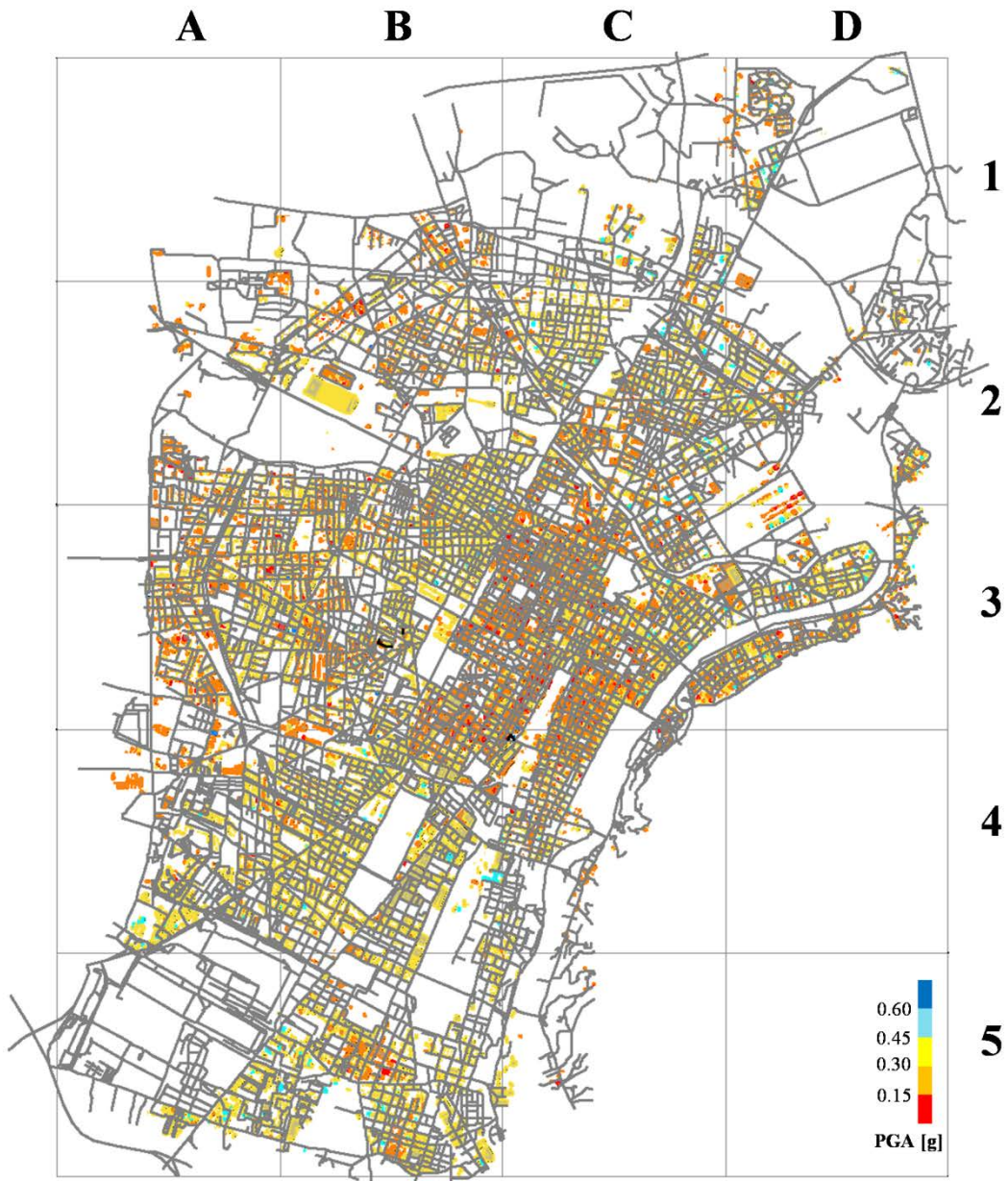
Figure 23. 2D visualization of the median PGA associated with Moderate Damage State.
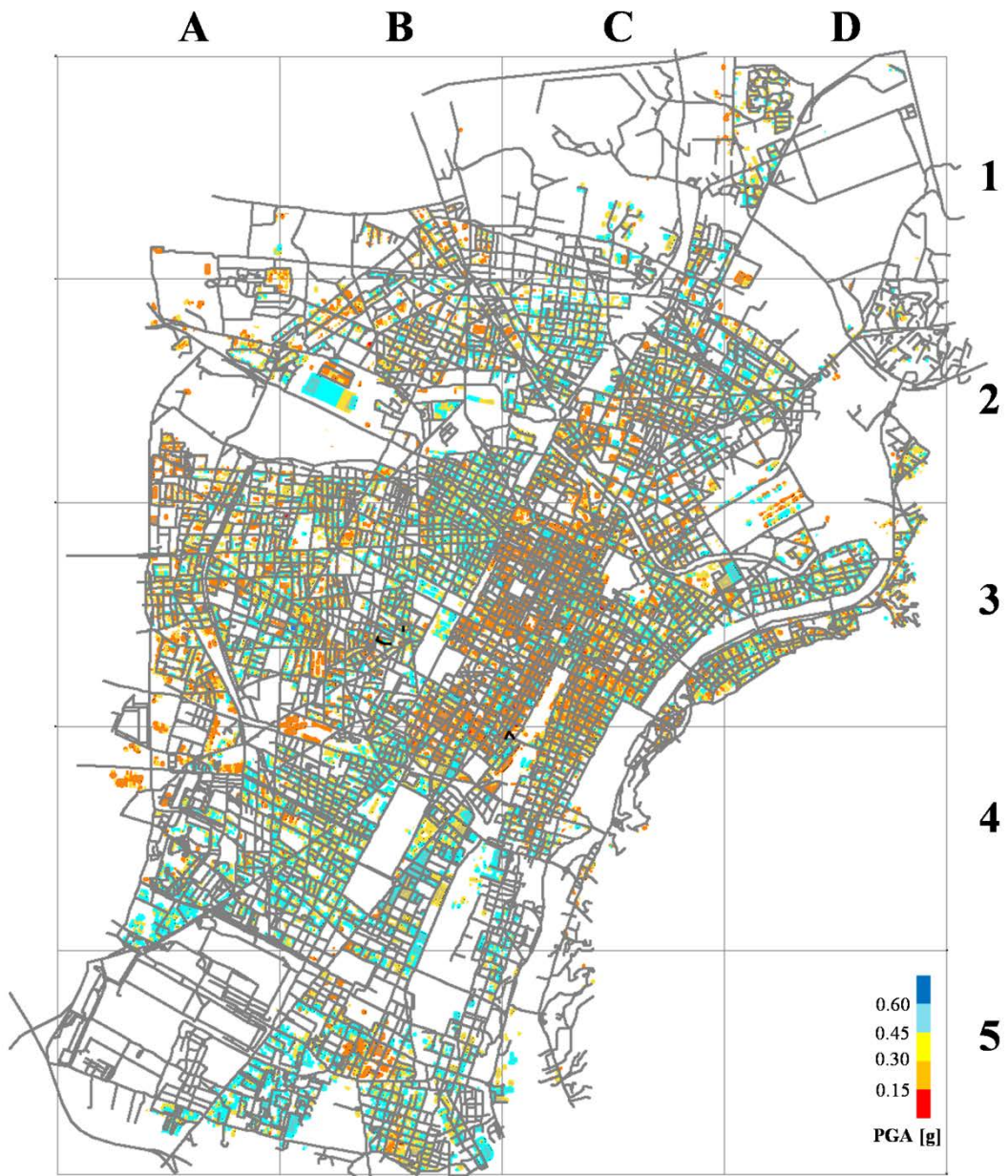
Figure 24. 2D visualization of the median PGA associated with Extensive Damage State.
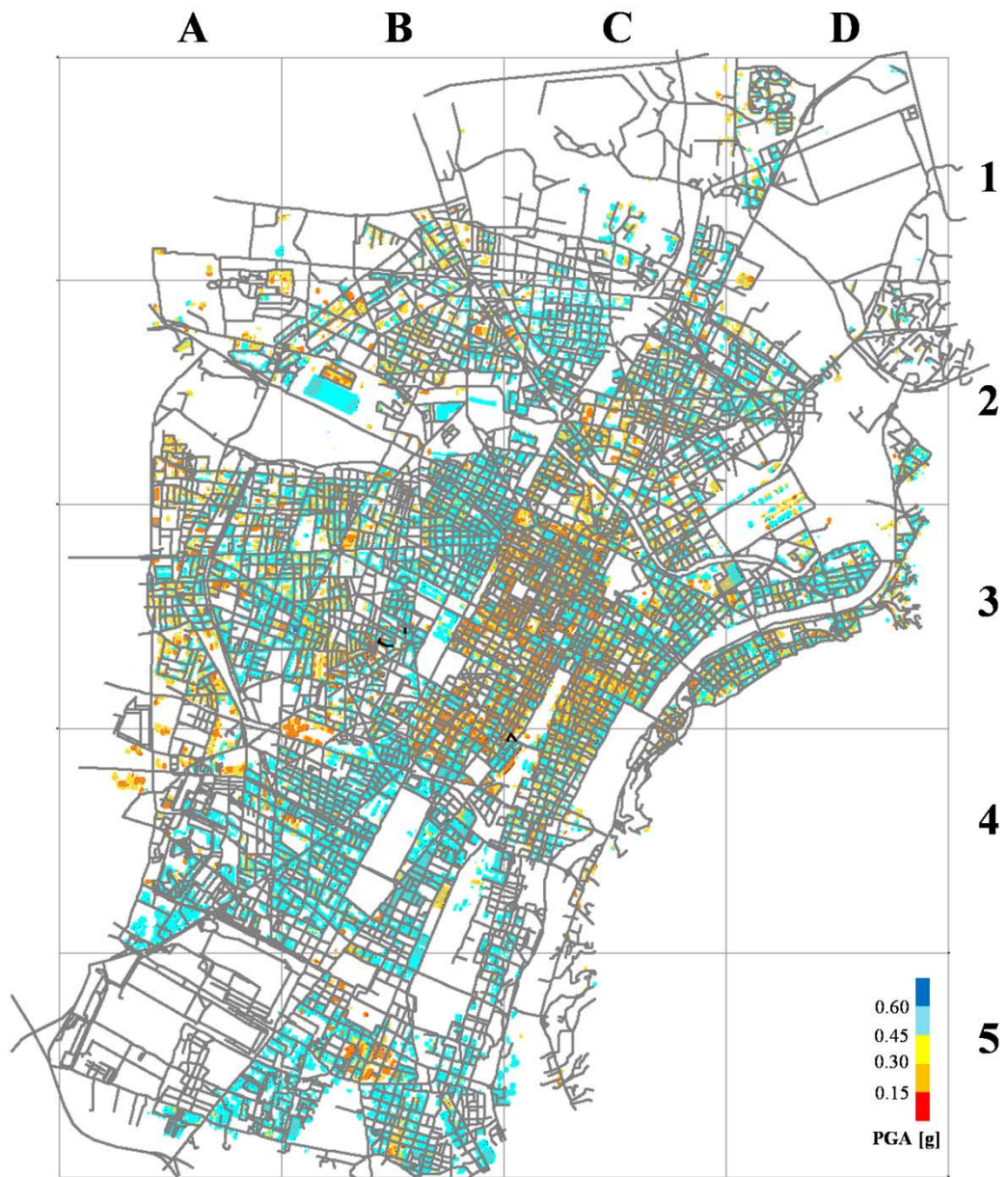
Figure 25. 2D visualization of the median PGA associated with Complete Damage State.
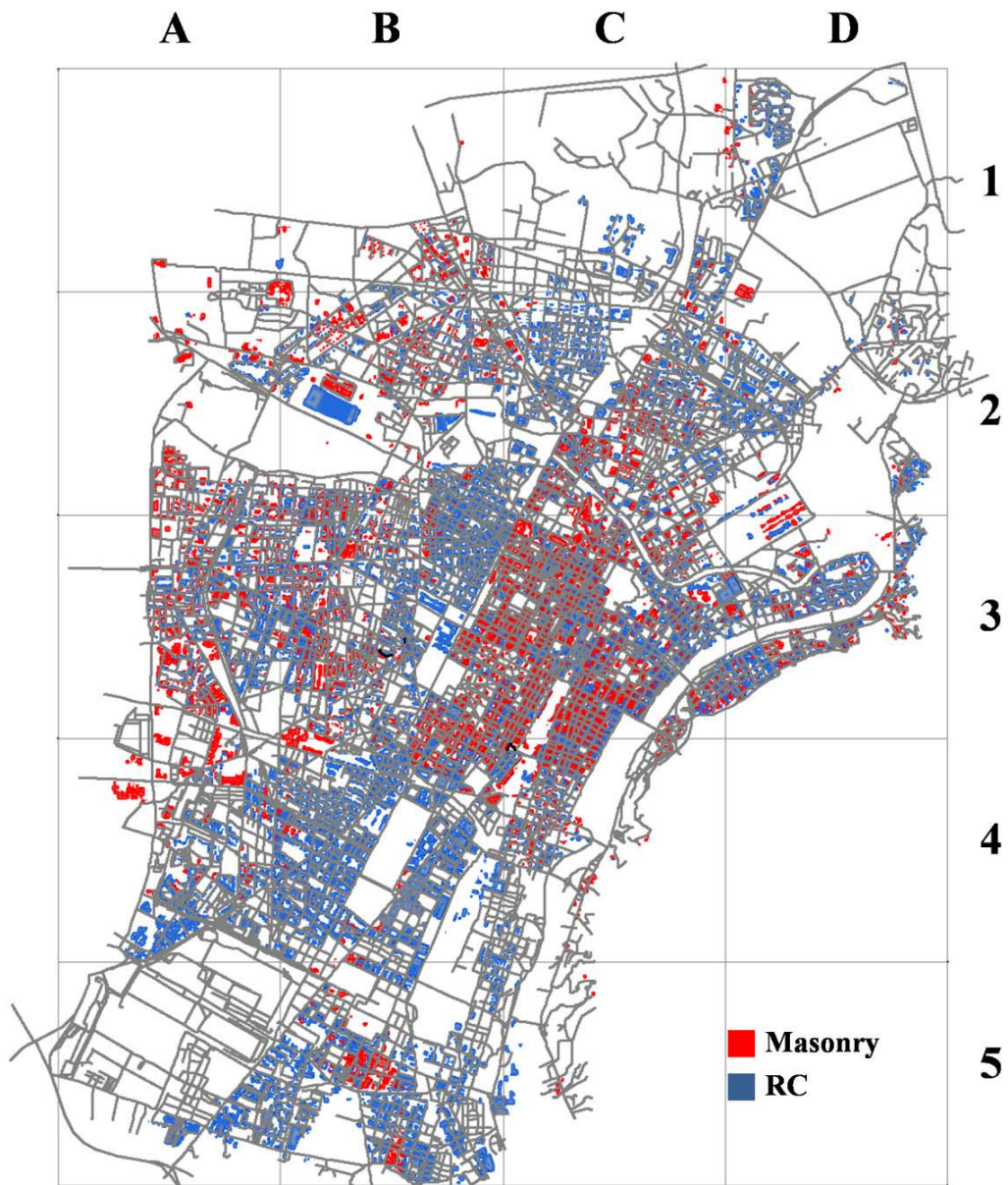
Figure 26. Spatial distribution of building archetype.
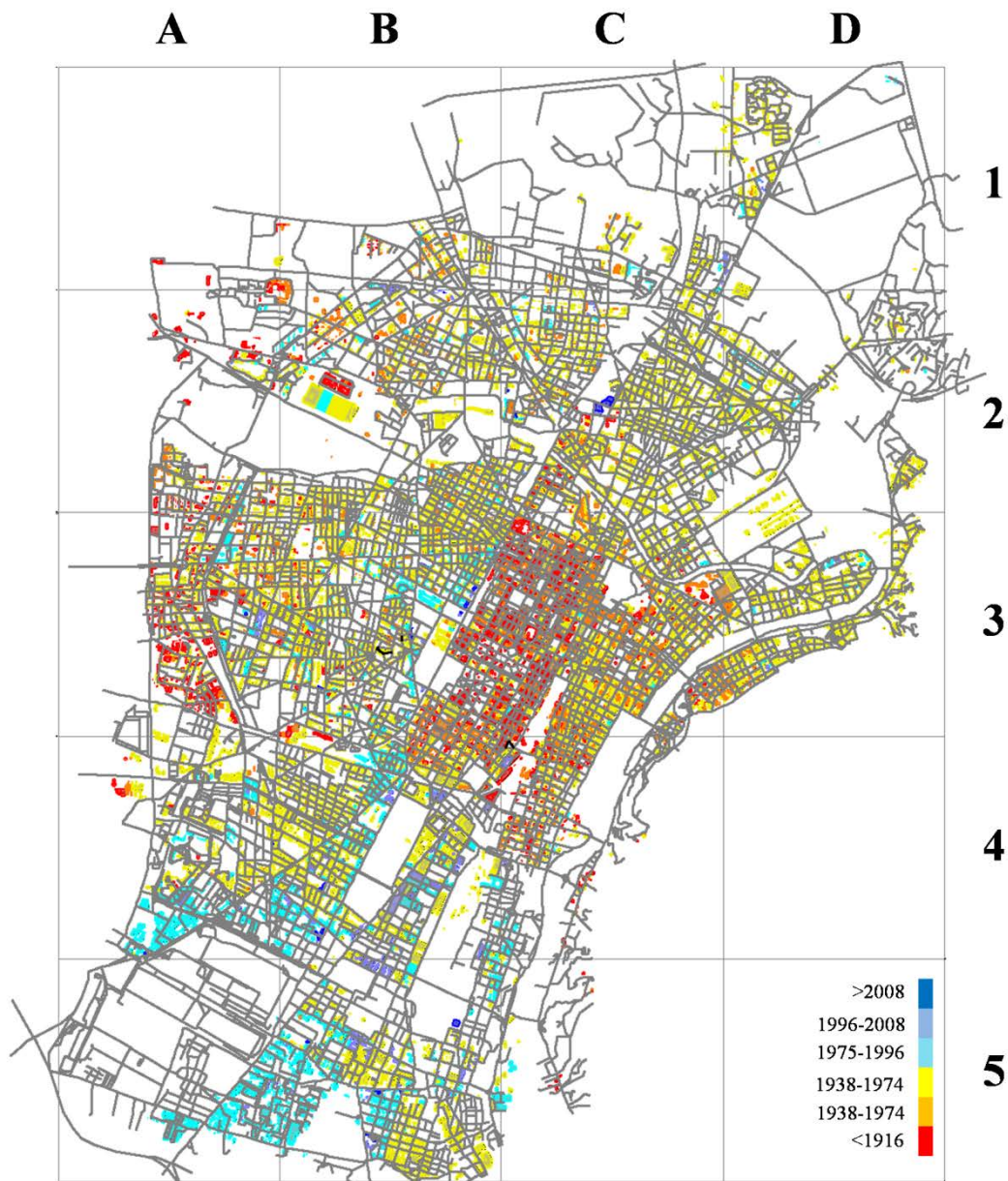
Figure 27. Spatial distribution of buildings based on year of construction.

The percentage of the buildings associated with the four Damage states has been calculated and normalized with respect to the total number of buildings built in the same construction period. Figure 28 shows the percentage of damaged building per year of construction based on the related DS. The percentage of buildings with complete DS is inversely proportional to the age of buildings. In other words, older buildings experienced a greater irreversible damage, whereas slight and moderate DSs are predominant for new buildings. In detail, 20 % of buildings built before 1916 have experienced complete DS and about 72 % are extensively damaged. The percentage of building with slight DS is increasing up to 22% for building built after 2008. For the same year of construction, the percentage of buildings with moderate damage reaches the value of 40 %. Thus, reversible damage is mostly observed for new buildings. This trend is consistent

51

with the newest seismic design procedures which aim to enhance the structural performance under seismic loads.
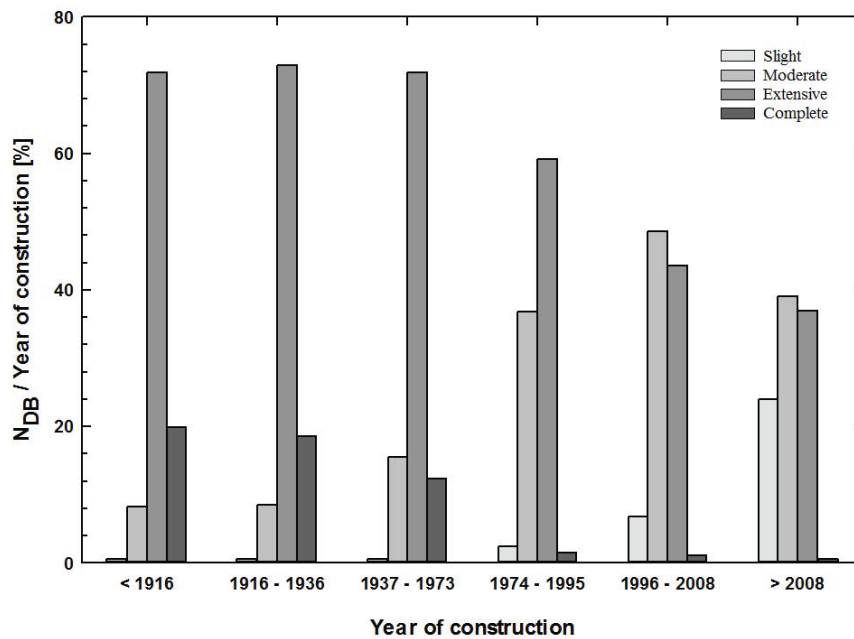
Figure 28. Percentage of buildings associated with the four DSs normalized with respect to the number of buildings built in the same period of construction.

4.3 Model validation

To validate the results in term of fragility curves, the proposed methodology in Chapter 3 has been applied to assess the response of two individual buildings described in Section 3.3. Thus, the results have been compared with fragility curves obtained from the FEM model performing nonlinear time history analyses. A set of ground motions on a rigid rock site has been selected according to the procedure describe in section 4.1. To assess the damage, direct integration dynamic nonlinear analyses have been performed in SAP2000 and the PGA has been assumed as Intensity Measure (IM). According to Ghobarah (2004), the fragility curves associated with the four DSs (Slight, Moderate, Extensive, and Complete) have been derived and compared with those ones obtained through the simulation model presented in Chapter 3. Fragility curves associated to moderate and complete Damage States for the first and second case study buildings are shown in Figure 29 and Figure 30, respectively. The confidence limits have been added both for the fragility curves obtained through the FEM analyses and proposed physical model.
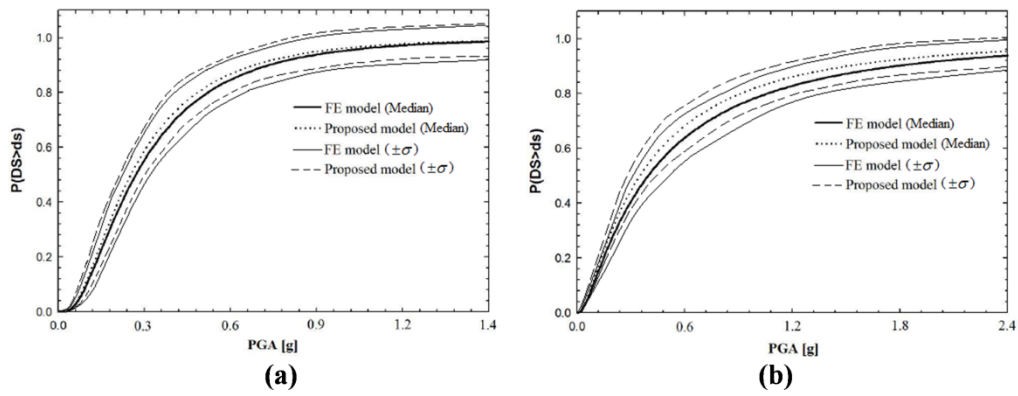
Figure 29. Comparison between fragility curves; moderate (a) and complete (b) DSs for the first case study.
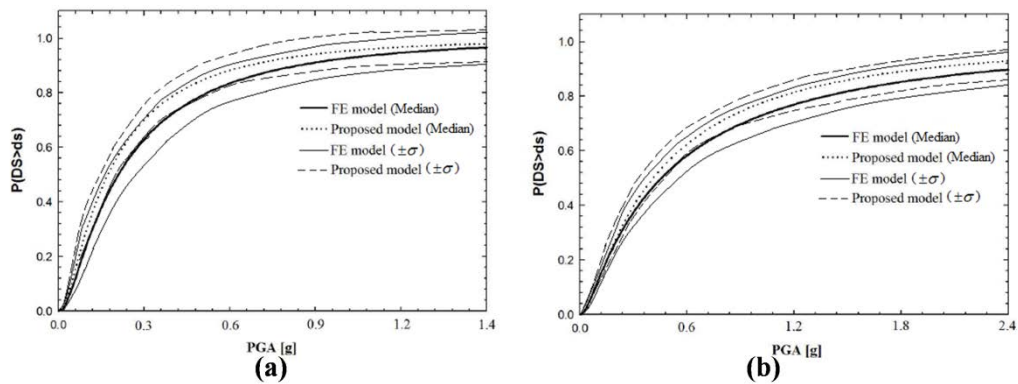
Figure 30. Comparison between fragility curves; moderate (a) and complete (b) DSs for the second case study.

Results shows that the proposed model provides comparable results in terms of fragility function with respect to the FEM model. Fragility functions associated with moderate DS are similar in terms of median demand and dispersion for both case study buildings. Besides, considering the complete DS, the median values among the PGAs obtained through the simulation model described in Chapter 3, are lower than those ones estimated through FEM analyses. Therefore, the simulation model results some extent more conservative for higher damage level.

4.4 Direct social loss: casualties

In this section a methodology to estimate casualties as direct economic loss is described based on the model provided by HAZUS (NIBS 2012). The number and severity of casualties have a strong correlation to the buildings level of damage. As an assumption, only the casualties caused by the structural damage is considered in this study, and the influence of nonstructural damage has been neglected since nonstructural damage will most likely control the injured in smaller earthquakes.

The casualties are classified to four severity levels as:

- *Severity 1* refers to minor injuries, meaning that patients need basic medical care that could be administered by nurses or paraprofessionals. This kind of patients could be associated with white or green triage codes;
- *Severity 2* represents serious injuries that require a greater degree of medical care. These patients are not in an immediate life threatening situation but they present a partial impairment of vital functions, hence they are coupled with yellow triage codes;
- Severity 3 is related to the patients with a severe injury level which means compromised vital functions. They need an immediate medical care so they are associated with yellow or red triage codes;
- Severity 4 refers to critical injury level. These patients are mortally injured or their lives are at risk so they may be associated with red triage codes.

The selection of the four severity division represents an achievable compromise between the demands of the medical infrastructure and the capability of the engineering in community to provide the required data (NIBS 2012).

4.4.1 Scenario time definition

Depending on when the earthquake happens, the number of injured and the severity of the injuries, can vary considerably. For example, during the night, most people are at home in residential buildings, whereas in the day-time, people are mostly at work or school in buildings with different structural characteristics. Instead, if the earthquake occurs during the day, the older buildings, which are mostly in the business areas located in downtown of the considered virtual city, will be responsible for the largest share of casualties. Similarly, if it occurs at night, the residential buildings will cause the most casualties and it will lead different patient distribution among the city. Since the buildings density, their archeology, and their occupancy vary by neighborhood in the considered virtual city, thus the time occurrence of the earthquake might affect considerably the number of injured and its distribution across the city. HAZUS (NIBS 2012) proposes three different time scenarios to estimate casualties:

- Scenario 1: Earthquake strikes at 2:00 a.m. (night time scenario);
- Scenario 2: Earthquake strikes at 14:00 p.m. (day time scenario);
- Scenario 3: Earthquake strikes at 17:00 p.m. (commute time scenario).

Scenario 1 expects to cause highest casualties for the population at home while scenario 2 generates most possible casualties for the population at work or schools. The third scenario aims to generate highest casualties during rush hour which also correlates the level of damage occurred in transportation system.

Furthermore, according to the time scenario the population distribution varies for each building stock. For example, for the time scenario 1 at time 2pm, the most percentage of population is distributed at educational, commercial, industrial

census tracts. According to HAZUS (NIBS 2012), for the time scenario 1 at 2am, the percentage of population staying at homes is 99%.

In study, casualties are estimated based on first time scenario (earthquake strikes virtual city at 2am). Population of city 908,000 is considered for virtual city, and then 99% of population is distributed within residential buildings. The population distribution map provided by Municipality of Turin has been implemented in order to distribute the population in each neighborhood (Figure 31). Accordingly, the number of habitants for each single building (considering the plan area and number of stories for each building) is calculated for further analysis.
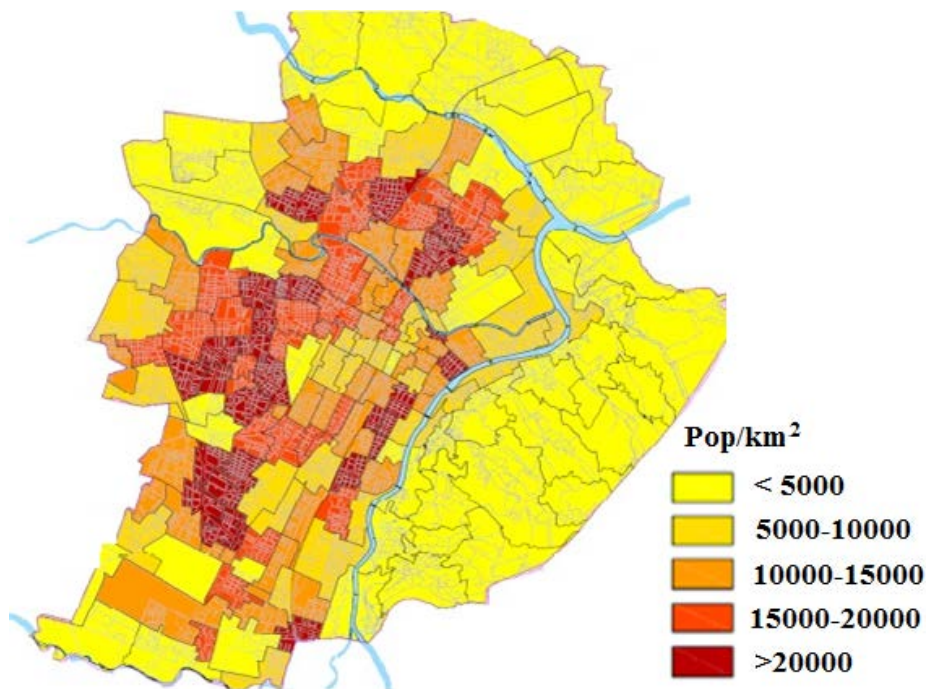
Figure 31. Population distribution map according to Municipality of Turin.

4.4.2 Description of methodology

The casualty model is based on building damage state (slight, moderate, extensive, and complete) computed by the direct physical damage described in Section 3.3. Casualties caused by an earthquake event can be modeled by a tree of events leading to their occurrence. For each building, the probability of the structure being in a certain level of damage is calculated (section 3.3) and it is assigned to each branch of tree. HAZUS (NIBS 2012) proposed structural casualty rates for model building type (concrete or masonry) for each damage state is implemented. The casualty rates caused from structural damage for both concrete and masonry buildings are presented in Table 8 and Table 9, respectively.

Table 8 and Table 9 imply that casualty rates at slight damage state for both concrete and masonry construction type is the same. This is due this fact that at low level of structural damage casualties most caused by non-structural components rather than structural elements. While, at high level of damage

(moderate or extensive), the casualties are caused from the falling of pieces of unreinforced masonry elements. Thus, the masonry buildings have more casualty rates in higher damage state with respect to concrete buildings.

Table 8. Casualty rates for concrete buildings for different structural damage.

Severity	Slight R_S	Moderate R_M	Extensive R_E	Complete (no collapse) R_{NC}	Complete (collapsed) R_C
Severity 1	0.05	0.25	1	5	40
Severity 2	0	0.03	0.1	1	20
Severity 3	0	0	0.001	0.01	5
Severity 4	0	0	0.001	0.01	10

Table 9. Casualty rates for masonry buildings for different structural damage.

Severity	Slight R_S	Moderate R_M	Extensive R_E	Complete (no collapse) R_{NC}	Complete (collapsed) R_C
Severity 1	0.05	0.35	2	10	40
Severity 2	0	0.04	0.2	2	20
Severity 3	0	0.001	0.002	0.02	5
Severity 4	0	0.001	0.002	0.02	10

Figure 32 shows an event tree to calculate the number of casualties after an earthquake scenario. The probability of the structure being in a certain level of damage (P_s, P_M, P_{CNC}, and P_{CC}) state is assigned in each branch corresponding to the "Damage states" component. The casualty rate associated for each severity level is defined at each branch of the component "Casualties" (R_1, R_2, R_3, and R_4).
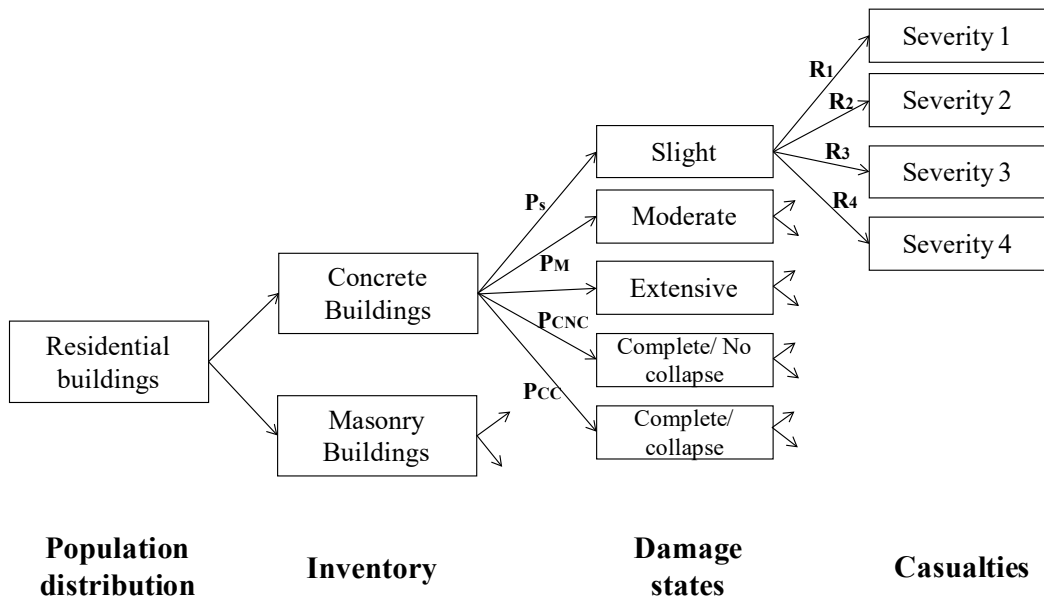
Figure 32. Event tree simulation model to estimate casualties.

According to Figure 32, for example the probability of a person being in severity level 3 in a given earthquake scenario can be calculated by:

$$P_{(Severity,3)} = \begin{cases} p(DM_S \mid EDP) \times R_{severity\,3/S} \\ \quad + \\ p(DM_M \mid EDP) \times R_{severity\,3/M} \\ \quad + \\ p(DM_E \mid EDP) \times R_{severity\,3/E} \\ \quad + \\ p(DM_{NC} \mid EDP) \times R_{severity\,3/NC} \\ \quad + \\ p(DM_C \mid EDP) \times R_{severity\,3/C} \end{cases} \tag{14}$$

where the terms $p(DM \mid EDP)$ refers to probabilities of a building being in a certain damage state (slight, moderate, extensive, not collapse, and collapse), and $R_{severity\,3}$ is the casualties rate for severity 3 associated with building type for each damage state.

According to HAZUS (NIBS 2012), probability of a building collapses given a complete damage state is considered equal to 10% for concrete buildings and 15% for masonry buildings, respectively. At the end, the expected number of injured in each severity level is a product of number of occupants in each building at the time of earthquake and the probability of a occupant being in a severity level.

The same methodology has been used to compute the number of injured for the virtual city under Norcia earthquake scenario. The casualty rates for each single building corresponding to the building damage state have been calculated. Figure 33 shows the total number of injured for each severity level for the virtual city. It confirms that the number of casualty in each severity level is proportional to the percentage of damaged buildings at each damage state. The major of casualty rates is related to severity 1. This is due to this fact that the most buildings experienced slight damage state (see Figure 19).

Figure 34 shows the casualty distribution based on the building archetype for each severity level. It shows that about 260 people will have critical injury level after the earthquake event. This is mostly caused by damaged building associated with complete damage state. In addition, results show that the expected number of casualties inside masonry buildings is about four times more than the one referred to concrete buildings. This is mainly due to two issues: firstly, masonry buildings were more vulnerable than concrete buildings since they were designed according to old design codes. Masonry buildings within the virtual city falls in the first and second categories of building year of construction (see Table 2), where design codes did not require to seismically design buildings or they had law seismic design requirements. Secondly, the casualty parameters defined for masonry

building in Table 9 are mostly higher (about twice) than the one referred to concrete buildings (Table 8).
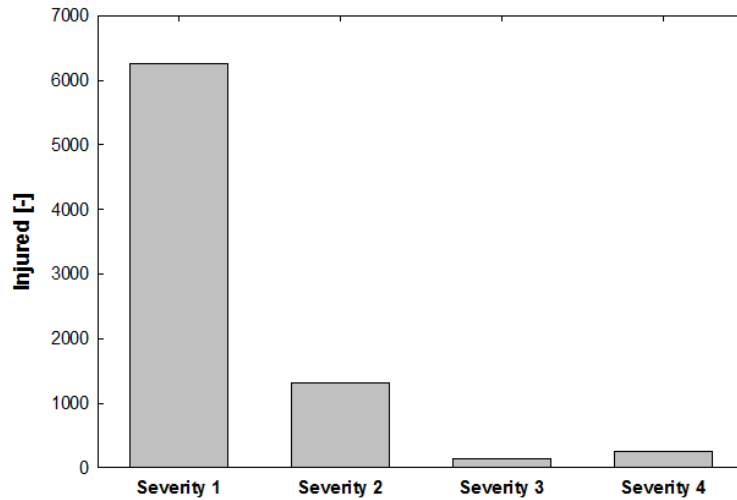
Figure 33. Total number of casualties corresponding to each severity level.
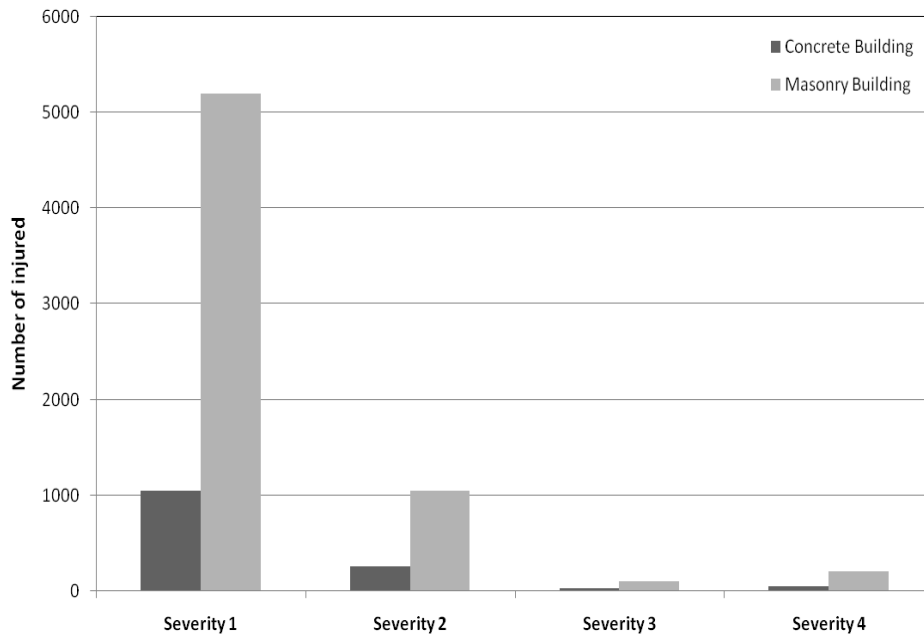
Figure 34. Casualty distribution based on the buildings archetype for different severity levels.

This chapter presented a simulation model to assess the seismic vulnerability of building stock. Fragility curves for each single building considering the buildings spatial distribution are developed and the level of damage for each building is evaluated. The methodology was applied to virtual city and social loss in term of casualty was estimated. The number of injured and their corresponding severities is used in Chapter 5 to evaluate the resilience of hospitals network of the virtual city.

Chapter 5

Resilience assessment of a hospital network

Healthcare facilities are recognized as critical infrastructure that must be able to supply essential health services to a community right after a disaster. In this chapter, a simplified methodology is presented in order to evaluate the performance of a hospital network after a strong earthquake. In particular, the performance of hospital network of the virtual city is analyzed after Norcia earthquake. The number of injured and their severity are estimated according to methodology provided in Chapter 4. The minimum targets indispensable to ensure adequate health care services during and after the earthquake is compared with the effective response of each hospital. The functionality of hospital network to coordinate the emergencies and to provide services to injured is evaluated using the waiting time (WT) spent by patients in the waiting room before receiving care.

An Overcrowded Emergency Department may lead delays in care and escalating the injured condition. Thus, the WT is selected as the main criterion to check how the hospital network responds to the earthquake. In addition, two different methodologies have been adopted to guarantee that hospital network can provide emergency care to all patients within the acceptable WT.

5.1 Existing methodologies

To respond adequately to an emergency situation, the hospital network should be remaining first safe and functional by having contingency plans. Recent earthquake events have shown that how moderate damages can become catastrophes if the communities are not prepared well to withstand and absorb the shock after an event (Arcidiacono, 2012).

Immediately after an earthquake a healthcare system within a city, comprising several hospitals, endures an extraordinary demand. When the earthquake occurs, the city will suffer from severe consequences. Even if it is almost impossible to

predict the exact location and time of earthquake occurrence, it is not equally impossible to predict its effects on the city and act consequently to make the city more resilient in the face of this disaster. In this sense hospitals play a critical role providing essential medical care during any type of disaster (Cimellaro et al 2010). Any event that causes casualties and injuries (e.g. earthquake) requires a solid hospital network for a rapid and effective response. In fact, the level of preparedness for an extreme event is critical for saving lives and reducing post-disaster consequences. Thus, hospital network should be able to immediately process the situation, to coordinate the emergencies, and manage resources right after a hazardous even (Downey et al 2013).

Some particular systems, such as a hospital emergency department, are designed to adapt to highly variable and uncertain inputs. The Emergency Departments should be able to provide acute ambulatory and inpatient care during 24 hours period (Morganti et al., 2013). Analyzing how these systems are able to cope with potentially changing demands and studying how they adapt to an emergency scenario can reveal a great deal about how to design resilient organizations (Anders et al 2006).

Lupoi et al. (2013) proposed a probabilistic framework to assess the effect of a seismic event on a healthcare system at the regional scale. In this study, the short-term period has been considered as a reference time and the estimation of an earthquake impact has been provided in terms of the number of un-hospitalized victims, hospitals functionality, demand of medical care, and hospitalization travel time. Furthermore, a single hospital has been described as a coupled system made of physical, human, and organizational dimensions.

The operating conditions of healthcare facilities after a natural disaster have been explored by Achour et al. (2014). A pluralistic qualitative and quantitative research approach has been used to measure the impact of healthcare supplies interruption during an emergency. A discriminant function analysis has been performed using the information collected from 66 different hospitals after three major seismic events occurred in Japan in 2003.

The performance of the Canterbury hospital system to the 2011 Christchurch Earthquake has been analyzed by Jacques et al. (2014) using a holistic approach. The functionality of healthcare services has been evaluated through a fault-tree analysis considering the hospital's staff, structure, and stuff as main factors. Estimation of the functional curve at the regional level has shown that the services' redundancy has increased the resilience of Christchurch Hospital of 12%.

In order to assess the seismic vulnerability of a hospital system, an integrated methodology has been proposed based on the theory of complex system analysis through input–output inoperability model of Leontief and rapid seismic vulnerability assessment (Miniati et al. 2012). The Leontief model allows defining the input failure vector, which describes the impact of an earthquake on the different elements of the hospital, causing their inoperability. The initial levels of inoperability are evaluated through a rapid seismic vulnerability approach which is based on the World Health Organization (WHO) evaluation forms. The

approach proposed by Miniati et al. (2012) has been applied to a system of five hospitals located near Florence, in central Italy and subjected to an Mw=6 earthquake scenario.

After a disaster, hospitals have to provide emergency services to injured in a setting of restricted resources through an accurate and effective collaboration with other healthcare facilities. The capacity of a healthcare system to coordinate the rescue and deliver emergency services after a disaster has been studied in several works (Zhong et al. 2014). Based on the 2008 Sichuan Earthquake, Zhou et al. (2014) studied how to build a valid communication system to ensure an effective flow of health information during major crises. According to Garshnek and Burkle (1999), sharing knowledge and experience during and after disasters is extremely important to develop a more effective emergency communication system. Furthermore, there is a strong need to integrate risk analysis with public health management at both the methodological and theoretical levels (Löfstedt et al. 2008).

5.2 Description of the methodology

During an emergency situation, the number of patients increases significantly with respect to the normal condition. It is essential that the entire network of hospitals will be able to respond to all the demands. A methodology for hospitals performance measurement has been provided to assess the response of a hospital network during a seismic event. An earthquake scenario has to be selected in order to analyze the consequences on the emergency framework of the considered city. First, the number of injured has been estimated taking into account the amount of damage that each building can experience after the earthquake scenario. In order to evaluate the number of injured, the methodology described in Chapter 3 has been applied and the number of injured people for each building then has been estimated. The number of patients in each Emergency Department of the hospital's framework has been evaluated assuming that patients during emergencies are directed to the closest hospital.

The estimation of an Emergency Department response is a complex procedure. The Emergency Plan, resources, location of the internal spaces, and paths should be considered and a simulation approach has to be used. A numerical simulation requires a long computational time to analyze the simulated scenario and it produces a significant amount of complex output data. Thus, an approximation of the simulation model is a preferable strategy to study the response of the Emergency Department within the healthcare network. The proposed methodology is based on the utilization of meta-models that are capable to assess the functional relationship between system behavior and selected input data parameters.

Meta-model definition consists in a structured approach focusing into the generic problem definition and model generation. The statement of the problem is necessary to identify the input, output, and response parameters to be used in the meta-model development. According to Cimellaro et al. (2010), the patients' WT

is one of the most representative parameters describing the hospital behavior during emergencies, while the time period (t), the seismic arrival rate (α), and the number of functional emergency rooms per color area (m) after earthquake occurrence are considered as input parameters (Cimellaro et al. 2017). After defining the input and output parameters, sensitivity analysis is performed in order to measure how the system output varies with respect to a change in system input parameters under emergency conditions.

The meta-model has been based on numerical simulation data obtained through the Discrete Event Simulation (DES) model applied to the case study of Umberto I Mauriziano Hospital located in Turin, Italy (Cimellaro et al. 2017). The model has been implemented using ProModel software (Price and Harrel 1999). The Patients' arrival rate, the path through the Emergency Department, the location of the rooms in which the patients are treated, the processing time, the resources involved (e.g. doctors, nurses, et.), and the operating conditions have been considered as input parameters in the simulation model. Some assumptions have been set to simplify the problem and to reduce the computational effort.

The hospital's structural and non-structural damage have not been considered as a parameter which can affect the patients' path within the hospital. However, the closure of some emergency rooms considering possible structural damage due to the earthquake has been preliminarily assumed. It consists of changing the values of *m* in the simulation model.

Furthermore, the patients have been divided into different codes from the beginning, without considering the first treatment at the "triage". The DES models have given as output the real time average patients' WT obtained through Monte Carlo simulations for different scenarios grouped according to the seismic input (α) and the number of functional rooms (m). In addition, the patient arrival rate collected in a Californian hospital during 1994 Northridge earthquake (Cimellaro et al. 2015) has been used as the seismic input parameter (Figure 35).
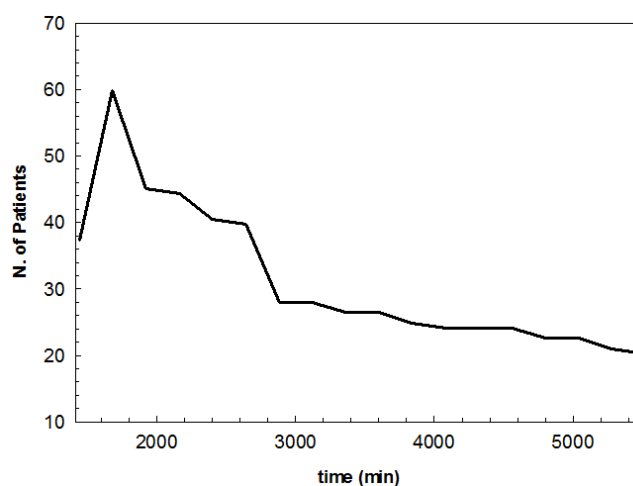
Figure 35. Patients arrival rates for 1994 Northridge earthquake.

According to Yi (2004), the seismic arrival rate has been divided in different patient's code for normal and emergency operating conditions (Table 10). The severity of an injury is represented by four different color codes: white, green,

yellow, and red. White codes include all patients who have not urgent injuries and they can be treated by a general doctor (no urgency). Patients with green codes have not critical situations, so their lives are not at risk, while yellow codes refer to the patients who have partial impairment of vital functions and then they need treatment in the Emergency Department. Finally, the red code refers to the patients with compromised vital functions, whose lives are at risk.

Table 10. Percentage of patients arriving in the Emergency Department in both normal and emergency operating conditions.

Color code	Normal operating conditions [%]	Emergency operating conditions [%]
White	11.47	7.81
Green	71.19	48.48
Yellow	16.78	40.1
Red	0.56	3.7

5.2.1 Scaling patient arrival rate

In order to consider the sensibility of the Emergency Department, the patient arrival rate has to be proportionally amplified using several scaling factors. The scaling procedure is necessary to adapt the available statistical data to the expected seismic intensity of the considered site and then provide a general definition of patients' arrival rate. A scaling procedure based on the Modified Mercalli Intensity (MMI) has been selected because it takes into account some important features such as the population density and the urbanization level which are important indexes for the assessment of seismic effects. Once the expected seismic arrival rate is defined, several increasing levels of seismic intensity have to be considered to cover the different possible scenario in the simulations.

The numerical results obtained in the case study of Umberto I Mauriziano Hospital which has been implemented in Cimellaro et al. (2017) can be used to build a meta-model. The main challenge is to provide a general meta-model which is capable to analyze healthcare facilities' capacity to cope with and respond to a catastrophic event, such as an earthquake. The problem is rather complex, considering that each hospital is substantially different from another and a considerable number of variables are needed to describe the behavior of a healthcare facility. Thus, the number of input variables has to be reduced to provide a general tool which may be applicable to any healthcare facility. Selecting the seismic input and the number of functional rooms as input parameters allows considering a set of representative variables which generally describe the trend of the patients' WT in given operative conditions for any hospital. Then a sensitivity analysis has to be performed to calibrate the meta-model and a specific mathematical form needs to be defined. This assumption is a key point in the definition of the meta-model for the operative conditions of an Emergency Department after a seismic event. Using the data from the

simulations, a lognormal function has been chosen as a representative to assess the patients' WT in the Emergency Department:

$$WT(t,\alpha,m) = \frac{a(\alpha,m)}{t} \cdot \exp\left(-0.5 \cdot \left(\frac{\ln\left(\frac{t}{b(\alpha,m)}\right)}{c(\alpha,m)}\right)^2\right)$$

(15)

where WT and the time range t are expressed in minutes. Parameters $a(\alpha,m)$, $b(\alpha,m)$, and $c(\alpha,m)$ are the nonlinear regression coefficients dependent on α and m values calculated in the considered operating conditions. These parameters have been calibrated based on the simulation results, first considering their dependency from the parameter α and then from the parameter m. It has been observed that a, b, and c coefficients can be expressed as a quadratic function of α, considering *m* as a constant parameter:

$$\begin{cases} a(\alpha) = a_0 + a_1 \cdot \alpha + a_2 \cdot \alpha^2 \\ b(\alpha) = b_0 + b_1 \cdot \alpha + b_2 \cdot \alpha^2 \\ c(\alpha) = c_0 + c_1 \cdot \alpha + c_2 \cdot \alpha^2 \end{cases}$$

(16)

Furthermore, the dependence from the parameter *m* has been studied considering a 4th order model to represent the coefficients a_0, a_1, a_2, b_0, b_1, b_2, c_0, c_1, and c_2:

$$\begin{cases} a_0(m) = a_{00} + a_{10} \cdot m + a_{20} \cdot m^2 + a_{30} \cdot m^3 + a_{40} \cdot m^4 \\ a_1(m) = a_{01} + a_{11} \cdot m + a_{21} \cdot m^2 + a_{31} \cdot m^3 + a_{41} \cdot m^4 \\ a_2(m) = a_{02} + a_{12} \cdot m + a_{22} \cdot m^2 + a_{32} \cdot m^3 + a_{42} \cdot m^4 \end{cases}$$

(17)

$$\begin{cases} b_0(m) = b_{00} + b_{10} \cdot m + b_{20} \cdot m^2 + b_{30} \cdot m^3 + b_{40} \cdot m^4 \\ b_1(m) = b_{01} + b_{11} \cdot m + b_{21} \cdot m^2 + b_{31} \cdot m^3 + b_{41} \cdot m^4 \\ b_2(m) = b_{02} + b_{12} \cdot m + b_{22} \cdot m^2 + b_{32} \cdot m^3 + b_{42} \cdot m^4 \end{cases}$$

(18)

$$\begin{cases} c_0(m) = c_{00} + c_{10} \cdot m + c_{20} \cdot m^2 + c_{30} \cdot m^3 + c_{40} \cdot m^4 \\ c_1(m) = c_{01} + c_{11} \cdot m + c_{21} \cdot m^2 + c_{31} \cdot m^3 + c_{41} \cdot m^4 \\ c_2(m) = c_{02} + c_{12} \cdot m + c_{22} \cdot m^2 + c_{32} \cdot m^3 + c_{42} \cdot m^4 \end{cases}$$

(19)

Therefore, all the parameters in Equations (17), (18), and (19) have been evaluated through nonlinear regression depending on the *m* values. Substituting these values in Equation (16), the three coefficients *a*, *b*, and *c* are obtained. This calibration procedure leads to express the influence of the seismic arrival rate (α) and the number of functional emergency rooms per color area (*m*) in given operating conditions for assessing the patients' WT.

Figure 36 shows the WT curve in emergency conditions, considering two functional emergency rooms *m*=2 for yellow code and a seismic arrival rate obtained using a scale factor α=1.20.

64

Table 11 summarizes the values obtained from the quadratic model based on the simulation results of the ED working when the Emergency Plan is applied.

Therefore, all the parameters in Equations (17), (18), and (19) have been evaluated through nonlinear regression depending on the m values. Substituting these values in Equation (16), the three coefficients a, b, and c are obtained. This calibration procedure leads to express the influence of the seismic arrival rate (α) and the number of functional emergency rooms per color area (m) in given operating conditions for assessing the patients' WT.

Figure 36 shows the WT curve in emergency conditions, considering two functional emergency rooms $m=2$ for yellow code and a seismic arrival rate obtained using a scale factor $\alpha=1.20$.

Table 11. Meta-model coefficients for patients treated with yellow codes in emergency operating conditions.

a_{00}	-894×10^5		b_{00}	285×10^2		c_{00}	5.57
a_{10}	139×10^6		b_{10}	-436×10^2		c_{10}	-9.34
a_{20}	-700×10^5		b_{20}	227×10^2		c_{20}	4.89
a_{30}	147×10^5		b_{30}	-4680		c_{30}	-1.04
a_{40}	-111×10^4		b_{40}	339		c_{40}	0.08
a_{01}	133×10^6		b_{01}	-438×10^2		c_{01}	-7.65
a_{11}	-233×10^6		b_{11}	742×10^2		c_{11}	13.7
a_{21}	124×10^6		b_{21}	-388×10^2		c_{21}	-7.34
a_{31}	-270×10^5		b_{31}	8010		c_{31}	1.58
a_{41}	207×10^4		b_{41}	-578		c_{41}	-0.12
a_{02}	167×10^5		b_{02}	116×10^2		c_{02}	2.79
a_{12}	223×10^5		b_{12}	-187×10^2		c_{12}	-4.78
a_{22}	-226×10^5		b_{22}	9200		c_{22}	2.54
a_{32}	623×10^4		b_{32}	-1810		c_{32}	-0.54
a_{42}	-544×10^3		b_{42}	123		c_{42}	0.04

According to the numerical example, the maximum time that patients with yellow code must wait to see a doctor at an emergency room at a given instant in time in emergency operating conditions is 553.20 min.

The meta-model has been built based on some assumptions. The configuration of the ED does not change during the emergency and the number of emergency rooms and the paths (surrounding conditions) are considered as constant parameters. Furthermore, the number of functional emergency rooms is assumed equal to the number of doctors. Generally, this assumption may be considered reasonable because one emergency room is equipped to provide care to only one patient, so the presence of additional doctors would be ineffective. Another assumption refers to the lognormal form of the output parameters. This

assumption leads to consider the same mathematical output trend for all the analyzed scenarios.
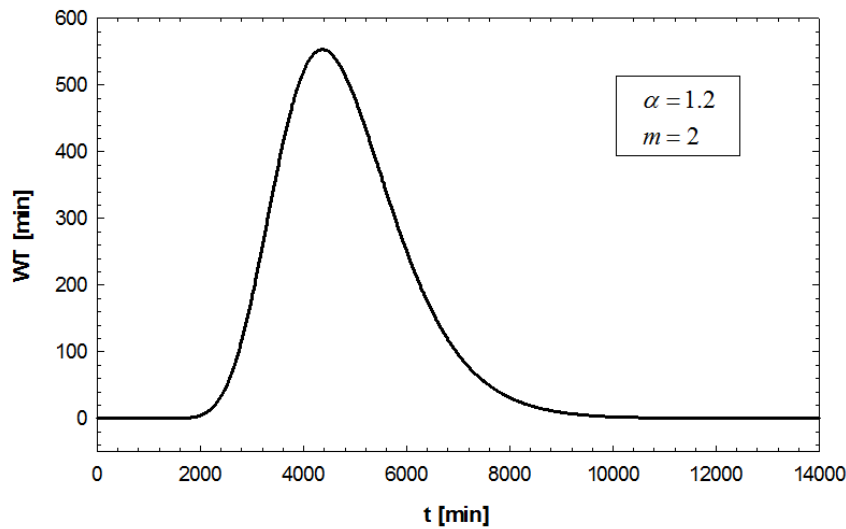
Figure 36. WT in emergency operating conditions for m=2 and α=1.2 for yellow code patients.

The proposed meta-model describes the performance of the ED under emergency using two parameters: the earthquake intensity (α) and the number of emergency rooms (m). The structural damage is taken into account as a penalty factor on this last parameter. The maximum admissible WT has to be estimated and compared with the WT evaluated through the proposed meta-model. For this purpose, interviews with medical staff of several hospitals have been carried out and the maximum acceptable WT, above which the hospital is considered not resilient, has been assessed. The questionnaire has been developed in order to quantitatively assess the disaster resilience capability of a healthcare facility. The survey conducted with Cimellaro et al. (2017) has been used to obtain the maximum WT.

This survey has been conducted by interviewing with emergency staff or by sending the questionnaire by e-mail for 16 Hospitals located in San Francisco. For each hospital the person who is familiar with emergency planning has been selected to fill out the questionnaire (in most cases the emergency department director). The collected information has been categorized into 8 sections: hospital safety, disaster leadership and cooperation, disaster plan, emergency stockpiles and logistics management, emergency staff, emergency critical care capability, emergency training and drills, recovery and reconstruction represented through 33 questions. All the questions are in the format of multiple choices, in which the only two possible answers are "yes" or "no". To the option of "yes" has been assigned the score "1", to the option of "no" the score "0". "Yes" answer represents the hospital's ability to resist and absorb the shock of disasters while the answer "no" is related to a "no resilient" hospital's behavior. The total score of each section has been obtained by summing the score of each question. Factor analysis has been performed to build a valid framework and measure the hospital

66

disaster resilience. The factor analysis results are shown in Figure 37 where the dashed line represents the average values estimated which has been considered as the maximum admissible WT.
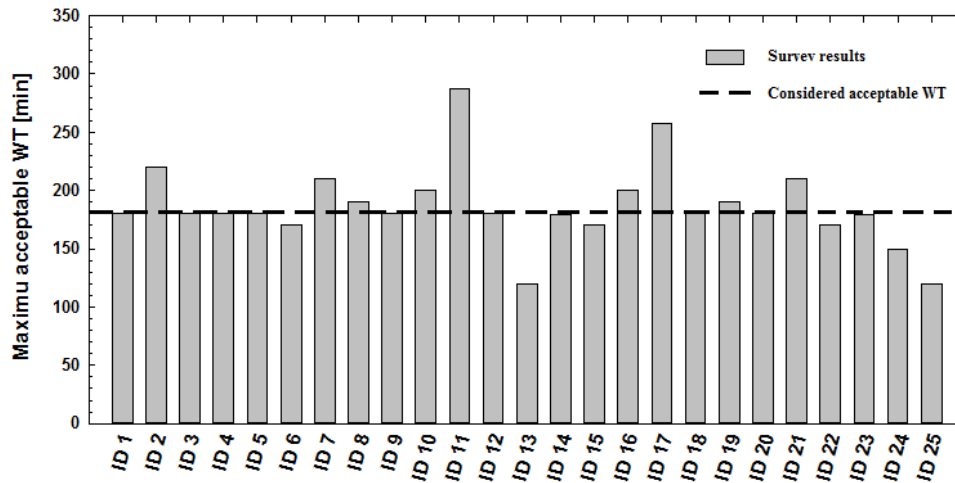
Figure 37. Results of the surveys and considered maximum acceptable WT.

The estimation of the number of injured for a given earthquake scenario has been carried out based on the methodology provided in Chapter 2 and Chapter 3, considering the level of damage that each building can experience after the earthquake. The patient arrival rate for each hospital is assessed and is used as input for the meta-model in order to estimate the trend of patients' WT. The capability of a given hospital to respond to an emergency situation is assessed by comparing the estimated WTs through the proposed meta-model and the maximum acceptable WT.

In cases where one or more hospitals of a network are not capable to guarantee emergency care to all the expected patients, different approaches may be considered to ensure that all patients receive emergency care within the maximum acceptable WT. Two different approaches are discussed in this chapter. The first approach assumes a resilient perspective in which the capacity of one or more healthcare facilities is used to guarantee emergency care to all the patients that cannot be treated in the nearest hospitals. This implies the presence of an Operative Center that manages the patients' flow in the hospitals. The second approach considers the possibility of increasing the number of hospitals by using another healthcare facility equipped with an efficient Emergency Department (mitigation action). In this case, different aspects of basic emergency planning need to be emphasized in these structures. Figure 38 summarizes the explained methodology for the general case of Emergency Department network.

```
┌──────────────┐         ┌──────────────────┐     ┌──────────────────┐     ┌──────────────────┐
│              │    ┌───▶│ Buildings damage │────▶│ Total number of  │────▶│ Injured distribution │
│              │    │    │   assessment     │     │ injured estimation│     │ based on closest │
│ Seismic scenario │──┤    └──────────────────┘     └──────────────────┘     │ distance criterion │
│              │    │                                                        └──────────────────┘
│              │    │    ┌──────────────────┐     ┌──────────────────┐     ┌──────────────────┐         │
└──────────────┘    └───▶│ Hospital damage  │────▶│ Total number of  │────▶│ Waiting time estimation │◀──┘
                         │   assessment     │     │ functional ED room│     │ considering meta-model │
                         └──────────────────┘     │   estimation     │     └──────────────────┘
                                                  └──────────────────┘              │
                                                                                    ▼
┌──────────────────────┐     ┌──────────────────┐            YES ◀───        ┌──────────────────┐
│ Patients redistribution │◀──│ Resilience approach │◀──────────────────────│ Are the hospitals │
│ according to Operative  │   │ with existing    │                          │ able to provide care │
│ Center               │     │   resource       │◀──┐                       │ to all the patients? │
└──────────────────────┘     └──────────────────┘   │                       └──────────────────┘
                                                     │          NO ◀───
┌──────────────────────┐     ┌──────────────────┐   │
│ Increase the number of │◀──│ Mitigation approach │◀─┘
│ Emergency department │     │ with additional  │
└──────────────────────┘     │   resources      │
                             └──────────────────┘
```

Figure 38. Flowchart of the methodology applied to the virtual city's Emergency Department network (ED).

5.3 Case study: virtual city

In this section application of proposed methodology is illustrated in the virtual city. The final evaluation of the capacity of the healthcare system, for almost all seismic scenarios and due to several uncertainties involved, may be complex. It is almost impossible to predict exactly the characteristics of next large earthquake will strike a city such as location, size, time, and many other parameters. Even if it is almost impossible to predict exactly the location and the time of the seismic event, it is not equally impossible to predict its effects.

Different parts of the city will be affected by earthquake depending on proximity to faults, underlying soil condition, and types of buildings. In addition, depending on when the earthquake happens, the number of injured and the severity of the injuries, can vary considerably. For example, during the night, most people are at home in residential buildings, whereas in the day-time, people are mostly at work or school in buildings with different structural characteristics. Instead, if the earthquake occurs during the day, the older buildings, which are mostly in the business areas located in downtown of the considered virtual city, will be responsible for the largest share of casualties. Similarly, if it occurs at night, the residential buildings will cause the most casualties and it will lead different patient distribution among the city. Since the buildings density, their archeology, and their occupancy vary by neighborhood in the considered virtual city, thus the time occurrence of the earthquake might affect considerably the number of injured and its distribution across the city.

5.3.1 Healthcare network model

This section aims to provide a valid first order methodology for assessing whether the network of hospitals in the considered virtual city will be able to deal with such a seismic event. The case study emergency network includes the six

most important hospitals in the virtual city, provided with a functioning Emergency Department. According to Municipality of Turin, the virtual city also has been divided into ten large neighborhoods listed in Table 12.

In this case study, only six hospitals have been considered, leaving aside all the other healthcare facilities among the considered virtual city. Actually, in the virtual city there are more than six hospitals but some of them do not have an emergency department while others are specialized hospitals (e.g. children's specialized hospital, geriatric psychiatry hospital, etc.). Therefore, only general hospitals provided with a functioning emergency department have been considered. Figure 39 shows the virtual city neighborhoods and the distribution of the six considered hospitals.

Table 12. Virtual city neighborhoods.

Number	Neighborhood
1	Centro, Crocetta
2	Santa Rita, Mirafioro Nord
3	Borgo San Paolo, Cenisia, Pozzo Strada, CitTurin, Borgata Lesna
4	San Donato, Campidoglio, Parella
5	Borgo Vittoria, Madonna di Campagna, Lucento, Vallette
6	Barriera di Milano, Regio Parco, Barca, Bertolla, Falchera, Rebaudengo, Villaretto,
7	Aurora, Vanchiglia, Sassi, Madonna del Pilone, San Sakvario, Cavoretto, Borgo Po
8	San Salvario, Cavoretto, Borgo Po
9	NizzaMillefonti, Lingotto, Filadelfia
10	MirafioriSud
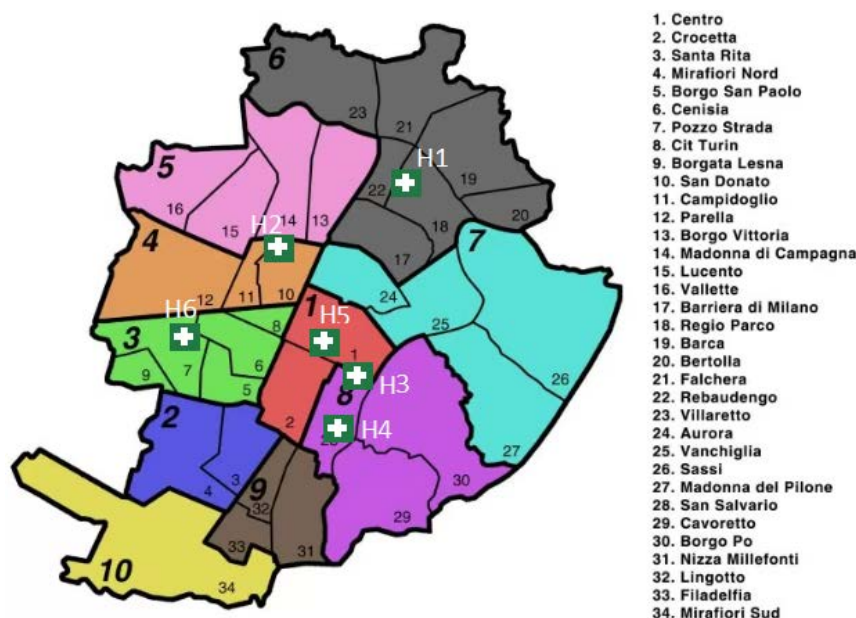
Figure 39. Virtual city's neighborhoods and hospitals distribution

The buildings density and their occupancy vary by neighborhood. Only the residential buildings have been considered in order to estimate their amount of damage and consequently the total number of injured. It is assumed that the earthquake happens at night-time (at 2:00 am) when they are mostly crowded.

69

According to HAZUS (NIBS 2012) this assumption implies that 99% of population is at their houses.

Post-earthquake damage to roads and infrastructures serving the healthcare system can affect both the number of injured and the patient's flow to hospitals. Studying the interdependencies between the infrastructures and the healthcare system is beyond the goal of this thesis. Therefore, the post-earthquake infrastructural damage and their cascading effects on the healthcare facilities have not been taken into account in this work. However, the consequences of infrastructure post-earthquake damage could be included in meta-model affecting the patient's arrival rate (α) as the future works.

Four severity levels have been considered in this study as described in Section 3.5. The estimated number of injured for each severity level after the Norcia earthquake scenario is estimated according to the methodology described in Chapter 3 and the results is reported in Table 13.

Table 13. Estimated number of injured for different levels of severity.

Levels of severity	Casualties
Severity 1	6251
Severity 2	1316
Severity 3	134
Severity 4	260

In this study, only patients with yellow code have been considered; thus, severity 1 and 4 are not taken into account. A total of 1450 injured with yellow triage code has been calculated. This number has been obtained by summing the injured number considering both severity 2 and severity 3. Thus, virtual city's hospitals have to provide care to 1450 patients distributed along different neighborhoods. According to the distribution of damage in buildings (Chapter 2) and to the population density (Chapter 3), the methodology described in Chapter 2 has been applied and the percentage of injured (summation of injured for severity 2 and severity 3) has been calculated (Figure 40). The total number of injured (for both severity 2 and severity 3) for each administrative neighborhood has been illustrated in Figure 41.
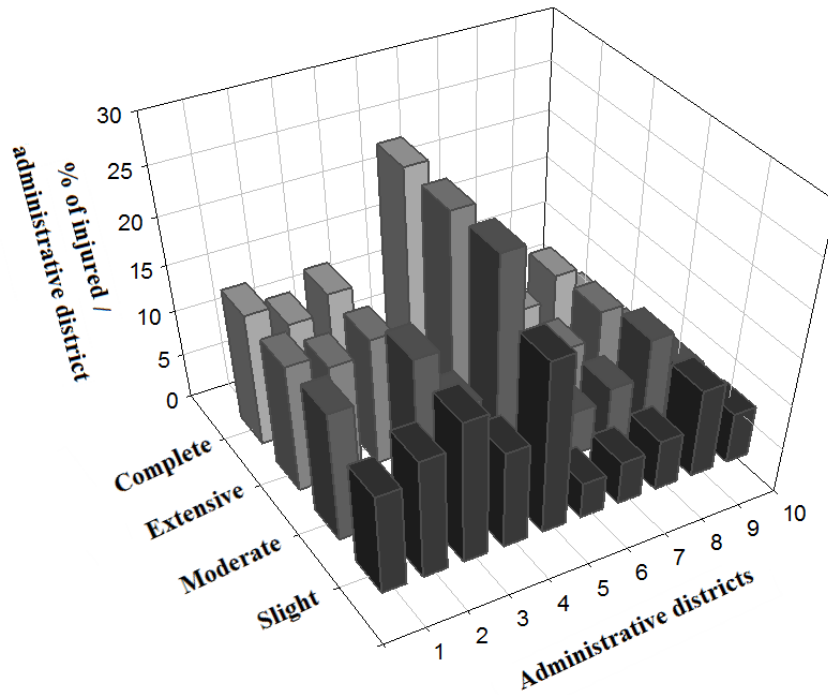
Figure 40. Percentage of injured per neighborhood for Norcia earthquake scenario.
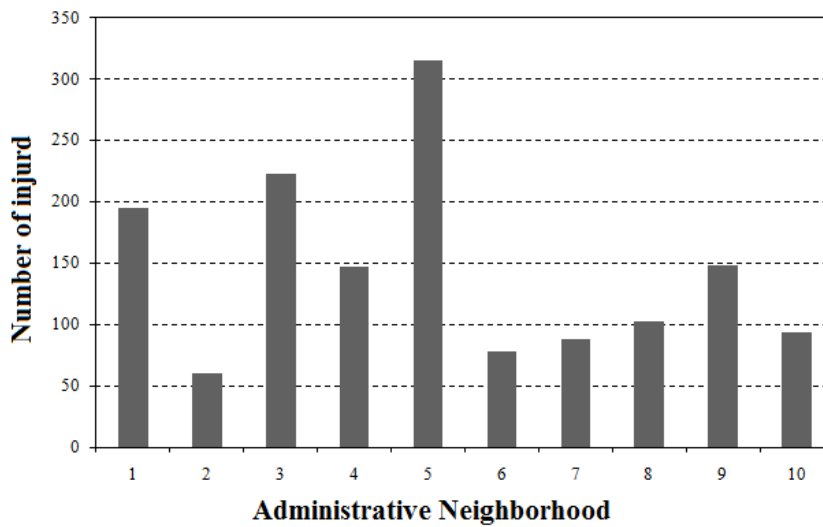
Figure 41. Number of injured per neighborhood for Norcia earthquake scenario.

After catastrophic events, all the injured patients have to reach one of the Emergency Departments located in the city. This travel has to be as short as possible because long average travel time to a trauma center could compromise the condition of the patients. Therefore, all the estimated injured have been distributed considering the distance between the position of the injured and the nearest hospital. A homogeneous distribution of the patients within a single neighborhood has been assumed. The percentage of patients for each hospital and the number of patients arriving at each hospital has been evaluated (Table 4).

71

Patients WT has been chosen as the most significant parameter in order to measure hospital resilience during emergencies. As illustrated in Figure 37, the survey has shown that the conditions of the patients may be compromised irreversibly after waiting more than 3 hours (180 min). In this study the estimation of the patient's WT in each hospital has been estimated through the meta-model developed by Cimellaro et al. (2017).

The number of functional emergency rooms treating patients with yellow codes (m) for each hospital has been obtained through the questionnaire and is reported in Table 14. It is assumed that the healthcare facilities remain fully functional after a seismic event.

In this case study, the patient arrival rate collected in a Californian hospital during 1994 Northridge earthquake (Cimellaro et al. 2015) has been assumed as seismic input parameter for the meta-model. Sensitivity analysis has been performed in the Emergency Departments and the patients' arrival rate has been proportionally amplified using a scaling procedure based on the MMI. First, the seismic intensity level of the considered scenario (6.5 M_W) has been converted in MMI. This value has been used as intensity scale factor (α_I) compared to the 1994 Northridge earthquake that is considered the reference scenario. The patients' arrival rate requires a further scaling procedure to take into account the total number of patients for the case study in comparison to the 1994 Northridge earthquake. The reported total number of patients who have received care in the Californian hospital during the 1994 Northridge earthquake is 559 (Cimellaro et al 2011). According to Yi (2004), 40.1% of the total patients are treated with yellow code in emergency operating conditions (Table 10). Hence, the total number of patients with yellow code in emergency operating conditions has been assumed equal to 223.

In the considered seismic scenario, the minimum value of the number of patients equal to 223 has been obtained for the fourth hospital (H4). The scaling procedure based on the total number of patients has been carried out and the related scale factors (α_{II}) are reported in Table 14. The total scale factor for each hospital has been obtained by multiplying the intensity scale factor (α_I) and scale factor based on the total number of patients in the Emergency Department (Table 14).

Table 14. Estimated percentage of total injured for each analyzed hospital and related meta-model parameters.

Hospital	N. of Patients	α_I	α_{II}	α	m	a	b	c
H1	224	1.12	1.01	1.13	1	188×10^4	4430	0.23
H2	231	1.12	1.04	1.16	4	233×10^3	3480	0.20
H3	225	1.12	1.02	1.14	2	196×10^4	4464	0.23
H4	223	1.12	1.00	1.12	2	180×10^4	4400	0.22
H5	237	1.12	1.08	1.21	4	296×10^3	3545	0.21
H6	310	1.12	1.39	1.56	3	407×10^3	3459	0.38

By knowing *m* and *α*, the trend of patients' WT for each assumed hospital has been obtained. Table 14 shows also the parameters *a*, *b*, and *c* derived for each hospital. A comparison between the estimated WTs and the maximum acceptable WT value (3 hours) has been carried out for each hospital as shown in Figure 42.

Figure 42 illustrates that hospital 1, hospital 3 and hospital 4 are unable to provide care to all the patients arriving at the Emergency Department. In particular, patients' WT for hospital 1 reaches a peak value of about 436 min while hospital 3 and hospital 4 of 450 min and 420 min, respectively. The results depend on the capability of the hospital that is determined by the number of available emergency rooms. According to the obtained results, the emergency framework of the virtual city has shown the inability to respond to an emergency situation caused by a 6.5 M_w earthquake. In the following section, two approaches have been considered to ensure that all patients receive emergency care within the maximum acceptable WT.
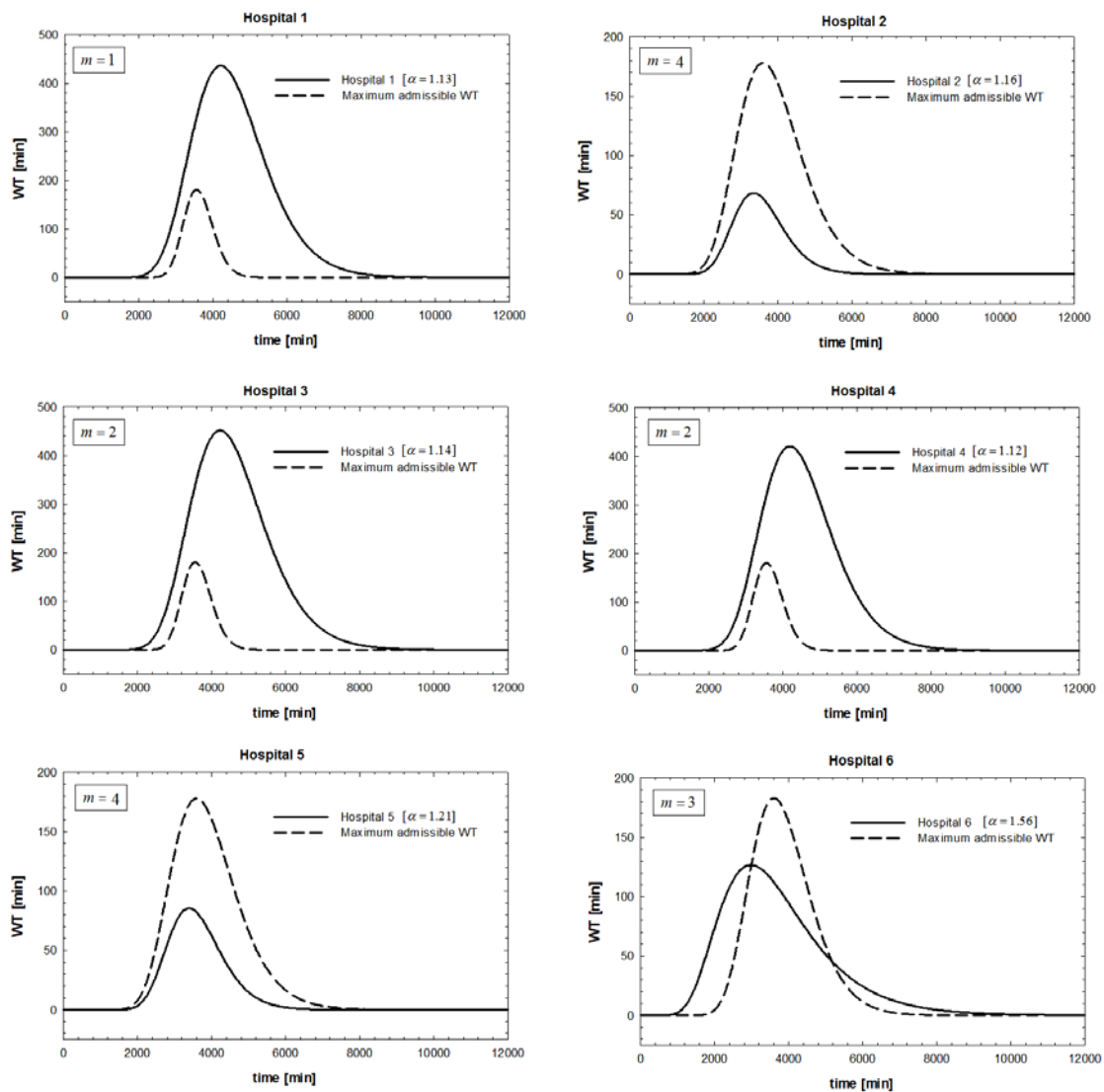
Figure 42. Patient's estimated WT vs maximum acceptable WT (3 hours)

73

5.4 Improvement of resilience of the emergency network

5.4.1 Approach 1: Emergency management with an Operative Center

For the considered case study, the distribution of the patients according to the closest distance criterion does not ensure that all patients receive emergency care within the maximum acceptable WT. Patient's redistribution approach has been developed to guarantee emergency care to all the injured in the virtual city under 6.5 M_w seismic event. The presence of an Operative Center has been assumed in order to manage the flow of patients in the hospitals. The predicted WT for hospital 1, hospital 3, and hospital 4 exceed the maximum acceptable WT. Therefore, the maximum number of patients that can be treated in each of the three hospitals has been obtained and the remaining patients have been distributed in the hospitals with higher capacity considering the minimum travel distance. Table 15 presents the new calculated α, and the parameters a, b, and c values considering the redistribution of the patients.

Table 15. Number of patients and related meta-model parameters after redistribution.

Hospital	N. of Patients	α	a	b	c
Hospital 1	174	0.88	648×10^3	3600	0.11
Hospital 2	281	1.27	398×10^3	3620	0.22
Hospital 3	172	0.88	648×10^3	3600	0.11
Hospital 4	176	0.88	648×10^3	3600	0.11
Hospital 5	284	1.40	716×10^3	3830	0.24
Hospital 6	363	1.81	675×10^3	3780	0.22

According to the new α values, the trend of patients' WT for each considered hospital after the redistribution has been obtained. A comparison between the estimated WTs and the maximum acceptable WT value has been carried out for each hospital (Figure 43).

As shown in Figure 43, the patients' WT never exceed the maximum acceptable limit of 3 hours. On the other hand, the travel time to reach hospital 2, hospital 5, and hospital 6 increases. The rate of increase in patients' travel time has been considered in order to evaluate the accuracy of the proposed solution. The maximum travel time between hospitals and their service areas has been calculated considering normal traffic conditions at the night-time. The results are listed in Table 16.

Table 16. Maximum travel time between hospitals and their service areas calculated considering normal traffic conditions.

Hospital	Travel time before redistribution	Travel time after redistribution	Increase in patients travel time
Hospital 1	14-17 min	14-17 min	0 min
Hospital 2	12-15 min	20-23 min	8 min
Hospital 3	20-23 min	20-23 min	0 min
Hospital 4	18-21 min	18-21 min	0 min
Hospital 5	13-16 min	17-20 min	4 min
Hospital 6	22-25 min	29-38 min	7 min

Table 16 shows that the maximum increasing rate is about 8 minutes. Thus, the proposed solution is a good option to manage the injured care in the virtual city's emergency network. In order to manage the patients' flow in the hospitals, the presence of an Operative Center has to be considered.

5.4.2 Approach 2: increase the emergency network capacity

An increase in the number of healthcare facilities has been considered as a second action to guarantee emergency care to all the injured. The possibility to locate a new hospital has been considered. The identification of the area in which the new hospital should be located is the first important step to perform to improve the network performance. Hospital 1, hospital 3, and hospital 4 are unable to provide care to all the patients arriving at their Emergency Departments after the earthquake. Thus, the new healthcare facility has to be placed in the service area of those three hospitals. This localized area includes neighborhoods 6,7, and 8.

In order to find the most appropriate location for the new hospital, the density of injured in each district has been considered according to the "center of gravity" method. The coordinates for the optimal location have been chosen as an average of the coordinates of the various neighborhoods weighted with the number of injured expected from each neighborhood. The center of gravity (G) of each neighborhood has been calculated using a Cartesian reference system. The center of gravity represents the geometric center of the neighborhood considering a uniform distributed density of patients in each area. Thus, the total number of patients per neighborhood has been used as weight. The center of mass has been calculated and the coordinates of the new hospital location have been determined. Figure 44 illustrates the position of the new hospital and the centers of gravity, as well as the number of patients per neighborhood.
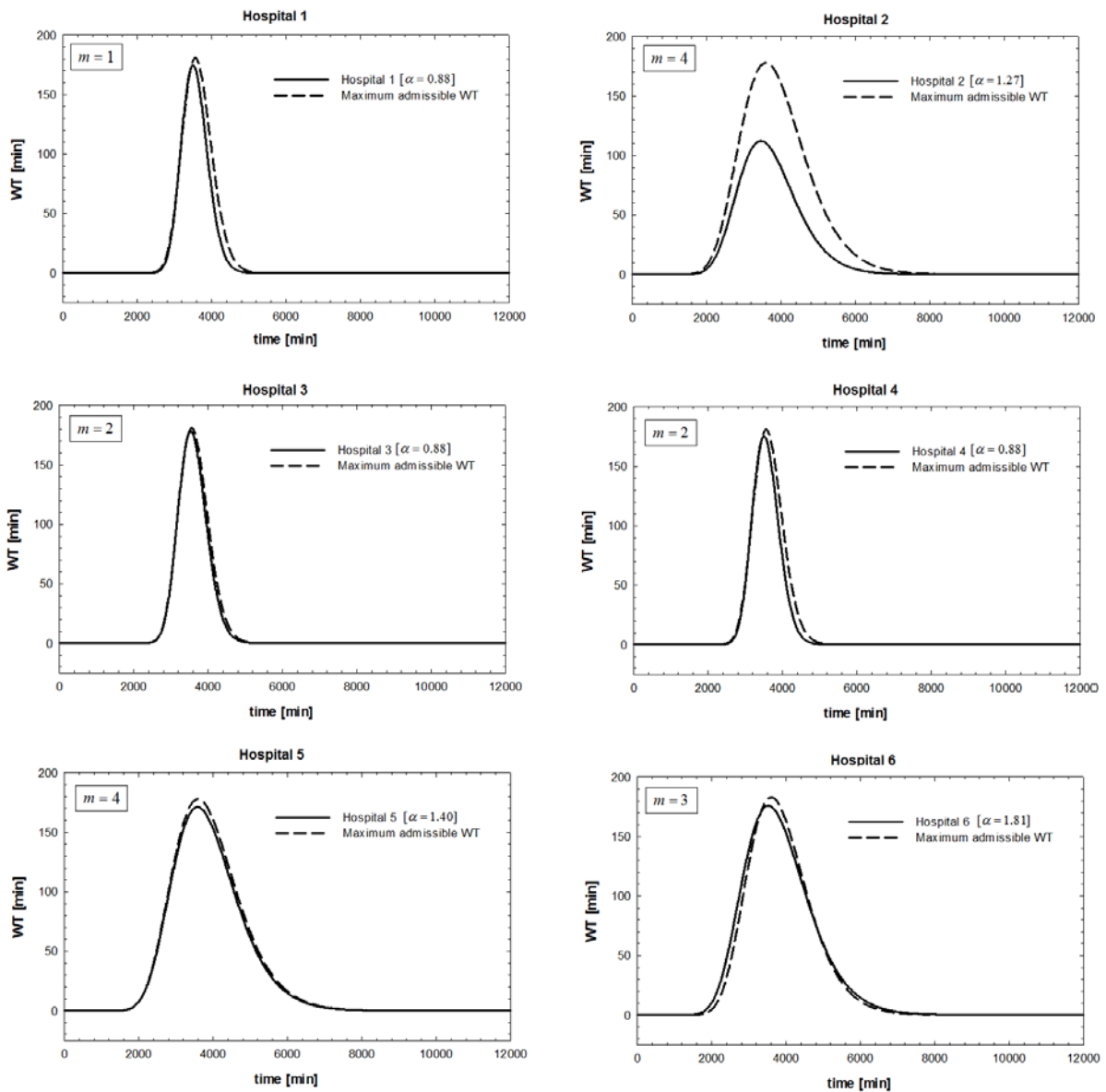
Figure 43. Patient's estimated WT with Operative Center vs maximum acceptable WT (3 h).

The proposed methodology might identify the location of the new hospital in an unfeasible region. In this case, the decision maker may choose another feasible location nearby the determined location. In fact, the calculation is based on estimates of the number of injured and the distances to the neighborhoods without taking into account the effective road paths. However, this first order method provides useful information that can help the decision makers during the design process. Once the most suitable position of the new facility has been identified, the number of patients arriving at each Emergency Department has been re-calculated considering the closest distance criterion. Results are listed in Table 17.
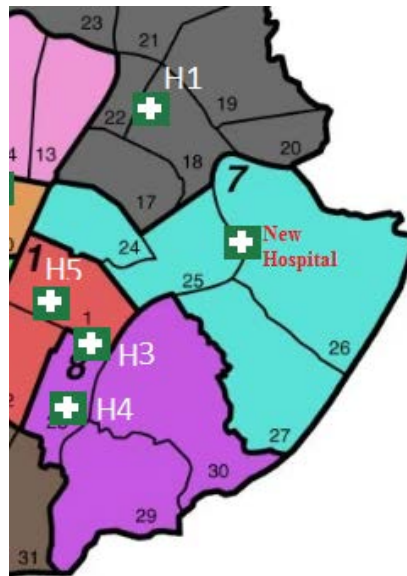
Figure 44. New hospital location.

In order to define the size of the new hospital, the expected number of patients has been used as input parameter. The minimum number of emergency rooms (m) for the new hospital has been obtained through an iterative procedure by fixing the seismic input corresponding to the number of expected patients, and the maximum allowable WT (180 min). Knowing the number of patients arriving at the Emergency Departments, the seismic input parameter α can be obtained (Table 17). Performing the iterative procedure, a minimum number of three rooms is identified to provide care to all the patients arriving in the new Emergency Department within a maximum waiting time of 3 hours. In order to evaluate the response of the new emergency network, the peak value of patients WT for each considered hospital has been assessed (Table 17).

Table 17. Estimated number of injured, α and WT for each analyzed hospital.

Hospital	N. of patients	α	Average WT peak
Hospital 1	174	0.88	175 min
Hospital 2	231	1.21	85 min
Hospital 3	172	0.88	173 min
Hospital 4	176	0.88	164 min
Hospital 5	237	1.16	68 min
Hospital 6	310	1.56	127 min
New Hospital	150	0.67	180 min

Comparing the estimated WTs and the maximum acceptable WT value, each hospital is able to provide timely and efficient care to all the patients arriving at their Emergency Departments. Therefore, the proposed solution appears to be a preliminary efficient guess to increase the resilience of the virtual city's emergency network.

5.4.3 Comparison between the two proposed approaches

Both proposed approaches are able to guarantee timely care to all the injured caused by the considered earthquake scenario, however limitations apply. *Approach 1* includes injured redistribution in the hospitals with higher capacity and allows optimizing resources. The preservation of the existing resources leads to avoid some issues like the planning phase for a new healthcare facility, the time necessary for the construction and the extremely high costs. Moreover, the presence of an Operative Center could allow managing in real time injured flow in the hospitals, ensuring that patients WT never exceed the maximum value of maximum acceptable WT. Nevertheless, the behavior of people during and after disasters strongly influences the management of the patients. Therefore, the Operative Center may not be able to manage the emergency. In addition, the virtual city's roads could be negatively affected by the earthquake causing unacceptable travel times to reach the healthcare facilities. *Approach 2* is based on mitigation by using additional resources. This approach is focusing in finding the location of a new hospital. The total construction cost is an important parameter in estimating the benefits of this action. Thus, a benefits-costs analysis has to be performed in order to evaluate the validity of the proposed approach.

This chapter presented a methodology to assess the resilience of the hospital network of the virtual city after Norcia earthquake scenario. The capability of the hospital network to provide emergency care to the injured after the earthquake was studied. The result shows that three hospitals located at the downtown of the virtual city are failed to treat injured within the maximum acceptable WT. Finally, two different methodologies evaluating the optimal recovery plans were proposed to improve the resilience of hospital network.

Chapter 6

An indicator based approach to measure community resilience

Measuring resilience is one of the most demanding tasks due to the complexity involved in the process. Recently, several studies have been conducted to address the community resilience quantification. Among the analytical measurement methods, the use of indicators usually is preferred as an affordable method to evaluate the resilience of a system. In this chapter, a new approach to quantitatively compute resilience exploiting an indicator based methodology from the PEOPLES framework is presented. The method is a deterministic and requires data on past earthquake events represented in the form of measure for the framework indicators. The method starts by collecting all community resilience indicators found in the literature. The collected indicators are first filtered to ensure a minimum overlapping between them, and then they are allocated to the PEOPLES' components. A single measure is assigned to each indicator allowing it to be quantified. The measure is not represented by a crisp value but rather a normalized function that marks the serviceability of the system in time. This method turns a resilience index and a performance function for the community as an output. In addition, a matrix interdependency approach is proposed to take into account the interdependencies between different indicators of a community. This chapter also introduces an open source online software tool to measure the resilience of communities. Then, the proposed methodology is applied to the virtual city to measure the resilience of physical infrastructures. At the end, two different strategies to improve the resilience of the virtual city including 'increasing the system robustness' and 'reducing recovery time' are investigated.

"Part of the work described in this chapter has been previously published in: "Deterministic and fuzzy-based methods to evaluate community resilience." Earthquake Engineering and Engineering Vibration 17, no. 2 (2018): 261-275.".

6.1 Indicator-based deterministic approach

6.1.1 PEOPLES' variables

PEOPLES is a framework for defining and measuring disaster resilience of a community at various scales. It is divided into seven *dimensions* and each of them is divided into several *components*. Further details on each of dimensions can be found in (Cimellaro et al. 2016). The framework does not identify a clear procedure to quantitatively compute resilience, but rather a qualitative assessment and description of resilience. The goal of this chapter is to convert PEOPLES from a qualitative to a quantitative framework. To achieve this, an extensive literature review was conducted to identify the existing *indicators* available in the literature describing the different aspects of a community. To translate these indicators from qualitative statement into a quantitative framework, they were first filtered to ensure a minimum overlapping between them, and then they have been allocated to the PEOPLES' components, creating a condensed list of 115 indicators. These indicators were selected in a way to be able to quantitatively compute the resilience of communities in different size and type. The list of the dimensions, components, indicators, and measures is presented in Appendix A. For each of the indicator collected from literature, the reference source has been cited in column "Ref." of the table provided in Appendix A. For the rest of the indicators, a new measure has been proposed to appropriately quantify the indicator. The developed indicators in this thesis have been highlighted in bold in Appendix A.

A single *measure* is assigned to each indicator to make it quantifiable. The measures are presented in the form of continuous functions instead of scalar values (crisp values). This allows identifying the performance of the indicator during an interval of time (i.e. the period following the disaster) rather than at a specific instance of time. The measures are then normalized to be ranged between 0 and 1. This is done by introducing a new parameter, the *standard value* (SV). SV is a quantity that represents the reference point of the corresponding measure, defined by the competent authority. The standard value is an essential quantity that provides the baseline to measure the resilience of a system. The system's existing serviceability at any instance of time is compared with the standard value to know how much serviceability deficiency is experienced by the system. Each measure is normalized with respect to a fixed quantity, the standard value (*SV*).

For example, if we consider the measure "*Red cross volunteers per 10,000 people*", the measure would give us an absolute number of volunteers as an output. This quantity cannot be integrated with other measures unless it is normalized; therefore, the result is divided over SV, which in this case represents the "BEST" number of volunteers per 10,000 people (e.g. SV=100 volunteers /10,000 people). If the ratio between the value of the measure and SV is less than one, it means that the indicator can still be improved, whereas if it is larger than one, the measure is considered "resilient", and a value of 1 is assigned to that

measure. Having all measures normalized enables the comparison among systems of similar or different types (e.g. hospitals and water networks).

Measures are classified according to their relationship (*Rel.*) with resilience. A letter "*P*" (positive effect) is assigned to the measures that contribute to the favor of increasing resilience, while a letter "*N*" (negative effect) is assigned to those that do the converse. In addition, two types of measures are identified: "static measures (*S*)", assigned to the measures that are not affected by the disastrous event, and "dynamic measure (*D*)" or event-sensitive measures, assigned to the measures whose values change after a hazard takes place. Appendix A summarizes the list of the dimensions, components, indicators, and measures, with relationships towards resilience (Rel. = N (negative) or P (positive)), and indicators' nature (Nat. = S (static) or D (dynamic)).

6.1.2 Interdependency factor

Interdependencies between the different variables of PEOPLES framework can highly affect the resilience result. Generally, the interdependency depends on several factors such as the disaster event and the type of the analyzed community (rural, urban and industry). To include interdependencies, factors are allocated to each variable through an interdependency analysis. The proposed interdependency technique returns as an output a factor for each variable. The technique assumes that the variable's interdependency factor is strictly related to the number of other variables in the same group that depend on it. For the purpose of the analysis, the variables of PEOPLES (see Appendix A) are classified into three major groups as follows:

- Indicators: that fall within a component are considered as a group (totally 29 groups that is equal to the total number of components);
- Components: classified under a dimension are taken as a group (totally 7 groups that is equal to the total number of dimensions);
- Dimensions: fall in one group (totally 1 group).

A square matrix for each group of variables is created (Figure 45), where each cell in the matrix represents the level of interdependency between two variables. This matrix is a [$n \times n$] square matrix where n is the number of variables in the analysed group. Each cell (a_{ij}) can take the values *0* or *1* indicating full independence and full interdependence, respectively. The number a_{ij} implies the dependency of variable *i* to variable *j*. This value can be identified either using descriptive knowledge in the form of a questionnaire filled by a group of experts or by relating to past data on previous events.

Figure 46 shows a sample questionnaire to portray, as an example, the interdependencies that exist among the indicators under the component "lifeline". This questionnaire form can be filled at least by one expert who has enough knowledge about the dynamics that exist between the variables. The expert responsibility is to identify whether two indicators have "low" or "high"

correlation. These descriptors are translated to 0 and 1 respectively in the matrix cells. The interdependency analysis is done in a hierarchical manner. That is, an interdependency matrix is built for each group of variables so that each variable is analyzed within the group it belongs to (Figure 47).
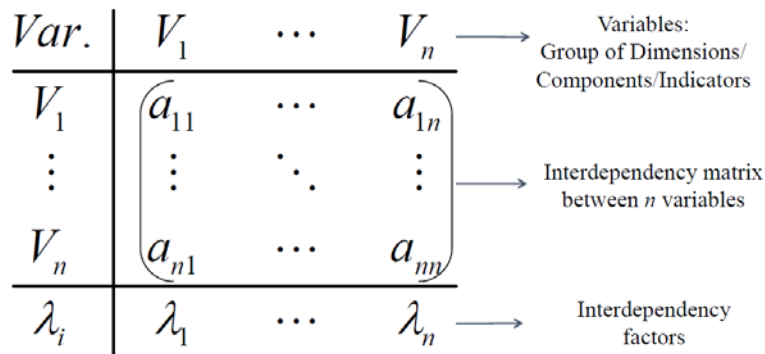
Figure 45. Interdependency matrix for the variables in a same group.

Name:
Designation:
Company:
Date:

Question: please fill the following table based on your expertise. Each cell represents the level of interdependency and its cascading effect of each indicator upon the other one (across each raw). Please use "L" for Low level of interdependency and "H" to display High level of interdependency.

Indicator	Telecommunication	Mental health support	Physician access	Medical care capacity	Evacuation routes	Industrial re-supply potential	High-speed internet infrastructure	Efficient energy use	Efficient Water Use	Gas	Access and evacuation	Transportation	Waste water treatment
Telecommunication	H												
Mental health support		H											
Physician access			H										
Medical care capacity				H									
Evacuation routes					H								
Industrial re-supply potential						H							
High-speed internet infrastructure							H						
Efficient energy use								H					
Efficient Water Use									H				
Gas										H			
Access and evacuation											H		
Transportation												H	
Waste water treatment													H

The level of interdependency on other indicators (read across each row)

Figure 46. Sample questionnaire to build the interdependency matrix for indicator under component "lifeline".

For instance, a single interdependency matrix $[M_R]$ is constructed for the seven dimensions of PEOPLES framework. This implies to create 7 interdependency matrices ($[M_{D1}]$, $[M_{D2}]$, ... , $[M_{D7}]$) for each group of components under the seven dimensions. Finally, each group of indicators under the components are analysed independently by performing the above introduced interdependency technique. This needs to create 27 interdependency matrices in total for all groups of indicators under the components (e.g. $[M_{C1-1}]$, $[M_{C1-2}]$,...), resulting in 37 matrices to perform a full interdependency analysis for the different variables under the PEOPLES framework. The number of matrices depends on the conceptual framework used. Frameworks that use less variables and simpler structure would require a smaller number of interdependency matrices.
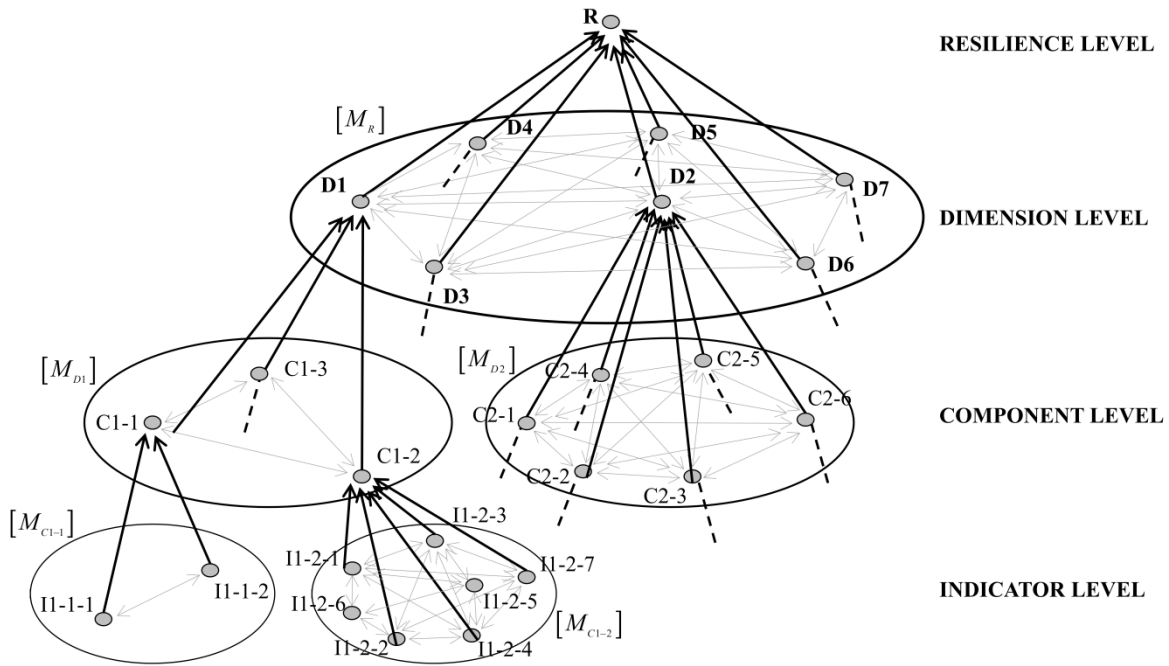
Figure 47. Interdependency matrices at the different levels.

These interdependency matrices are not symmetrical because if a variable i is dependent on a variable j, the reverse is not necessarily true. The interdependency factor of a variable i is obtained by normalizing the summation of the values in column i with respect to the maximum value among all the columns' summations. A high value means high importance of the corresponding variable. The interdependency factor for a variable i is mathematically calculated as follows:

$$\lambda_i = \frac{\sum_{j=1}^{n} a_{ji}}{\max(\sum_{j=1}^{n} a_{j1},...,\sum_{j=1}^{n} a_{jn})} \tag{20}$$

where λ_i is interdependency factor for variable i, a_{ji} is the interdependency level that variable j has on a variable i, n is the number of variables in the studied group.

The interdependency between the variables is greatly related to the community type (e.g. urban, rural, etc.).For instance, the "economic development" dimension is significantly less dependent on "physical infrastructure" dimension in a rural community with respect to an urban community. As an example, to illustrate how the proposed interdependency method can include the community type, three different communities including urban, rural, and industrial have been considered and the interdependency matrices at the dimension level have been created. The interdependency matrices were defined through a questionnaire identifying whether two dimensions are "independent", "low dependent", "medium dependent", "high dependent", or "fully dependent". These descriptors were then translated to 0, 0.25, 0.50, 0.75, and 1, respectively in the matrix cells. Equations(21), (22), and (23) show the interdependency matrices for rural, urban and industrial communities, respectively.

$$[M_{R,Urban}] = \begin{bmatrix} 1 & 1 & 1 & 1 & 1 & 1 & 1 \\ 0.25 & 1 & 0.5 & 0.5 & 0.5 & 0.75 & 0.25 \\ 0.5 & 0.5 & 0.75 & 1 & 0.75 & 0.75 & 1 \\ 0.75 & 0.5 & 1 & 1 & 0.75 & 1 & 0.75 \\ 1 & 1 & 0.5 & 1 & 1 & 0.5 & 1 \\ 0.75 & 1 & 0.75 & 1 & 0.5 & 1 & 0.5 \\ 1 & 0.5 & 1 & 0.5 & 1 & 0.5 & 1 \end{bmatrix} \tag{21}$$

$$[M_{R,Rural}] = \begin{bmatrix} 1 & 1 & 0 & 0 & 0 & 0 & 0 \\ 0 & 1 & 0 & 0 & 0 & 0 & 0 \\ 0 & 0 & 1 & 0.5 & 0.25 & 0.5 & 0 \\ 0 & 0.5 & 0.25 & 1 & 0 & 0.25 & 0 \\ 0 & 1 & 0 & 0 & 1 & 0 & 0 \\ 0 & 0 & 0.5 & 0.25 & 0 & 1 & 0 \\ 0 & 0 & 0 & 0 & 0.25 & 0 & 1 \end{bmatrix} \tag{22}$$

$$[M_{R,Industrial}] = \begin{bmatrix} 1 & 0 & 0.5 & 0.25 & 0 & 1 & 0 \\ 0 & 1 & 0 & 0.25 & 0 & 1 & 0 \\ 0 & 0 & 1 & 0.5 & 0 & 1 & 0.5 \\ 0 & 0 & 1 & 1 & 0 & 1 & 0 \\ 0.5 & 0.5 & 0.75 & 1 & 1 & 0.75 & 0.25 \\ 0.25 & 0.25 & 0.75 & 1 & 0 & 1 & 0 \end{bmatrix} \tag{23}$$

At each matrix, cell a_{ij} represents the dependency level of dimension i (Di) on dimension j (Dj), while the seven analysed dimensions are: Population and demographics ($D1$), Environmental and ecosystem ($D2$), Organized governmental services ($D3$), Physical infrastructure ($D4$), Lifestyle and community competence ($D5$), Economic development ($D6$), and Social-cultural capital ($D7$).

Table 18 lists the interdependency factors for the urban, rural, and industrial communities obtained using Equation (20). It shows that in industrial communities, the economic development (*D6*) is the dimension that most other dimensions or dependent on it ($\lambda_6 = 1$). It implies that after a disaster for a fast and efficient recovery, resources should be allocated mainly to this dimension since the others are heavily dependent on it. It helps the decision makers to better distribute the resources during the recovery process. Furthermore, Table 18 shows that for a rural community the dimension with the higher interdependency factor is Environmental and ecosystem (*D2*) which is more important for rural communities. Figure 48 shows the level of interdependency between the seven dimensions for urban, rural, and industrial communities. The area enclosed by the interdependency polygon for the urban community is greater than the others. This shows a high level of interaction and interdependency for urban communities. Also, the development level of the community plays a role in identifying the interdependency among resilience components because developed communities require more interdependent systems to increase service efficiency.

Table 18. Interdependency factor (λ) for urabn, rural, and industrial communites based on PEOPLES framwork.

Community	PEOPLES Dimension						
	D1	D2	D3	D4	D5	D6	D7
Urban	0.88	0.92	0.92	**1.00**	0.92	0.92	0.92
Rural	0.29	**1.00**	0.50	0.50	0.43	0.50	0.29
Industrial	0.30	0.30	0.70	0.67	0.22	**1.00**	0.26
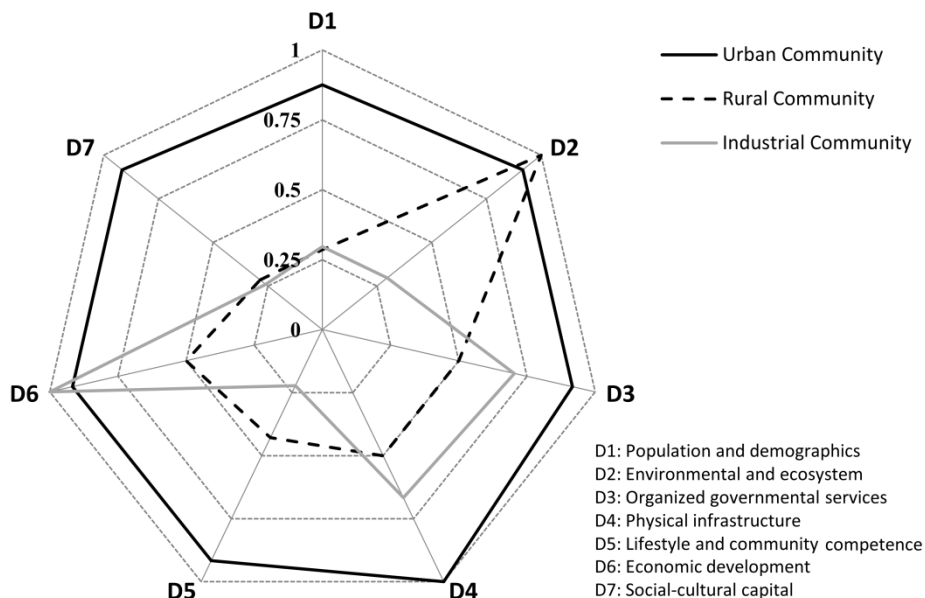
Figure 48. Interdependency level between the seven dimensions of the PEOPLES framework for urban, rural, and industrial communities.

To better consider the uncertainties and reduce the subjectivity, the questionnaire can be filled by a group of experts. In this case, a statistical analysis is carried out. A probability distribution function (PDF) with normal distribution is considered for each variable based on the data collected from the experts (Figure 46), and three values are used in the subsequent analysis to address the uncertainties in final resilience output: (1) the mean (λ), (2) mean + standard deviation ($\lambda + \sigma$), (3) mean – standard deviation ($\lambda - \sigma$) (Figure 49). This results in a final resilience output with the uncertainty bound being considered.
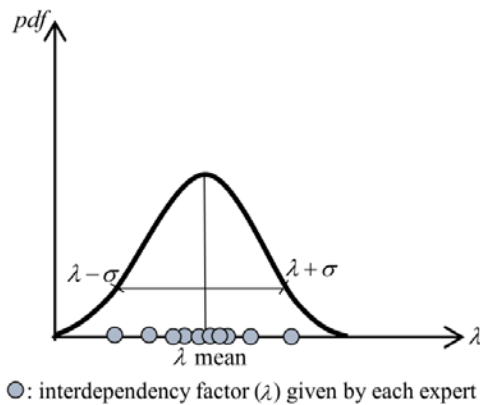
Figure 49. Statistical analysis for the expert responses about the interdependency factor of each variable.

6.1.3 Importance factor

Variables do not contribute equally to the overall resilience output and each of them contributes with a certain degree towards the goal of achieving resilience. The importance of variables strictly depends on the type of community. For example, in a rural community, Lifestyle and community competence (*D5*) has not the same contribution toward the overall community resilience as Environmental and ecosystem (*D2*), while in an urban community it is an important dimension. To include this, each of the dimensions, components and indicators is given an importance factor (*I*) ranging from 1 to 3, where 1 means low importance and 3 means high importance. This factor represents the extent to which a variable (component, sub-component, or indicator) contributes towards achieving resilience. This factor can be chosen by experts or decision makers.

Table 19 shows a first order evaluation of importance factors at the dimension level for rural, urban, and industrial communities under the PEOPLES framework. The importance factors "*I*" for all variables including dimensions, components and indicators have been provided for an urban community in Appendix A. These values have been obtained through questionnaires and can be modified based on the community type.

86

Table 19. Importance factor (I) for urabn, rural, and industrial communites based on PEOPLES framwork.

Community	PEOPLES Dimension						
	D1	D2	D3	D4	D5	D6	D7
Urban	2	2	3	3	1	3	2
Rural	3	3	1	2	1	2	2
Industrial	1	2	2	3	1	3	1

6.1.4 Weighting factor

The final weighting factor for each variable (w_i) is calculated considering both interdependency and importance factors. Equation (24) translates an interdependency factor (λ_i) and importance factor (I_i) of variable i into a final weighting factor (w_i):

$$w_i = \frac{\lambda_i.I_i}{mean(\lambda_1.I_1,...,\lambda_n.I_n)} = \frac{\lambda_i.I_i}{\sum_{j=1}^{n}\lambda_j.I_j}n \tag{24}$$

where w_i is weighting factor of variable i, I_i is importance factor of variable I, λ_i is interdependency factor of variable i, n is the number of variables in the studied group. Table 20 presents the weighting factors at the dimension level for rural, urban, and industrial communities under the PEOPLES framework. It shows that for an urban community, all seven dimensions mostly have the same weighting factors (with the standard deviation of 0.35 with respect to the mean) while for a rural community the distribution of weighting factors are less uniform (with the standard deviation equal to 0.85).

This kind of analysis can help decision makers to study better the community variables, to allocate the resources to variables with higher contribution in total community resilience (both in terms of importance and interdependency), and finally to plan a better recovery process.

Table 20. Weighting factor (w) for urabn, rural, and industrial communites based on PEOPLES framwork.

Community	PEOPLES Dimension						
	D1	D2	D3	D4	D5	D6	D7
Urban	0.83	0.87	1.30	**1.42**	0.43	1.30	0.87
Rural	0.82	**2.85**	0.48	0.95	0.41	0.95	0.54
Industrial	0.27	0.53	1.27	1.80	0.20	**2.70**	0.23

6.1.5 Final resilience

After obtaining weighting factors for the variables of the PEOPLES framework, a serviceability function is built for each variable: uniform for event-non-sensitive measures "static measures", and non-uniform for event-sensitive

measures "dynamic measures", as shown in Figure 50. The serviceability function can be defined using a set of parameters that mark the outline of resilience graph (e.g. initial serviceability q_0, post disaster serviceability q_1, restoration time T_r, recovered serviceability q_f). These parameters can be obtained from the past events and/or by performing a hazard analysis specific to each variable. In addition, the shape of restoration curve (sometimes referred to as *slope* or *rapidity*) during the recovery affects the resilience quantity and therefore it should be taken into account in the resilience computation. However, the restoration rapidity depends on many variables such as the spatial dimension, the temporal dimension, the hazard type, the available resources (including financial and human resources), the restoration plan, etc. Thus, modeling the restoration curve of a single system is complex and it could be defined graphically in infinite shapes (Kammouh et al., 2017b).

Different types of restoration shapes such as linear, exponential, step function, trigonometric and random function can be selected based on the available system information. For example, the exponential shape can be selected when the initial speed recovery is high due to an initial inflow of resources and it decreases as the recovery reaches the end (Kafali and Grigoriu, 2005). HAZUS (FEMA, 2011) adopted the linear trend as a simplest restoration shape that is generally used when there is not enough available data regarding the system resources and recovery plans (Whitman et al., 1997). In this study, as not much information about the restoration rapidity is available, the linear shape for restoration curve is selected to build the serviceability function. All serviceability functions are weighted using the weighting factors described in section 6.3.
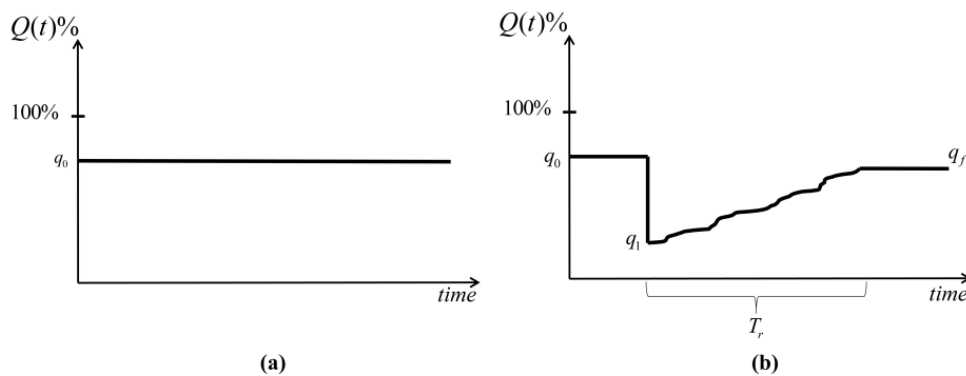
Figure 50. Serviceability functions (a) static, (b) dynamic.

Prior to obtaining the weighted serviceability function for each indicator, the final resilience function is obtained through a hierarchical aggregation procedure (Figure 51). The average of the weighted serviceability functions of the variables belonging to the same group is considered to move to an upper layer. That is, to obtain the serviceability function of component i, the average of the weighted serviceability functions of the indicators under component i is considered. Similarly, to get the serviceability function of dimension j, the average of the weighted serviceability functions of the components under dimension j is

considered. Finally, the serviceability function of the community is the average of the weighted serviceability functions of the seven dimensions. The proposed aggregation methodology is shown as a flowchart in Figure 52. The resilience index of the community is then evaluated as the area under the final serviceability function using Equation (2).
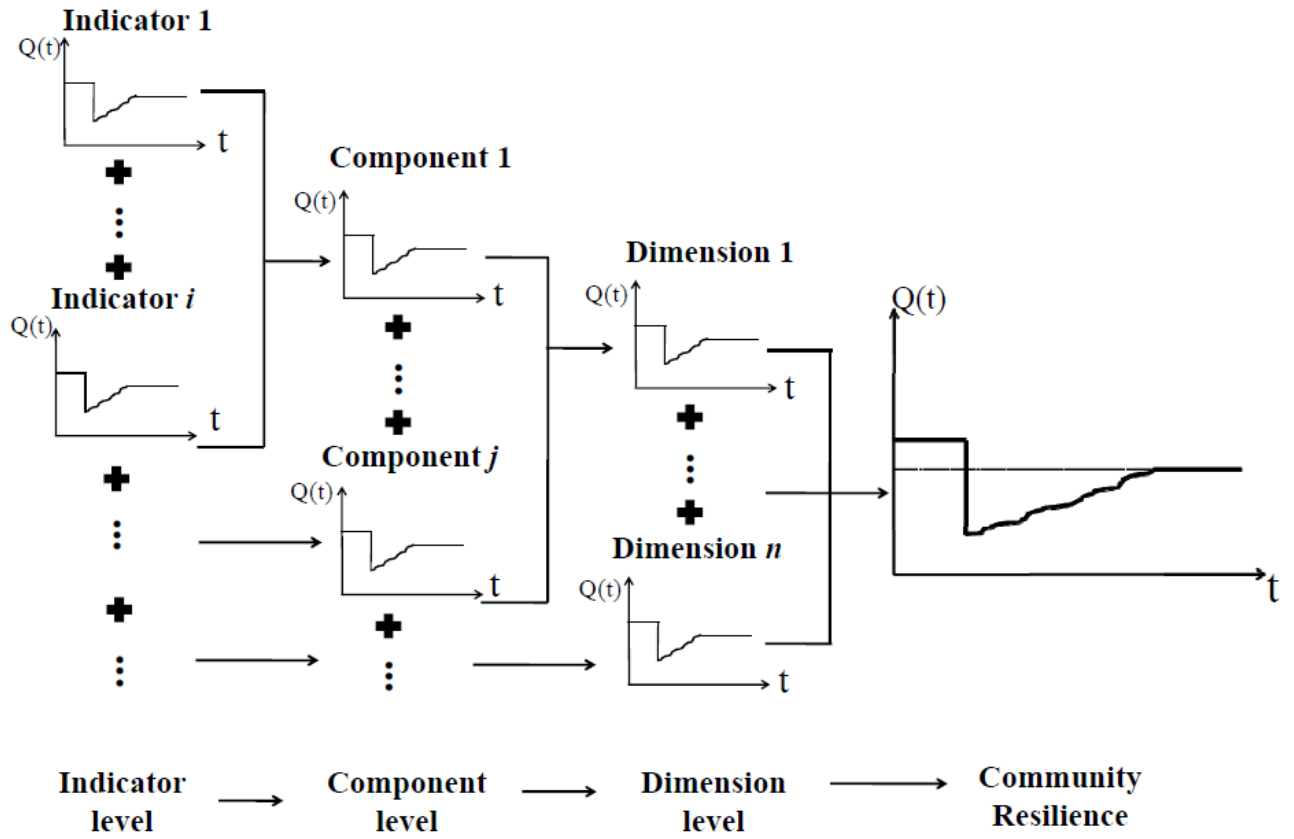
Figure 51. Hierarchical scheme of the adopted indicator-based resilience methodology.
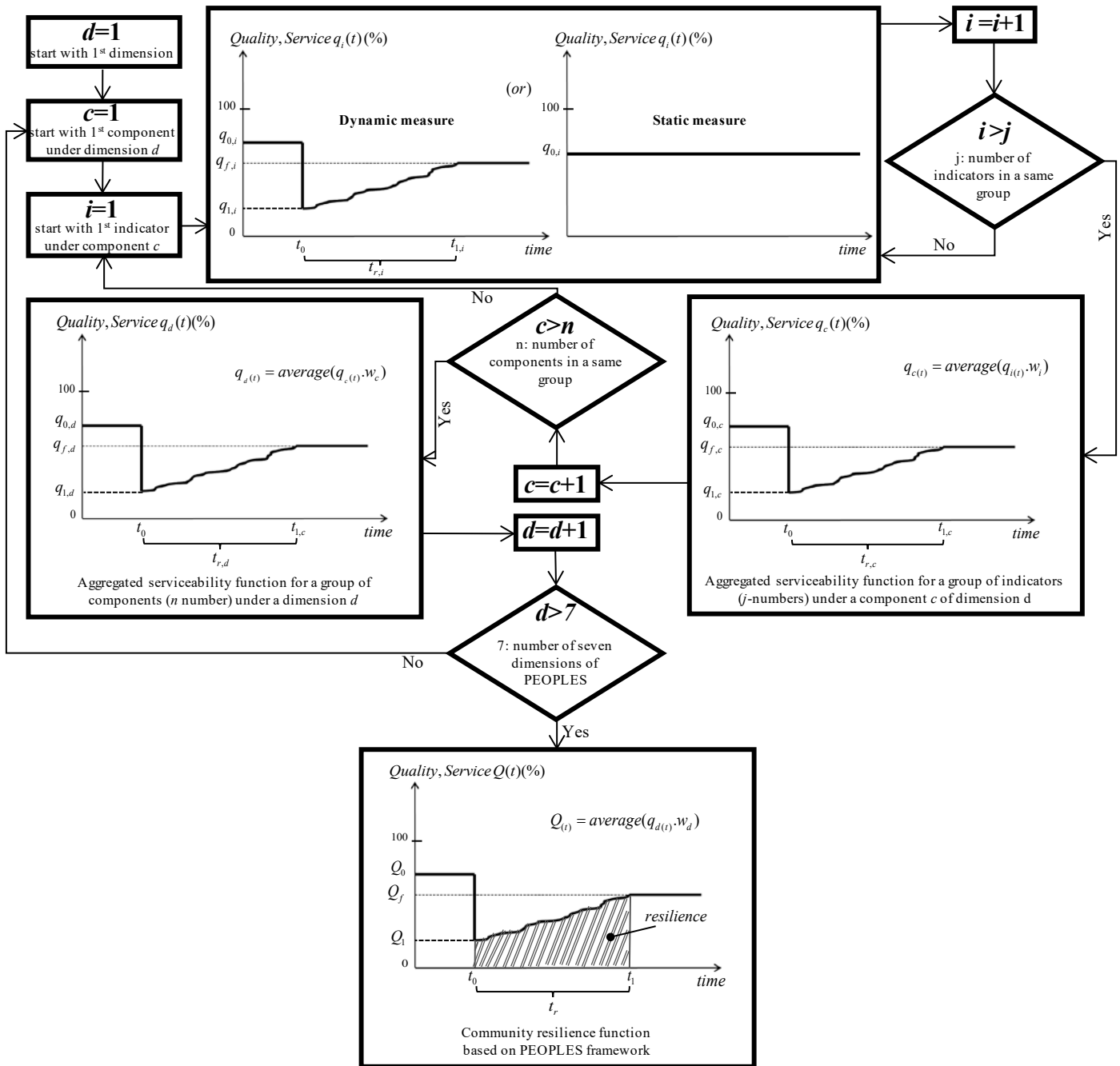
Figure 52. Flowchart to compute the final resilience of a community based on PEOPLES framework.

6.2 Open source resilience computation tools

This section introduces a software tool developed in conjunction with research group working on the European research project "IDEAL_RESCUE" implementing the community resilience approach described in Section 6.1. Specifically this tool was extended in this thesis by including the interdependencies matrix approach presented in section 6.1.2. The developed tool is an online open source software. The user is asked to insert information about the specific community resilience indicators based on PEOPLES framework

before and after a disaster event. The output is presented in the form of a resilience curve of the whole community.

To use the software, a Login/Register window appears when accessing the website link http://borispio.ddns.net/PEOPLES/login.php (Figure 53a). The user must register prior to using the tool. Once registered, she can start a new scenario for which the resilience is to be evaluated (Figure 53b). The scenario is composed of two main ingredients: (1) the analyzed community (i.e. city, country, etc.), and (2) the hazard considered (e.g. earthquake, tsunami, fire, etc.).
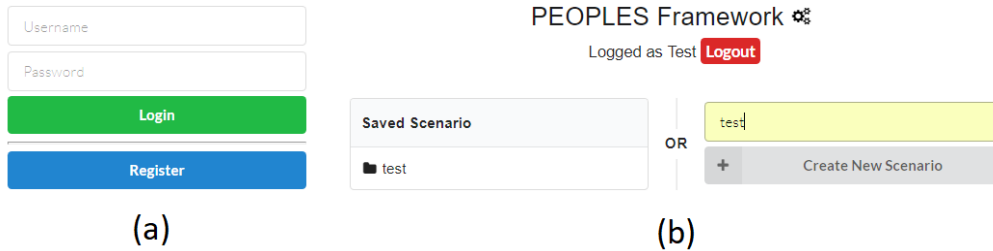
Figure 53. (a) Registration/login page, (b) new scenario definition/load scenario.

After defining the scenario, a data-entry page that displays the various variables of the PEOPLES framework appears (Figure 54). A full list of the components and indicators presented in Appendix A is implemented in the developed tools. On the left side of the webpage, the seven dimensions of PEOPLES framework are listed. For each dimension, a list of components and indicators (based on Appendix A) is shown with blank spaces to be filled with the parameters required for the resilience evaluation. A pop-up description is triggered when hoovering the mouse over a parameter in the window. This is to get extra information that helps the users identifying what kind of information they should insert. The parameters are:

- Importance factor (I): each indicator is associated with an importance factor that represents the weight of the indicator towards the resilience output.
- Indicator nature *(Nat)*: the indicators are classified according to their nature: "Static *(S)*", assigned to the measures that are not affected by the disastrous event, and "Dynamic *(D)*" or event-sensitive measures, assigned to the measures whose values change after a hazard takes place;
- Un-normalized serviceability before the event (q_{0u}): is the un-normalized initial serviceability of the measure;
- Standard value (SV): represents the optimal quantity for the indicator in order to be considered as fully resilient;
- Normalized serviceability before the event (q_0): is the normalized initial serviceability of the measure. It is obtained automatically by the software by dividing the un-normalized serviceability q_{0u} over the standard value SV;
- Serviceability after the event (q_1): The residual serviceability after the disaster. This quantity should be normalized by the user with respect to SV;

91

- Serviceability after recovery (q_r): it is the recovered serviceability, which can be equal, higher, or lower than the initial serviceability (q_{0u}). The recovered serviceability q_r is assumed equal to the initial serviceability q_0;
- Restoration time (T_r): It is the time needed to finish the recovery process. This value is usually determined using probabilistic or statistical approaches.

A list of importance factors (I) has been set as default in the software. At the indicator level, the users can change the importance factors between 1 and 3 according to their preference. The importance factors can also be set all to "1" in case the user finds no justification to change the weights of the indicators; in this case, the indicators will be equally weighted. The importance factors at the level of dimensions and components have been set by default to the program according to Table 19 and Appendix A, respectively. In this software, the community type has been considered by default as an urban community. Future works will focus to include different types of communities inside the software.

Virtual City

- 1. Population and demographics
- 2. Environmental and ecosystem
- 3. Organized governmental services
- 4. Physical infrastructure
- 5. Lifestyle and community competence
- 6. Economic development
- 7. Social-cultural capital
- The community resilience curve

1.1 Distribution/Density — Importance: 3

Index	Indicator	Measure	I	Nat	q_{0u}	SV	q_0	q_1	q_r	T_r
1.1.1	Population density	1-(Average number of people per area ÷ SV)	3	D	q0u	sv	q0	q1	qr	tr
1.1.2	Population distribution	% population living in urban area	2	D	q0u	sv	q0	q1	qr	tr

1.2 Composition — Importance: 2

Index	Indicator	Measure	I	Nat	q_{0u}	SV	q_0	q_1	q_r	T_r
1.2.1	Age	% population whose age is between 18 and 65	3	S	q0u	sv	q0	-	-	-
1.2.2	Place attachment-not recent immigrants	1-(% population not foreign-born persons who came within previous five years)	1	S	q0u	sv	q0	-	-	-
1.2.3	Population stability	1-% population change over previous five year period	2	S	q0u	sv	q0	-	-	-
1.2.4	Equity	% nonminority population – % minority population	3	S	q0u	sv	q0	-	-	-
1.2.5	Race/Ethnicity	1-Absolute value of (% white – % nonwhite)	1	S	q0u	sv	q0	-	-	-
1.2.6	Family stability	% two parent families	2	S	q0u	sv	q0	-	-	-
1.2.7	Gender	Absolute value of (%female–%male)	1	S	q0u	sv	q0	-	-	-

1.3 Socio-Economic Status — Importance: 2

Index	Indicator	Measure	I	Nat	q_{0u}	SV	q_0	q_1	q_r	T_r
1.3.1	Educational attainment equality	% population with college education – % population with less than high school education	3	S	q0u	sv	q0	-	-	-

Figure 54. User interface and data entry environment.

The nature of the indicator "Nat" can also be changed by the user because this parameter depends on the type of hazard and type of community considered in the analysis. If the indicator is *Static 'S'*, it is enough for the user to insert data about the initial serviceability of the system q_{0u}, and the standard value *SV*. If the indicator is *Dynamic 'D'*, the user should proceed and insert data about the post-event damage q_1, serviceability level after restoration q_r, and restoration time T_r. The parameter q_{0u} is inserted as un-normalized value while other serviceability parameters q_1 and q_r have to be normalized by the user with respect to *SV* (by dividing over *SV*). A serviceability curve for each component is shown at the

bottom of the page when filling all data. The serviceability curve of the analyzed dimension, which is the weighted average of all serviceability functions of the components, is also shown on the same graph.

After inserting all the required data for all the dimensions, the user will be able to see the resilience graph of the community by clicking on the 'The community resilience curve' on the left side of the screen. For each of the serviceability curves, the software automatically evaluates the *LOR*, which is an indicator for the serviceability loss incurred during the event.

One of the main challenges that needs to be included in the next version of the software, is how to consider interdependency factors between different variables. The current version of the software is not able to include interdependency factors, as only the importance factors can be defined. In order to solve this problem, all the importance factors (I_i) can be set as 1, which means all variables will be equally weighted. Therefore, user must normalize directly the serviceability functions (q_0, q_1, q_r) by multiplying the weighting factors (w_i) obtained from Equation (24). However, in the case that the user is not interested to consider the interdependency analysis (i.e. not considering λ_i), the current form of software is suitable by defining only importance factors (I_i).

6.3 Case study: virtual city resilience computation

The resilience of the virtual city is evaluated using the proposed resilience methodology in this section. The Norcia earthquake scenario, which is characterized by a moment magnitude of 6.5 M_w, is considered as the disaster event. Only the 'Physical Infrastructure' (D_4) has been considered in the case study for simplicity reasons. Thus, a resilience function for each variable under this dimension is computed to calculate the total virtual city resilience index. Later, two different approaches including increasing the system robustness and reducing the recovery time have been explored to improve the virtual city resilience. It is worth to mention that the case study shows only the applicability of the proposed methodology and not the actual evaluation of the resilience.

6.3.1 Physical infrastructures (*D4*)

The 'Physical infrastructure' dimension has two components including 'Facilities' (C_{4-1}) and 'Lifelines' (C_{4-2}). Each component has different indicators that are linked to measures to describe the indicators numerically using a set of parameters. To aggregate the different variables (including group of indicators and group of components), interdependency analyses for each group of variables should be performed. This requires creating two interdependency matrices for each group of indicators under the components and an interdependency matrix for two components.

Table 21 and Table 22 show the interdependency matrices for groups of indicators under the 'Facilities' and 'Lifelines' components, respectively. The report by the National Institute of Standards and Technology (NIST 2015) and the

Lifelines Council (CCSF Lifelines Council 2014) have been used to fill the interdependency matrix for the group of indicators under 'lifelines', while questionnaires and recommendations of some expertswere used to create the 'Facilities' interdependency matrix.In each matrix, the number '1' represents a significant interdependency while '0' means limited interaction and interdependency between the variables.

Table 21. Matrix of interdependency for indicators under component 'Facilities'.

Indicators		Interdependency coefficient							
		$I_{4.1.1}$	$I_{4.1.2}$	$I_{4.1.3}$	$I_{4.1.4}$	$I_{4.1.5}$	$I_{4.1.6}$	$I_{4.1.7}$	$I_{4.1.8}$
Sturdy (robust) housing	$I_{4.1.1}$	1	0	1	0	0	0	0	0
Temporary housing availability	$I_{4.1.2}$	0	1	1	0	0	0	0	0
Housing stock construction quality	$I_{4.1.3}$	0	0	1	0	0	0	0	0
Community services	$I_{4.1.4}$	1	0	1	1	1	1	1	1
Economic infrastructure exposure	$I_{4.1.5}$	0	0	1	0	1	1	0	0
Distribution commercial facilities	$I_{4.1.6}$	0	0	0	0	1	1	0	0
Hotels and accommodations	$I_{4.1.7}$	0	0	1	0	0	0	1	0
Schools	$I_{4.1.8}$	0	0	1	0	0	0	0	1

Table 22. Matrix of interdependency for indicators under component 'Lifelines'.

Indicators		Interdependency coefficient												
		$I_{4.2.1}$	$I_{4.2.2}$	$I_{4.2.3}$	$I_{4.2.4}$	$I_{4.2.5}$	$I_{4.2.6}$	$I_{4.2.7}$	$I_{4.2.8}$	$I_{4.2.9}$	$I_{4.2.10}$	$I_{4.2.11}$	$I_{4.2.12}$	$I_{4.2.13}$
Telecommunication	$I_{4.2.1}$	1	0	0	0	0	0	1	1	0	0	1	1	0
Mental health support	$I_{4.22}$	0	1	0	1	0	0	0	0	0	0	0	0	0
Physician access	$I_{4.2.3}$	0	0	1	1	0	0	0	0	0	0	0	0	0
Medical care capacity	$I_{4.2.4}$	1	0	1	1	0	0	0	1	1	1	0	1	1
Evacuation routes	$I_{4.2.5}$	0	0	0	0	1	1	0	1	1	1	0	1	1
Industrial re-supply potential	$I_{4.2.6}$	0	0	0	0	1	1	0	1	0	0	1	1	0
High-speed internet infrastructure	$I_{4.2.7}$	1	0	0	0	0	0	1	1	0	0	0	0	0
Efficient energy use	$I_{4.2.8}$	0	0	0	0	0	0	0	1	1	0	1	0	0
Efficient Water Use	$I_{4.2.9}$	1	0	0	0	0	0	0	1	1	0	1	1	1
Gas	$I_{4.2.10}$	1	0	0	0	0	0	0	1	1	1	1	1	1
Access and evacuation	$I_{4.2.11}$	1	0	0	0	1	0	0	1	1	1	1	1	1
Transportation	$I_{4.2.12}$	1	0	0	0	1	1	0	1	0	1	1	1	0
Waste water treatment	$I_{4.2.13}$	1	0	0	0	0	0	0	1	1	0	1	1	1

The interdependency factor (λ_i) for each indicator has been calculated using Equation (20) and the results have been used to calculate finally the weighting

94

factor (w_i) for each indicator. The weighting factors have been obtained using Equation (24) including contribution of both interdependency factors (λ_i) and importance factors (I_i). The results for 'Facilities' and 'Lifelines' components have been presented in Table 23 and Table 24, respectively.

The weighting factors represent the contribution of each indicator in the overall resilience of the component. They are used to allow the combination of different indicators by normalizing the serviceability functions (q_o and q_1).

Table 23. Interdependency factor (λ), importance factor (I), and weighting factors (w) for indicators under component 'Facilities'.

Indicator	interdependency factor (λ)	importance factor (I)	weighting factor (w)
Sturdy (robust) housing	0.29	3	0.81
Temporary housing availability	0.14	3	0.41
Housing stock construction quality	1.00	3	2.85
Community services	0.14	2	0.27
Economic infrastructure exposure	0.43	2	0.81
Distribution commercial facilities	0.43	3	1.22
Hotels and accommodations	0.29	3	0.81
Schools	0.29	3	0.81

Table 24. Interdependency factor (λ), importance factor (I), and weighting factors (w) for indicators under component 'Lifelines'.

Indicator	interdependency factor (λ)	importance factor (I)	weighting factor (w)
Telecommunication	0.73	3	1.56
Mental health support	0.09	2	0.13
Physician access	0.18	2	0.26
Medical care capacity	0.27	3	0.59
Evacuation routes	0.36	2	0.52
Industrial re-supply potential	0.27	3	0.59
High-speed internet infrastructure	0.18	3	0.39
Efficient energy use	1.00	3	2.15
Efficient Water Use	0.64	3	1.37
Gas	0.45	3	0.98
Access and evacuation	0.73	3	1.56
Transportation	0.82	3	1.76
Waste water treatment	0.55	3	1.17

Data collection corresponding to the serviceability function (q_{0u}) and standard value (SV) is the most challenging part of the analysis since data about the serviceability of community systems is scarce and not shareable with the public. However, interested parties, such as decision makers and authorities, can use the framework with its full potential since data is usually available to them. In this

study, the parameters have been obtained using open database sources such as Data World Bank, City Data, Census Data, City Assessor's Data, and Dept of Numbers. Since the case study aims to show only the applicability of the proposed methodology for a virtual city, for some indicators that the data was not found in literature, a number according to past earthquake data has been assumed.

Table 25 summarizes the serviceability parameters of the indicators within the 'Physical Infrastructure' dimension for the virtual city. In this table, q_{0u} is the un-normalized initial serviceability of the measure. The normalization of this quantity is necessary in order to combine it with the other measures that fall in the same group. This is done by dividing the un-normalized serviceability q_{0u} over the standard value (SV). Right after the disaster, the serviceability function of a dynamic measure drops to q_1 (see Figure 50b). In this example, the recovered serviceability q_r is assumed equal to the initial serviceability q_0. It is worth to note that not all facilities can be restored immediately after the disaster due to limitation of resources (financial, man power, etc.) and due to the lack of recovery plans. In addition, restoring some facilities is sometimes done in series with (after the completion of) other facilities, which poses some delay to the restoration process.

The restoration time (T_r) is usually determined using probabilistic or statistical approaches. In this case study, restoration fragility curves recently developed by Kammouh et al. (2017) have been used to determine the restoration time for the different variables. In their work, they introduced an empirical probabilistic model to estimate the downtime of lifelines following an earthquake. Different restoration functions were derived for various earthquake magnitudes using a large earthquake database that contains data on the downtime of infrastructures. These functions were presented in terms of probability of recovery versus time. The downtime corresponding to 95% of exceedance probability of recovery has been used as a deterministic downtime for the considered infrastructure. As for the rate of restoration, in this section a linear interpolation is assumed for all measures.

Table 25. Serviceability parameters of the indicators within the Physical Infrastructure dimension for the virtual city after Norcia earthquake scenario.

Component /indicator	Measure	N.	q_{0u}	SV	q_0	q_1	q_r	T_r (days)
4.1 Facilities								
4.1.1 Sturdy (robust) housing types	% housing units that are not manufactured homes	D	1	1	1.00	0.60	1.00	120
4.1.2 Temporary housing availability	% vacant units that are for rent	D	1.55	5	0.31	0.08	0.31	620
4.1.3 Housing stock construction quality	100-% housing units built prior to 1970	D	0.351	1	0.35	0.15	0.35	700
4.1.4 Community services	%Area of community services (recreational facilities, parks, historic sites, libraries, museums) total area ÷	D	0.18	0.2	0.90	0.35	0.90	430

96

			q_{0u}	SV	q_0	q_1	q_r	T_r
4.1.5 Economic infrastructure exposure	% commercial establishments outside of high hazard zones ÷ total commercial establishment	S	0.64	1	0.64	-	0.64	-
4.1.6 Distribution commercial facilities	%Commercial infrastructure area per area ÷ SV	D	0.12	0.15	0.80	0.48	0.80	160
4.1.7 Hotels and accommodations	Number of hotels per total area ÷ SV	D	115	128	0.90	0.52	0.90	130
4.1.8 Schools	Schools area (primary and secondary education) per population ÷ SV	D	112	140	0.80	0.48	0.80	90
4.2 Lifelines								
4.2.1 Telecommunication	Average number of Internet, television, radio, telephone, and telecommunications broadcasters per household ÷ SV	D	5.5	6	0.92	0.50	0.92	90
4.2.2 Mental health support	number of beds per 100 000 population ÷ SV	D	66	75	0.88	0.64	0.88	40
4.2.3 Physician access	Number of physicians per population ÷ SV	S	2.8	3	0.93	-	0.93	-
4.2.4 Medical care capacity	Number of available hospital beds per 100000 population ÷ SV	D	440	600	0.73	0.64	0.73	40
4.2.5 Evacuation routes	Major road egress points per building ÷ SV	S	0.45	1	0.45	-	0.45	-
4.2.6 Industrial re-supply potential	Rail miles per total area ÷ SV	D	4890	6000	0.82	0.63	0.82	50
4.2.7 High-speed internet infrastructure	% population with access to broadband internet service	D	0.9	1	0.90	0.45	0.90	300
4.2.8 Efficient energy use	Ratio of Megawatt power production to demand	D	0.75	1	0.75	0.16	0.75	30
4.2.9 Efficient Water Use	Ratio of water available to water demand	D	0.9	1	0.90	0.24	0.90	60
4.2.10 Gas	Ratio of gas production to gas demand	D	0.8	1	0.80	0.05	0.80	70
4.2.11 Access and evacuation	Principal arterial miles per total area ÷ SV	D	187212	2e5	0.94	0.60	0.94	50
4.2.12 Transportation	Number of rail miles per area ÷ SV	D	5891	6000	0.98	0.63	0.98	80
4.2.13 Waste water treatment	Number of WWT units per population ÷ SV	D	3.7	4	0.93	0.30	0.93	70

- Note: q_{0u} = initial serviceability; SV = standard value; q_0 = initial normalized serviceability; q_1 = post disaster serviceability; q_r = recovered serviceability; T_r = restoration time.

The weighted serviceability functions are combined and the final resilience curve for the 'Facilities' component is shown in Figure 55. It illustrates that the serviceability of the 'Facilities' prior to earthquake is about 63.2%. After the earthquake, the serviceability function of a 'Facilities' drops to 36.8%. In addition, Figure 55 shows that the serviceability function of 'Facilities' can be

recovered to 53.3% after 120 days. This figure graphically can help decision makers to distribute better the resources for a more efficient restoration process.
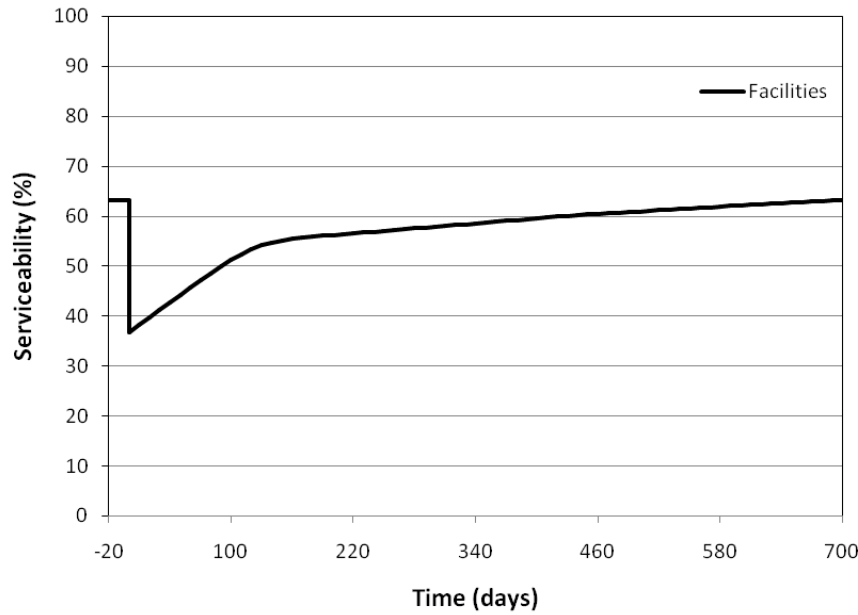
Figure 55. Resilience curve of component 'Facilities' for the virtual city.

The loss of resilience corresponding to 'Facilities' component ($LOR_{facilities}$) can be calculated using Equation (2):

$$LOR_{Facilities} = \int_{t_0=0}^{t_0=700} \frac{[100-Q(t)]}{T_C} dt = 44.79\% \qquad (25)$$

The time interval for calculation of resilience is considered from the time that the event occurs ($t_0=0$) until the end of full recovery ($t_1=t_r=700$ days). The control time (T_c) can be determined based on the user's period of interest and in this example is set equal to t_r ($T_c=700$days).

The same procedure has been applied to 'Lifelines' component and the combined resilience curve is shown in Figure 56. It illustrates that the serviceability of the 'Facilities' prior to earthquake is about 85.8%, while after the earthquake, it drops to 41.3%. In addition, Figure 56 shows that the serviceability function of 'Facilities' can be recovered to the preliminary functionality (84.3%) after 80 days of recovery. This graph shows that, despite there is one indicator 'High-speed internet infrastructure' with recovery time of 300 days, the component mostly can be recovered after 80 days. It is due to the effect of indicators aggregation considering different weighting factors. The weighting factor for 'High-speed internet infrastructure' with respect to the other indicators such as 'Efficient energy use' or 'Transportation' is much lower (see Table 24). Thus, the overall serviceability of the system and its corresponding recovery time is mostly dependent on indicators with higher weighting factors. This graphical information can help community decision makers to better plan their restoration strategies.

98
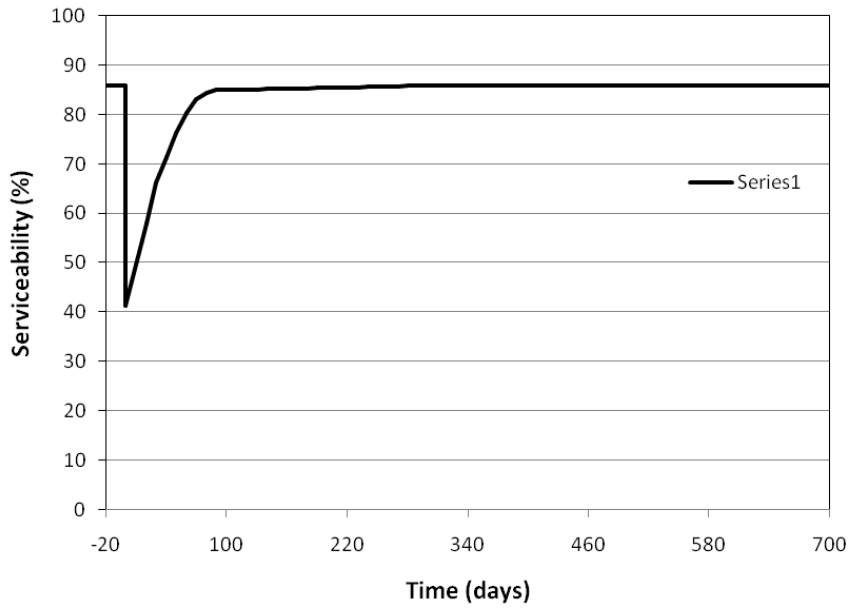
Figure 56. Resilience curve of component 'Lifelines' for the virtual city.

The loss of resilience corresponding to 'Lifelines' component ($LOR_{lifelines}$) has been calculated using Equation (2):

$$LOR_{Lifelines} = \int_{t_0=0}^{t_0=700} \frac{[100-Q(t)]}{T_C} dt = 17.22\% \tag{26}$$

where the control time (T_c) has been considered equal to 700 days. It is clear that the virtual city has more problems in facilities ($LOR=44.79\%$) than lifelines ($LOR=17.22\%$); therefore, it is suggested that the authority focuses more on enhancing their facilities.

Finally, the total resilience of 'Physical infrastructure' dimension is calculated by combining the individual resilience curve for each component. For the purpose of aggregation, first the interdependency analysis has been performed.

Table 26 presents the matrix of interdependency for components under 'Physical infrastructure' dimension. This matrix is not a symmetric matrix and it shows that 'Facilities' is fully dependent on 'Lifelines' component while the 'Lifelines' is independent.

The interdependency factor (λ_i) for each component has been calculated using Equation (20) and the results have been used to calculate the weighting factors (w_i). Table 27 summarizes the results for the importance factor (I), interdependency factor (λ), and weighting factor (w) for each component. It shows the component 'Lifelines' has three times more contribution than the 'Facilities' toward the total dimension resilience.

Table 26. Matrix of interdependency for components under dimension 'Physical infrastructures'.

Component		interdependency coefficient	
		$C_{4.1}$	$C_{4.2}$
Facilities	$C_{4.1}$	1	1
Lifelines	$C_{4.2}$	0	1

Table 27. Interdependency factor (λ), importance factor (*I*), and weighting factors (*w*) for components under 'Physical infrastructure' dimension.

Component	interdependency factor (λ)	importance factor (*I*)	weighting factor (*w*)
Facilities	0.50	2	0.50
Lifelines	1.00	3	1.50

The total resilience for 'Physical infrastructure' dimension has been obtained similarly by combining 'Lifelines' and 'Facilities' components. The result has been presented in Figure 57. It shows that the combined curve is closer to the 'lifelines' component since it has more weighting factor. Thus, loss of resilience for 'Physical infrastructure' ($LOR_{Phys.inf.}$) setting control time (T_c) equal to 700 days is calculated:

$$LOR_{\text{Physic.infra.}} = \int_{t_0=0}^{t_0=700} \frac{[100-Q(t)]}{T_C} dt = 24.11\% \tag{27}$$

In order to compute the resilience index for the whole community, the serviceability functions of other dimensions must be calculated and aggregated similarly.
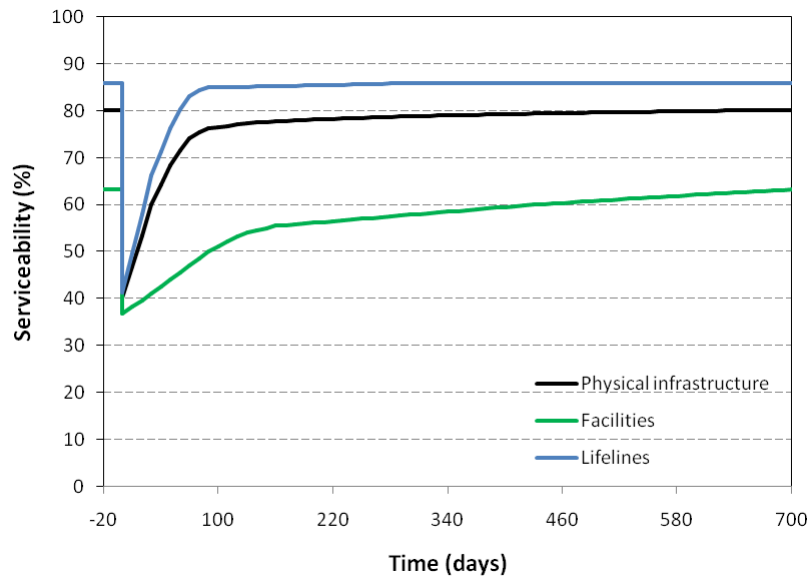
Figure 57. Resilience curve of 'Physical infrastructure' dimension for the virtual city.

6.4 Resilience improvement strategies

In this section, two different approaches including increasing the system robustness (first strategy) and reducing the recovery time (second strategy) have been explored to improve the virtual city resilience. The first strategy can increase directly the initial system serviceability (q_{0u}). Furthermore, it can enhance the post disaster serviceability (q_1) that leads to improve the overall system resilience. The second strategy can be achieved by better distribution of resources during the restoration phase. This leads to reduce the loss of resilience and therefore to increase the system functionality. To do that, the main challenge is first to determine the critical variables (i.e. indicators and components) that have more contribution toward the final resilience.

6.4.1 Increasing system robustness

In this example, it is assumed that initial functionality of some indicators is improved due to strengthening and robustness strategies. The two indicators corresponding to minimum and maximum weighting factors (see Table 23 and Table 24) among the group of indicators under each component have been selected. This will allow evaluating the influence of different indicators in total resilience index. Therefore, 'Housing stock construction quality' and 'community services' corresponding to maximum (w=2.85) and minimum (w=0.27) weighting factors have been selected among the group of indicators under 'Facilities' component (see Table 23). Similarly, 'Efficient energy use' (w=2.15) and 'Mental health support' (w=0.13) have been chosen as strengthening strategy for group of indicators under 'Lifelines' component (see Table 24). In addition, to show better the effect of different indicators, other two indicators with a weighting factor close to the median value have been selected. Thus, 'Schools' and 'Gas' indicators are also considered.

For each indicator the initial strengthened serviceability (q^*_{0u}) is considered equal to standard value (SV) due to performing retrofitting plans, so that the initial normalized serviceability (q^*_0) will be equal to 100%. Furthermore, it is assumed the post disaster serviceability (q^*_r) will be improved by 30%. This is only an assumption to perform a parametric study to show how the methodology enables including retrofitting strategies. The recovery time (T_r) in analysis has been sets same as before. Table 28 lists the strengthening plans and corresponding indicator's parameters.

To evaluate how each indicator improves, the loss of resilience for each indicator individually before retrofitting and after strengthening is calculated and the result is presented in Table 29. It is clear that the strategy 1 is more efficient in decreasing the indicator loss of resilience, since the initial normalized serviceability function of 'Housing stock construction quality' with respect to the other indicators (strategies 2-6) was much lower before strengthening.

Table 28. System strengthening plan and related serviceability parametrs.

Strategy	Component	Strengthened indicator	w	q_{0u}	q^*_{0u}	SV	q^*_0	q^*_1	q^*_r	T_r days
1	Facilities	Housing stock construction quality	2.85	0.35	1	1	1.0	0.195	1.0	700
2	Facilities	Schools	0.81	112	140	140	1.0	0.624	1.0	90
3	Facilities	Community services	0.27	0.18	0.2	0.2	1.0	0.455	1.0	430
4	Lifelines	Efficient energy use	2.15	0.75	1	1	1.0	0.208	1.0	30
5	Lifelines	Gas	0.98	0.80	1	1	1.0	0.065	1.0	70
6	Lifelines	Mental health support	0.13	66	75	75	1.0	0.837	1.0	40

Table 29. Loss of resilience for different strengthening strategies for each individual indicator.

Strategy	Component	Strengthened indicator	Not-strengthened ($LOR\%$)	Strengthened ($LOR^*\%$)
1	Facilities	Housing stock construction quality	78.13	40.83
2	Facilities	Schools	23.18	2.69
3	Facilities	Community services	27.71	17.13
4	Lifelines	Efficient energy use	27.76	2.26
5	Lifelines	Gas	25.14	5.34
6	Lifelines	Mental health support	13.36	0.58

The total resilience for each component corresponding to different strengthening strategies is obtained by combining indicator's serviceability functions. Figure 58 and Figure 59 show the comparison of resilience curves for 'Facilities' and 'Lifelines' components for different strengthening strategies. It shows that most efficient strategies are 'strategy 1' and 'strategy 4' in which the indicators with higher waiting factors were rehabilitated. Furthermore, the total loss of resilience (*LOR*) corresponding different strategies has been calculated and the result is presented in Table 30. The total loss of resilience for the original system (non-strengthened) for the 'Facilities' and 'Lifelines' are 44.79% and 17.22%, respectively (Equation (25) and Equation (26)). For 'Facilities', strengthening the 'Housing stock construction quality' reduces *LOR* about 13.1% while the other strategies were less efficient. Similarly, 'strategy 4' can increase the virtual city resilience by reducing 4.2% of *LOR*.

Comparing the results between strategies 1 and 4, it can be stated that strategy 1 is more efficient due to three major reasons: 1) the percentage of initial serviceability improvement for 'Housing stock construction quality' with respect to the other indicators is higher (see Table 28); 2) it has higher weighting factors comparing to strategy 4 (see Table 28); and 3) the standard deviation of weighting factors related to group of indicators under 'Facilities' ($\sigma_{wi,facilities} = 0.80$) is greater than the corresponding number for the 'lifelines' ($\sigma_{wi,lifelines} = 0.64$). It causes more contribution for 'Housing stock construction quality' toward the final resilience.

Table 30. Total loss of resilience (*LOR*) corresponding to each strengthening
strategy.

Strategy	Component	Strengthened indicator	*LOR%*
1	Facilities	Housing stock construction quality	31.58
2	Facilities	Schools	42.81
3	Facilities	Community services	44.53
4	Lifelines	Efficient energy use	13.07
5	Lifelines	Gas	15.73
6	Lifelines	Mental health support	17.09
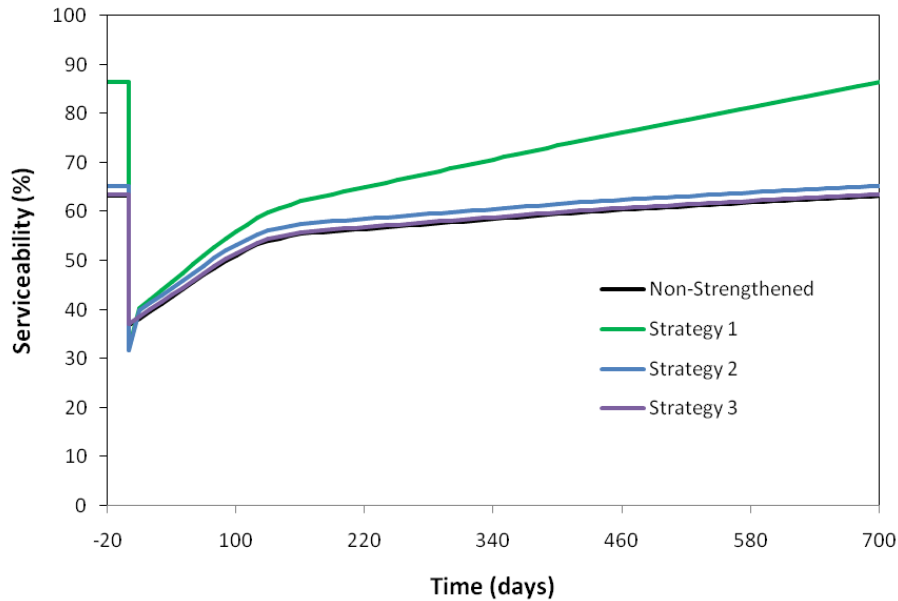
Figure 58. Resilience curves for 'Facilities' corresponding to different
strengthening strategies.
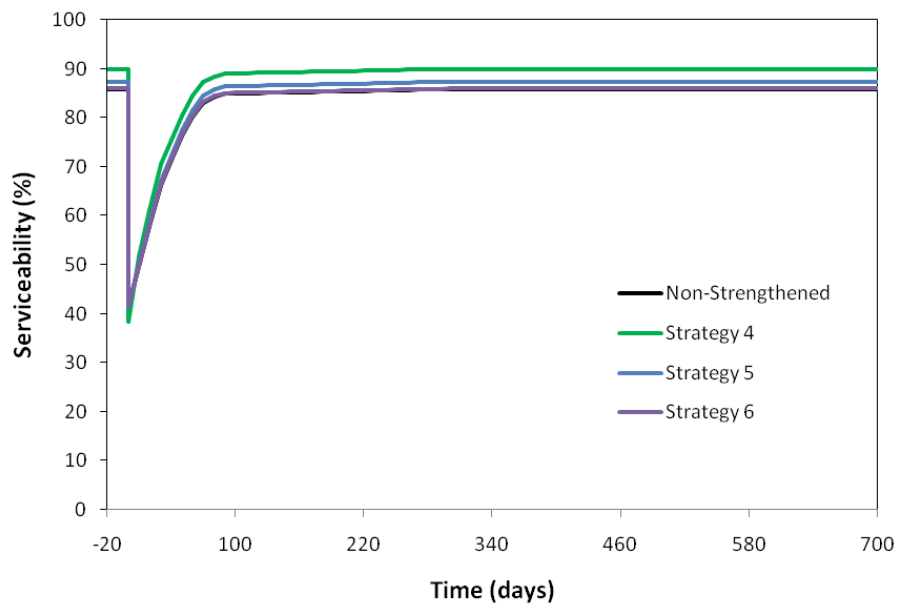
Figure 59. Resilience curves for 'Lifelines' corresponding to different
strengthening strategies.

103

6.4.2 Reducing recovery time

As another solution to improve the virtual city resilience, the effect of improvement in recovery time is studied. To do that, recovery time for the six indicators identified in the previous section is reduced and the total loss of resilience for each component has been computed. For each strategy, the recovery time is reduced in a way that the loss of resilience (*LOR*) for each indicator remains same as the loss of resilience corresponding to the strengthening strategies. Figure 60 shows schematically the strategies for reducing recovery time and strengthening. The reduced recovery time is calculated considering that the area enclosed by ABCD in Figure 60a should be same as the area enclosed byABC in Figure 60b.In this case, it is possible to compare the effectiveness of reducing recovery time strategies with the results of strengthening plans. The new reduced recovery time (T_r*) can be obtained by:

$$T_r* = \frac{LOR_{Strength}}{100 - 0.5*(q_{0,r} - q_{1,r})} \tag{28}$$

where T_r* is the new reduced recovery time, $LOR_{strength}$ is the loss of resilience corresponding to strengthening strategies, q_0 and q_1 are initial and post disaster serviceability, respectively.

Six new plans (strategy 7-12) for improvement the system resilience by reducing recovery time have been considered. The new recovery time (T_r*) for each strategy is obtained using Equation (28) and results have been presented in Table 31. The other serviceability parameters such as q_{0u}, SV, q_0, q_1, q_r, and T_r considered same as Table 25 in computation of resilience.

Table 31. Strategies for improvement of recovery time.

Strategy	Component	Strengthened indicator	T_r (days)	T_r* (days)
7	Facilities	Housing stock construction quality	700	286
8	Facilities	Schools	90	19
9	Facilities	Community services	430	120
10	Lifelines	Efficient energy use	30	16
11	Lifelines	Gas	70	37
12	Lifelines	Mental health support	40	4

The total resilience of each component for each strategy is computed by combining indicator's serviceability functions. In order to compare different strategies effectiveness, loss of resilience for each strategy has been calculated and results have been presented in Table 32. It shows that the strategies corresponding to indicators with higher weighting factors (strategy 7 and strategy 10) are considered more efficient because they have more contribution in total resilience. In addition, comparing the results provided in Table 30 and Table 32, strengthening strategies were more efficient with respect to the reduction of recovery time plans. This parametric analysis can help the community planner to

organize better the retrofitting strategies and allocate better the resources to where can improve more the community resilience.
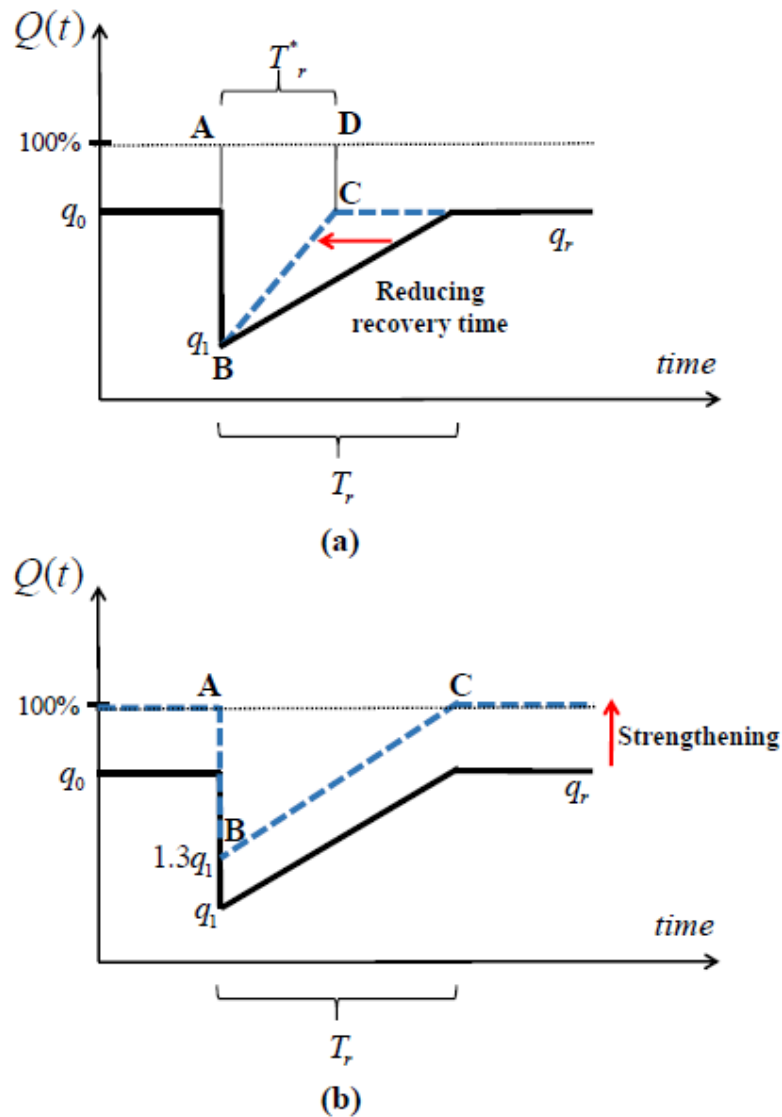
Figure 60. Improving recovery time strategy (a) and increasing system robustness (b) to increase the virtual city resilience.

Table 32. Total loss of resilience (*LOR*) corresponding to each reducing recovery time strategy.

Strategy	Component	indicator	*LOR%*
7	Facilities	Housing stock construction quality	36.67
8	Facilities	Schools	42.63
9	Facilities	Community services	44.38
10	Lifelines	Efficient energy use	17.08
11	Lifelines	Gas	17.10
12	Lifelines	Mental health support	17.18

In this chapter an indicator-based approach to compute the community resilience using the PEOPLES framework structure was proposed. Each indicator is defined with a dynamic measure illustrating the functionality of indicator over the time. Then, the indicators were aggregated into a single functionality function, which describes the functionality of the whole community. The methodology was applied to the virtual city to evaluate the resilience of physical infrastructure under Norcia earthquake scenario. To enhance the city resilience, two strategies including 'increasing system robustness' and 'reducing recovery time' were studied. Results show the effectiveness of the proposed methodology to indicate in detail whether the resilience deficiency is caused by the system's lack of robustness or by the slow restoration process.

Chapter 7

Concluding remarks

7.1 Summary

In this dissertation, a computational framework was developed for a comprehensive and efficient assessment of the impacts to the building asset caused by a seismic event at the urban scale. The methodology aims at representing the complex problem of quantifying earthquake damage to a city-level community by characterizing a building portfolio as a system of interconnected components.

Existing earthquake-induced damage assessment methodologies were reviewed and four main aspects were identified to be addressed in the proposed approach: 1) provide an analytical approach to evaluate appropriately the response of each single building; 2) explicit modeling of uncertainties associated with mechanical and geometrical parameters of an individual building; 3) modeling of spatial buildings distribution for a variety of possible earthquake scenarios; 4) computational efficiency. In the end, an indicator-based model was developed to evaluate the resilience of communities considering multiple dimensions and an interdependence matrix approach using PEOPLES framework.

A virtual city was designed based on the buildings stock of the city of Turin in Italy as testbed to validate the developed methodology. To build the city's database, the structural design parameters were determined according to the seismic design codes associated to buildings' year of construction, while the average mechanical, geometrical, and construction parameters were identified through a typological approach for each building.

In the proposed simulation model, the dynamic structural responses of each single building were evaluated through a tri-linear backbone curve for a MDOF system. The methodology explicitly included the uncertainties related to buildings' geometric and mechanical parameters, and hazard intensities. A global capacity curve representative of the seismic behavior of each building was

evaluated taking into account the aleatory uncertainties associated with building attributes. MCSs were performed by repeating random input sampling and, thus, the median global capacity curve for each individual building was obtained. The proposed methodology was applied to the virtual city and the fragility curves representative of the probability of buildings' failure given a damage state as a function of the earthquake intensity were developed. As expected, results show that the level of the damage is directly proportional to the building's year of construction. This is consistent with the fact that recent design codes have more stringent seismic design requirements. In virtual city, masonry buildings were mostly designed according to old design codes where either there was no seismic design procedure or less seismic design requirements. Also, results confirm that the main share of damaged buildings to the city belongs to masonry buildings rather than reinforced concrete ones.

To enable computation of the likely casualty rates of the city inhabitants, a human casualty assessment model based on HAZUS methodology was developed combining the collapse fragility data for typical built inventory with the occupancy data. Results show that the expected number of casualties inside masonry buildings is about four times more than the one referred to concrete buildings. This is due to the fact that in the virtual city masonry buildings are more vulnerable than concrete buildings. Furthermore, the defined casualty coefficient by HAZUS specific to masonry buildings, are mostly higher (about twice) than the one referred to concrete buildings

The proposed simulation model was then extended to assess the resilience of a hospital network in virtual city combining the casualty model. The goal is to develop a risk-informed model for patient arrival rate taking into account the geography, hazard intensity, and inventory distribution of the virtual city. Two different solutions were proposed in order to make the city capable of managing the post-earthquake scenarios. The two approaches evaluate the optimal recovery plan that increases the resilience of healthcare facilities, so that all Emergency Departments can guarantee timely and efficient care to all the injured. The described method helps to estimate the capacity of cities' emergency network and provides an efficient and simple tool for evaluating the first order response of the healthcare facilities of a city.

Finally, a new indicator-based methodology for computing community resilience based on PEOPLES framework was introduced. The approach evaluates a multitude of resilience dimensions with the intent to quantify the community properties in each dimension using indicator values. Two different weights based on the importance and interdependency factors are assigned to each variable to allow aggregation of the variables in a same level. The methodology was applied to virtual city to measure the resilience of the physical dimension. The approach is deterministic and allows to understand how different dimensions of a community, considered within PEOPLES framework, affect community disaster resilience. Two objectives, namely 'increasing the system robustness' and 'reducing recovery time', were set as targets to see the effectiveness of the proposed methodology. Results show that 'increasing system robustness' strategy is more

efficient than the 'reducing recovery time' one in improving the resilience of the virtual city. In addition, an open-source tool was developed to compute the community resilience combining the resilience curves for individual elements of the community into a final measure. The methodology presented in this dissertation is considered a promising attempt to evaluate the resilience of any system ranging from small to large-scale community.

7.2 Originality

This dissertation has two primary objectives: 1) the definition of a simulation model to evaluate the earthquake-induced damage to a building portfolio for a variety of possible earthquake scenarios; 2) the development of a model to quantify the community resilience based on an indicator approach.

The first objective was achieved by implementing mathematical simulation models and nonlinear time history analysis to assess the vulnerability of each individual building of an urban area. The new advancements in the proposed approach relative to existing methods include:

1) **Analytical formulation**: the existing simulation models evaluate vulnerability of building stock by using fragility curves available from the literature or by development of fragility curves specific to group of buildings classified according to the height of the building, year of construction, structure type etc. It is too approximate, however, to assume all buildings under the same category will experience an identical level of damage given an earthquake. The response of each building exclusively depends on building specific parameters. The proposed simulation model leads to an accurate identification of the capacity curve for each building without losing accuracy and consistency with the expected results.

2) **Uncertainties**: many existing simulation models limit the inclusion of the uncertainties by alternating the fragility curves used for vulnerability assessment (e.g. changing structural system type). While, there are several uncertainties associated with building material characteristics, structural element design parameters, building geometry and occupancy type, that can affect the capacity curve and therefore the vulnerability assessment of a building. The proposed simulation model is able to explicitly model aleatory uncertainties associated with construction elements, mechanical and geometrical parameters.

3) **Modeling spatial distribution**: the inclusion of correlations between spatial distribution of the building portfolio, buildings' level of damage, and hazard intensity is one of the strengths of the proposed methodology. These correlations are shown to be very significant in computing the variance of total loss specifically in the calculation of the interaction with other infrastructures (e.g. hospital network).

4) **Computational efficiency**: a notable advantage in using this simulation model is its computational efficiency. The proposed method significantly reduces

the computational and time efforts providing an efficient perspective to estimate the potential seismic vulnerability of a large-scale built environment.

The second objective of the dissertation is addressed using an indicator-based approach for computing community resilience based on PEOPLES framework. In this respect, the methodology offers the following advantages:

1) **Dynamic resilience analysis**: while all previous works generally provide a single index to measure community resilience, here a dynamic index is introduced in order to represent the community functionality over time (starting from the time right after the disaster to the end of the restoration process). Thus, multiple dynamic serviceability functions for different dimensions can be aggregated into the model.

2) **Interdependency analysis**: the inclusion of interdependencies between multitude dimensions of a community is one of the strengths of the discussed method. It is done by defining an interdependence matrix approach resulted from a weighting factor allowing the combination of different dimensions of a community.

3) **Graphical representation**: the presented graphical representation helps decision makers to take proper actions to improve community resilience. Providing the dynamic resilience index, it is possible to describe in details whether the resilience deficiency is caused by the system's lack of robustness or by the slow restoration process. It identifies where exactly resources should be spent to efficiently improve resilience.

7.3 Limitation and future research

Five main issues have been identified as potential shortcomings in using the proposed methodology for earthquake damage assessments. These are outlined below, accompanied by suggested future research steps to address these limitations.

1) **Data collection:** the definition of a comprehensive building database is the first step required by the simulation model. A detail database that includes buildings' geometry, height, archetype, occupancy, construction elements, structure type, and year of construction, is necessary to assess the vulnerability of each single building. In the case of large applications (e.g. regions, states), the aforementioned information is not easily available. Thus, different data acquisition approach such as satellite images and available GIS inventory data can be used. Further investigation would be required to develop more realistic modeling assumptions to limit the uncertainties and maintain computational efficiency.

2) **Simulation model:** the vulnerability of building portfolio is assessed through obtaining the global capacity curve for each single building and then by performing nonlinear time history analysis to evaluate its response under a given earthquake scenario. While results are fairly accurate, the procedure requires an excessive computational effort for larger application such as regional seismic loss

estimation. Future research aims at improving the procedure specifically for regional or country levels by estimating the building responses directly through capacity curves. To do that, SPO2IDA methodology proposed by Vamvatsikos and Cornell (2006) can be adopted by connecting directly the capacity curve and the results of incremental dynamic analysis.

3) **Seismic scenario definition:** in this research, a simplified seismic input was defined in order to perform nonlinear time history analyses. This was used only to test and show the effectiveness of the proposed methodology. In future work this limitation needs to be overcome to obtain even more accuracy in the results. For example, a seismic hazard map of Intensity Measure parameters (e.g. PGA, response spectrum parameters) can be defined through soil response modeling.

4) **Hospital network:** some assumptions were made in the evaluation of the hospital network's resilience. These can certainly be corrected by means of additional data and accordingly the model should be improved. The damage to hospitals was neglected assuming that all hospitals remain fully functional after the earthquake. Future research aims at considering the effect of structural damage to the hospital for estimation of patient waiting time. In addition, the estimation of damage to non-structural components is another important aspect to address, since providing service to the patients strictly depends on availability of resources after the earthquake. A solution could consist in changing the values of m (number of available emergency room) corresponding to hospital damage state. Also, the serviceability of hospitals depends on functionality of critical infrastructures such as power and water networks. Further investigation would be required to develop more realistic modeling assumptions performing interdependency analysis between different infrastructures of the city.

5) **Resilience quantification:** the methodology is a deterministic approach and is operable only if indicators can be numerically quantified, which may not be the case in some situations. The methodology requires input data for each indicator including the system initial functionality, level of damage after disaster (post-disaster functionality), and recovery time. Some of these can be obtained from vulnerability assessment but some are not easily accessible. Future studies can focus in the implementation of a method that does not require detailed deterministic data to compute the resilience of a community. Probabilistic indicator-based resilience metrics using the fuzzy logic-based modeling of PEOPLES indicators can be used in accordance with the level of details available. Moreover, the open source resilience tool will be improved to enable users to perform interdependency analysis, including the uncertainties in input data.

References

Abeling, T., Huq, N., Wolfertz, J., Birkmann, J. (2014). Interim Update of the Literature. Deliverable 1.3, *emBRACE project*.

Achour, N., Miyajima, M., Pascale, F., and DF Price, A. (2014). Hospital resilience to natural hazards. classification and performance of utilities. *Disaster prevention and management*, 23(1), 40-52.

AISC (2005). Specification for Structural Steel Buildings. AISC 360, American Institute of Steel Construction, Chicago, IL.

Allenby, B., Fink, J. (2005). Toward Inherently Secure and Resilient Societies Science 309.1034-1036 doi.10.1126/science.1111534

Alesch, D. J., Arendt, L. A., Petak, W. J. (2012). SB 1953. The Law, the Program, and the Implementation Challenge. *Natural Hazard Mitigation Policy*, Springer, 45-60.

Anders, S., Woods, D., Wears, R., Perry, S., and Patterson, E. (2006). Limits on adaptation. modeling resilience and brittleness in hospital emergency departments. *Symposium on Resilience Engineering*, 8-10.

ASCE. (2010). Minimum design loads for buildings and other structures. 7-10, Reston, VA.

Asprone, D., Jalayer, F., Prota, A., Manfredi, G. (2010). Proposal of a probabilistic model for multi-hazard risk assessment of structures in seismic zones subjected to blast for the limit state of collapse. *Structural Safety*, Volume 32, Issue 1, Pages 25-34.

ATC (2012). Seismic Performance Assessment of Buildings. *ATC-58, Applied Technology Council,* Redwood City, CA.

ATC-21. (2017). *Rapid visual screening of buildings for potential seismic hazards. A handbook*. Federal Emergency Management Agency, US. Government Printing Office.

Babrauskas, V., Krasny, J.F. (1985). Fire Behaviour of Upholstered Furniture. *NBS Monograph* 173 (U.S.), National Bureau of Standards.

Baker, J. W. (2010). Conditional mean spectrum. Tool for ground-motion selection. *Journal of Structural Engineering*, 137(3), 322-331.

Baker, J. W., Jayaram, N. (2008). Correlation of spectral acceleration values from NGA ground motion models. *Earthquake Spectra*, 24(1), 299-317.

Baker, J. W., ornell, A. (2006). orrelation of Response Spectral Values for Multicomponent Ground Motions. *Bulletin of the Seismological Society of America*, 96(1), 215–227.

Barbato, M., Petrini, F., Unnikrishnan, V.U., and Ciampoli, M. (2013). Performance-Based Hurricane Engineering (PBHE) framework. *Structural Safety*, 45, 24-35.

Beatley, T., Newman, P. (2013). Biophilic Cities Are Sustainable, Resilient Cities. *Sustainability*, 5(8), 3328.

Berardi, G., Paci-Green, R., Hammond, B. (2011). Stability, sustainability, and catastrophe. applying resilience thinking to US agriculture. *Research in Human Ec*ology, 18(2), 115.

Biggs, J. M. (1964). Introduction to structural dynamics, McGraw-Hill, New York.

Birkmann, J., UNU-EHS Expert Working Group on Measuring Vulnerability. (2006). Measuring vulnerability to natural hazards. towards disaster resilient societies. United Nations University New York.

Bonstrom, H., Corotis, R.B. (2016). First-Order Reliability Approach to Quantify and Improve Building Portfolio Resilience. *Journal of Structural Engineering* 142.C4014001 doi.doi.10.1061/(ASCE)ST.1943-541X.0001213.

Boore, D. M., Atkinson, G. M. (2008). Ground-motion prediction equations for the average horizontal component of PGA, PGV, and 5%-damped PSA at spectral periods between 0.01 s and 10.0 s. *Earthquake Spectra*, 24(1), 99-138.

Bosher, L. (2008). *Hazards and the built environment. attaining built-in* resilience. Routledge.

Bowman, A., Parsons, B.M. (2009). Vulnerability and resilience in local government. assessing the strength of performance regimes. State & Local Government Review, 13-24.

Bradley, D., Grainger, A. (2004). Social resilience as a controlling influence on desertification in Senegal. Land Degradation & Development, 15(5), 451-470.

Brody, S.D., Peacock, W.G., Gunn, J. (2012). Ecological indicators of flood risk along the Gulf of Mexico. Ecological Indicators, 18, 493-500.

Bruneau, M., Chang, S. E., Eguchi, R. T., Lee, G. C., O'Rourke, T. D., Reinhorn, A. M., Shinozuka, M., Tierney, K., Wallace, W. A., and Von Winterfeldt, D. (2003). A framework to quantitatively assess and enhance the seismic resilience of communities. Earthquake spectra, 19(4), 733-752.

Bruneau, M., Lopez-Garcia, D., and Fujikura, S. Multihazard-resistant highway bridge bent. *Proc., Proc., Structures Congress*, ASCE New York, 1-4.

Burton. C.G. (2015). A Validation of Metrics for Community Resilience to Natural Hazards and Disasters Using the Recovery from Hurricane Katrina as a Case Study. *Annals of the Association of American Geographers*, 105(1), 67-86.

Chandra, A., Acosta, J., Stern, S., Uscher-Pines, L., Williams, M.V. (2011). Building community resilience to disasters. A way forward to enhance national health security. Rand Corporation.

Chang, S.E., McDaniels, T., Fox, J., Dhariwal, R., Longstaff, H. (2014). Toward Disaster-Resilient Cities. Characterizing Resilience of Infrastructure Systems with Expert Judgments Risk Analysis 34.416-434.

Cimellaro, G.P. (2016). Urban Resilience for Emergency Response and Recovery. Springer.

Cimellaro, G. P., Malavisi, M., and Mahin, S. (2017). Using Discrete Event Simulation Models to Evaluate Resilience of an Emergency Department. *Journal of Earthquake Engineering*, 21(2), 203-226.

Cimellaro, G. P., and Marasco, S. (2015). A computer-based environment for processing and selection of seismic ground motion records. Opensignal. *Frontiers in Built Environment*, 1, 17.

Cimellaro, G.P., Reinhorn, A.M., and Bruneau, M. (2010a). Framework for analytical quantification of disaster resilience. *Engineering Structures*, vol. 32, pp. 3639-3649.

Cimellaro, G. P., Reinhorn, A. M., and Bruneau, M. (2010b). Seismic resilience of a hospital system. *Structure and Infrastructure Engineering*, 6(1-2), 127-144.

Cimellaro, G. P., Reinhorn, A. M., and Bruneau, M. (2011). Performance-based metamodel for healthcare facilities. *Earthquake Engineering & Structural Dynamics*, 40(11), 1197-1217.

Cimellaro, G.P., Renschler, C., Reinhorn, A.M., Arendt, L. (2016) PEOPLES. A Framework for Evaluating Resilience. *Journal of Structural Engineering*, 04016063.

Cimellaro, G.P., Solari, D., Bruneau, M. (2014). Physical infrastructure interdependency and regional resilience index after the 2011 Tohoku Earthquake in Japan. *Earthquake Engineering & Structural Dynamics*, 43 (12). 1763-1784.

Cimellaro, G.P., Tinebra, A., Renschler, C. and Fragiadakis, M. (2016b), New Resilience Index for Urban Water Distribution Networks. *Journal of Structural Engineering*, **142**(8). C4015014.

Cimellaro, G.P., Zamani-Noori, A., Kammouh, O., Terzic, V., Mahin, S.A. (2016a). Resilience of Critical Structures, Infrastructure, and Communities. *Pacific Earthquake Engineering Research Center (PEER)*, Berkeley, California.

Comerio, M.C. (2006), Estimating downtime in loss modeling, *Earthquake Spectra*, **22**(2). 349-365.

Computer and Infrastructure Inc. Sap2000, Version 17.3, Berkeley, CA.

Corrado, V., Ballarini, I., Corgnati, S.F. (2012). National scientific report on the TABULA activities in Italy. Politecnico di Torino.

Costin, N. S. (2014). Numerical simulation of detonation of an explosive atmosphere of liquefied petroleum gas in a confined space. Defence Technology, 10(3), 294-297.

Cumming, G.S., Barnes, G., Perz, S., Schmink, M., Sieving, K.E., Southworth, J., Van Holt, T. (2005). An exploratory framework for the empirical measurement of resilience. Ecosystems, 8(8), 975-987.

Cutter, S.L., Ash, K.D., Emrich, C.T. (2014). The geographies of community disaster resilience. *Global Environmental Change* , 29. 65-77.

Cutter, S.L., Barnes, L., Berry, M., Burton, C., Evans, E., Tate, E., Webb, J. (2008a). A place-based model for understanding community resilience to natural disasters. Global Environmental Change, 18(4), 598-606.

Cutter SL, Barnes L, Berry M, Burton C, Evans E, Tate E, Webb J (2008b). Community and regional resilience. Perspectives from hazards, disasters, and emergency management. Community and Regional Resilience Initiative (CARRI) Research Report, 1.

Cutter SL, Burton CG, Emrich CT (2010). Disaster resilience indicators for benchmarking baseline conditions. *Journal of Homeland Security and Emergency Management*, 7 (1).

Davis E, Phillips B (2009). Effective Emergency Management. Making Improvements for Communities and People with Disabilities. Washington, DC.

Delmonaco, G., Margottini C., and Spizzichino D. (2006). Report on new methodology for multi-risk assessment and the harmonisation of different natural risk maps. *Deliverable 3.1, ARMONIA*.

Didier, M., Broccardo, M., Esposito, S., & Stojadinovic, B. (2018). A compositional demand/supply framework to quantify the resilience of civil infrastructure systems (Re-CoDeS). *Sustainable and Resilient Infrastructure*, 3:2, 86-102, DOI: 10.1080/23789689.2017.1364560.

Didier M, Sun L, Ghosh S, Stojadinovi (2015). Post-earthquake recovery of a community and its electrical power supply system. 5th International Conference on Computational Methods in Structural Dynamics and Earthquake Engineering, Greece.

Downey, E. L., Andress, K., and Schultz, C. H. (2013). External factors impacting hospital evacuations caused by Hurricane Rita. the role of situational awareness. *Prehospital and disaster medicine*, 28(3), 264-271.

EC (2002). Eurocode 1. Actions on structures. Part 1-1. General actions - Densities, self-weight, imposed loads for buildings, EC1, European Committee for Standardization, Bruxelles, BG.

EC (2005). Design of steel structures - Part 1-2. General rules -Structural fire design. *EC3, European Committee for Standardization,* Bruxelles, BG.

EC2. (2004). Eurocode 2. Design of concrete structures-Part 1-2. General rules-Structural fire design. *European Standards, London*.

Fabbrocino G., Iervolino I., Orlando F., and Salzano E. (2005).Quantitative risk analysis of oil storage facilities in seismic areas. *Journal of Hazardous Materials*, Volume 123, Issues 1–3, Pages 61-69.

Félix D, Branco JM, Feio A (2013). Temporary housing after disasters. A state of the art survey. Habitat International, 40, 136-141.

FEMA (2000). Prestandard and Commentary for the Seismic Rehabilitation of Buildings.

FEMA 356, Federal Emergency Management Agency, Washington, D.C.

FEMA (2009). Effects of Strength and Stiffness Degradation on Seismic Response. FEMA P440A, Federal Emergency Management Agency, Washington, D.C.

FEMA (2011). HAZUS FEMA's methodology for estimating potential losses from disasters , FEMA Federal Emergency Management Agency, Washington, D.C.

FEMA P-58. (2012). Seismic Performance Assessment of Buildings. Vol. 1. Methodology. FEMA P-58.

Gernay, T., Khorasani, N. E., and Garlock, M. (2016). Fire fragility curves for steel buildings in a community context. a methodology. Engineering Structures, 113, 259-276.

Garshnek, V., and Burkle, F. M. (1999). Telecommunications systems in support of disaster medicine. applications of basic information pathways. *Annals of emergency medicine*, 34(2), 213-218.

Ghobarah, A. (2004). *On drift limits associated with different damage levels.* Paper presented at the Performance-Based Seismic Design Concepts and Implementation. Proceedings of the International Workshop, Bled, Slovenia.

Godschalk, D. R. (2003). Urban hazard mitigation. creating resilient cities. Natural hazards review, 4(3), 136-143.

Hilfinger Messias, DK, Barrington C, Lacy E (2012). Latino social network dynamics and the Hurricane Katrina disaster. Disasters, 36(1), 101-121.

Hori, M, Ichimura, T, Oguni, K. (2006). Development of Integrated Earthquake Simulation for estimation of strong ground motion, structural responses and human actions in urban areas.

Hosseini S, Barker K, Ramirez-Marquez JE (2016) A review of definitions and measures of system resilience *Reliability Engineering & System Safety* 145.47-61 doi.http.//dx.doi.org/10.1016/j.ress.2015.08.006

IAOGP (2010). Ignition probabilities. *Risk Assessment Data Directory*, International Association of Oil & Gas Producers, Report No. 434-6.1.

IOTWSP (2007). How resilient is your coastal community? A guide for evaluating coastal community resilience to tsunamis and other coastal hazards. Bangkok, Thailand. U.S. Agency for International Development.

Jacques, C. C., McIntosh, J., Giovinazzi, S., Kirsch, T. D., Wilson, T., and Mitrani-Reiser, J. (2014). Resilience of the Canterbury hospital system to the 2011 Christchurch earthquake. *Earthquake spectra*, 30(1), 533-554.

Jayaram, N., and Baker, J. W. (2010). Efficient sampling and data reduction techniques for probabilistic seismic lifeline risk assessment. *Earthquake Engineering & Structural Dynamics*, 39, 1109–1131.

Kafali C and Grigoriu M (2005), Rehabilitation decision analysis, In Proceedings of the Ninth International Conference on Structural Safety and Reliability (ICOSSAR'05).

Kammouh O, Cimellaro GP (2017). Restoration Time Of Infrastructures Following Earthquakes. *12th International Conference on Structural Safety & Reliability,* Vienna, Austria.

Kammouh O, Dervishaj G, Cimellaro GP (2017a). A New Resilience Rating System for Countries and States. *Procedia Engineering*, 198 (Supplement C). 985-998.

Kammouh O, Dervishaj G, Cimellaro GP (2018). Quantitative Framework to Assess Resilience and Risk at the Country Level. *ASCE-ASME Journal of Risk and Uncertainty in Engineering Systems, Part A. Civil Engineering* 4(1), p.04017033

Kammouh O, Zamani-Noori A, Cimellaro GP, Mahin S. (2018). Deterministic And Fuzzy-Based Methods to Evaluate Community Resilience Based on The Peoples Framework. *Earthquake Engineering and Engineering Vibration.*

Kammouh O, Zamani-Noori A, Cimellaro GP, Mahin S. (2018). Resilience Evaluation of Urban Communities Based on Peoples Framework. *ASCE-ASME Journal of Risk and Uncertainty in Engineering Systems, Part A. Civil Engineering.*

Kammouh O, Zamani-Noori A, Renschler C, Cimellaro GP (2017b). Resilience Quantification of Communities Based on Peoples Framework. *16th World Conference on Earthquake Engineering (16WCEE)*, Santiago, Chile.

Kappos, AJ, Stylianidis, KC, & Pitilakis, K. (1998). Development of seismic risk scenarios based on a hybrid method of vulnerability assessment. *Natural Hazards, 17*(2), 177-192

Komatitsch, D., and Vilotte, J.P. (1998). The spectral element method. an efficient tool to simulate the seismic response of 2D and 3D geological structures. *Bulletin of the seismological society of America, 88*(2), 368-392.

Lie, T. T. (1974). Characteristic temperature curves for various fire severities. *Fire Technology, 4pp. 315-326.*

Liu, X., Ferrario, E., Zio, E. (2017). Resilience analysis framework for interconnected critical infrastructures. *ASCE-ASME Journal of Risk and Uncertainty in Engineering Systems, Part B. Mechanical Engineering*, 3 (2). 021001.

Löfstedt, R. E., and 6, P. (2008). What environmental and technological risk communication research and health risk research can learn from each other. *Journal of risk research*, 11(1-2), 141-167.

Lupoi, A., Cavalieri, F., and Franchin, P. (2013). Seismic resilience of regional health-care systems. *11th International Conference on Structural Safety and Reliability, ICOSSAR 2013.*

Maio, R., and Tsionis, G. (2015). Seismic fragility curves for the European building stock. *Review and evaluation of analytical fragilitycurves.*

Malalgoda, Chamindi, Amaratunga, Dilanthi, & Haigh, Richard. (2014). Challenges in creating a disaster resilient built environment. *Procedia Economics and Finance, 18*, 736-744.

Mannakkara, S., Wilkinson, S. (2013). Build back better principles for post-disaster structural improvements. *Structural Survey, 31*(4), 314-327.

Manyena SB (2006), The concept of resilience revisited, *Disasters*, **30**(4). 434-450.

Marasco, S., and Cimellaro, GP. (2018). A new energy-based ground motion selection and modification method limiting the dynamic response

dispersion and preserving the median demand. *Bulletin of Earthquake Engineering, 16*(2), 561-581.

MATLAB Version 2018b, *Version 2018b Edition. Natick, MA*. The MathWorks Inc., 2018.

Mayunga, J.S. (2007), Understanding and applying the concept of community disaster resilience. a capital-based approach, *Summer academy for social vulnerability and resilience building*, 1. 16.

Mendel J (1995), Fuzzy logic systems for engineering. a tutorial, *Journal*, 83(Issue). 345-377.

Miniati, R., and Iasio, C. (2012). Methodology for rapid seismic risk assessment of health structures. Case study of the hospital system in Florence, Italy. *International journal of disaster risk reduction*, 2, 16-24.

Morrow B (2008). Community Resilience. A Social Justice Perspective. Oak Ridge, TN.

Murphy BL (2007). Locating social capital in resilient community-level emergency management. Natural Hazards, 41(2), 297-315.

National Institute of Building Sciences (NIBS). (2012). *Multi-hazard Loss Estimation Methodology, Earthquake Model, HAZUS-MH 2.1 Technical Manual*. Federal Emergency Management Agency, Washington, D.C.

Norris FH, Stevens SP, Pfefferbaum B, Wyche KF, Pfefferbaum RL (2008). Community Resilience as a Metaphor. *Theory, Set of Capacities*.

NTC-08. (2008). Nuove Norme Tecniche per le Costruzioni (NTC08) (in Italian). Gazzetta Ufficiale Della Repubblica Italiana. Rome. Consiglio Superiore dei Lavori Pubblici, Ministero delle Infrastrutture, 29.

NFPA 30 (2013). Flammable and Combustible Liquids Code. Committee on Tank Storage and Piping Systems.

Padgett, J., Ghosh, J., and Ataei, N. (2010). Sensitivity of dynamic response of bridges under multiple hazards to aging parameters. *Proc., 19th analysis and computation specialty conference. ASCE*.

Park, J., Bazzurro, P., and Baker, J. W. (2007). Modeling Spatial orrelation of Ground Motion Intensity Measures for Regional Seismic Hazard and Portfolio Loss Estimation. Tenth International Conference on Application of Statistic and Probability in Civil Engineering (ICASP10), Tokyo, Japan.

Peacock WG, Brody S, Seitz W, Merrell W, Vedlitz A, Zahran S, Stickney R (2010). Advancing Resilience of Coastal Localities. Developing, Implementing, and Sustaining the Use of Coastal Resilience Indicators. A Final Report. Hazard Reduction and Recovery Center.

Pietrzak RH, Tracy M, Galea S, Kilpatrick DG, Ruggiero KJ, Hamblen JL, Norris FH (2012). Resilience in the Face of Disaster. Prevalence and Longitudinal Course of Mental Disorders following Hurricane Ike. PLoS ONE, 7(6).

Pingali P, Alinovi L, Sutton J (2005). Food security in complex emergencies. enhancing food system resilience. Disasters, 29(s1), S5-S24.

Poland, C. (2009). The resilient city. Defining what San Francisco needs from its seismic mitigation polices. *San Francisco Planning and Urban Research Association report, San Francisco, CA, USA*.

Porter, K.A. (2003). An overview of PEER's performance-based earthquake engineering methodology. *Proc. Ninth International Conference on Applications of Statistics and Probability in Civil Engineering (ICASP9)* July 6-9, 2003, San Francisco, CA. Civil Engineering Risk and Reliability Association (CERRA), 973-980. http://www.sparisk.com/pubs/Porter-2003-PBEE-Overview.pdf.

Price, R.N., and Harrell, C.R. (1999). Simulation modeling and optimization using ProModel. *Proceedings of the 31st conference on Winter simulation. Simulation---a bridge to the future-Volume 1*, 208-214.

Renschler CS, Frazier AE, Arendt LA, Cimellaro GP, Reinhorn AM and Bruneau M (2010), *A framework for defining and measuring resilience at the community scale. The PEOPLES resilience framework*, MCEER Buffalo.

Rose A (2007). Economic resilience to natural and man-made disasters. Multidisciplinary origins and contextual dimensions. Environmental Hazards, 7(4), 383-398.

Rose A, Krausmann E (2013). An economic framework for the development of a resilience index for business recovery. International Journal of Disaster Risk Reduction, 5, 73-83.

Rossetto, T, Ioannou, I, & Grant, DN. (2013). Existing empirical fragility and vulnerability relationships. compendium and guide for selection. *Pavia, Italy. GEM Foundation*.

Rubinoff P, Courtney C (2008). How resilient is your coastal community. A guide for evaluating coastal community resilience to tsunamis and other hazards. Basins Coasts, 1(1), 24-28.

SAP2000 (2018). Integrated Finite Element Analysis and Design of Structures Basic Analysis Reference ManualComputers and Structures, Inc., Berkeley, California, USA.

SBEDS (2008). Methodology Manual for the Single-Degree-of Freedom Blast Effects Design Spreadsheets. *PDC TR-06-01 Rev 1*, Protective Design Center Technical Report, U.S. Army Corps of Engineers.

Sherrieb K, Norris FH, Galea S (2010). Measuring capacities for community resilience. *Social Indicators Research,* **99**(2), 227-247.

Sutton, S.B., and McCauley, E. W. (1975). Assessment of Hazards Resulting from Atmospheric Propane Explosions at Lll., US Energy Research and Development Administration, California Univ., Livermore Lawrence Livermore Lab.

Takeda, T., Sozen, M., Nielsen, N N. (1970). Reinforced concrete response to simulated earthquakes. *Journal of the Structural Division, 96*(12), 2557-2573.

TM5-1300 (1990). The Design of Structures to Resist the Effects of Accidental Explosions.US Department of the Army, Navy, and Air Force, Washington DC.

Tierney K (2009). Disaster Response. Research Findings and Their Implications for Resilience Measurement. CARRI Research Report 6 Community and Regional Resilience Institute, Oak Ridge, TN.

Tierney K, Bruneau M (2007). Conceptualizing and measuring resilience. A key to disaster loss reduction. TR news(250).

Tagawa, H., Miyamura, T., Yamashita, T., & Kohiyama, M. (2015). Detailed Finite Element Analysis of Full-scale Four-story Steel FrameStructure. *International Journal of High-Rise Buildings, 1*.

Thompson, E. M., Baise, L. G., Kayen, R. E., Tanaka, Y., and Tanaka, H. (2010). A Geostatistical Approach to Mapping Site Response Spectral Amplifications. *Engineering Geology*, 114(3-4), 330–342.

Tobin, G.A. (1999). Sustainability and community resilience. the holy grail of hazards planning. Global Environmental Change Part B. Environmental Hazards, 1(1), 13-25.

Tobin. T., and Samant L. (2009). San Francisco's Earthquake Risk - Report on Potential Earthquake Impacts in San Francisco. The Community Action Plan for Seismic Safety (CAPSS), Internal report.

Twigg, J. (2009). Characteristics of a disaster-resilient community. a guidance note (version 2).

UNDE (2007). Indicators of sustainable development. Guidelines and methodologies. United Nations Publications.

UNISDR (2011). Hyogo Framework for Action 2005-2015 mid-term review.

UNISDR (2012). How to Make Cities More Resilient. A Handbook for Local Government Leaders, a Contribution to the Global Campaign 2010-2015. United Nations Office for Disaster Risk Reduction.

USGS (2013). Seismic Hazard Analysis tools. U.S. Geological Survey. < http.//earthquake.usgs.gov/hazards/designmaps/grdmotion.php>.

Voogd, H. (2004). Disaster prevention in urban environments. *European Journal of Spatial Development, 12*, 1-20.

Wagner, I., Breil, P. (2013). The role of ecohydrology in creating more resilient cities Ecohydrology&Hydrobiology13.113doi.http.//dx.doi.org/10.1016/j.ecohyd.2013.06.002

Whitman, R.V., Anagnos, T., Kircher, C.A., Lagorio, H.J., Lawson, R.S. and Schneider, P. (1997), Development of a national earthquake loss estimation methodology, Earthquake Spectra, 13(4).643–661.

Yi, P. (2004). Real-time generic hospital capacity estimation under emergency situations.

Zhong, S., Clark, M., Hou, X.-Y., Zang, Y., and FitzGerald, G. (2014). Validation of a framework for measuring hospital disaster resilience using factor analysis. *International journal of environmental research and public health*, 11(6), 6335-6353.

Zhou, H., Shi, L., Mao, Y., Tang, J., and Zeng, Y. (2014). Diffusion of new technology, health services and information after a crisis. a focus group

study of the Sichuan 5.12 Earthquake. *The International journal of health planning and management*, 29(2), 115-123.

Appendix A

PEOPLES' dimensions, components, indicators, and measures.

Component/ sub-component/indicator	Measure (0 ≤value ≤1)	Ref.	Rel.	I	Nat.
1- Population and demographics				2	
1-1- Distribution\ Density				3	
-Population density	Average number of people per area ÷ SV		N	3	D
-Population distribution	% population living in urban area		P	2	D
1-2- Composition				2	
-Age	% population whose age is between 18 and 65		P	3	S
-Place attachment-not recent immigrants	% population not foreign-born persons who came within previous five years	(Sherrieb et al. 2010)	N	1	S
-Population stability	% population change over previous five year period	(Sherrieb et al. 2010)	N	2	S
-Equity	% nonminority population – % minority population		P	3	S
-Race/Ethnicity	Absolute value of (% white – % nonwhite)		N	1	S
-Family stability	% two parent families	(Sherrieb et al. 2010)	P	2	S
-Gender	Absolute value of (%female– %male)		N	1	S
1-3- Socio- Economic Status				2	
-Educational attainment equality	% population with college education – % population with less than high school education		P	3	S
-Homeownership	% owned-occupied housing units	(Cutter et al. 2014)	P	2	S
-Race/ethnicity income equality	Gini coefficient	(Sherrieb et al. 2010)	N	3	S
-Gender income equality	Absolute value of (% male median income – % female median income)		N	2	S
-Income	Capita household income ÷ SV	(Tobin 1999)	P	3	S
-Poverty	% population whose income is below minimum wage		N	3	S
-Occupation	Employment rate %		P	3	S
2- Environmental and ecosystem				2	
2-1- Water				3	
-Water quality/quantity	Number of river miles whose water is usable ÷ SV		P	3	D
2-2- Air				1	
-Air pollution	Air quality index (AQI) ÷ SV		N	2	D
2-3- Soil				2	
-Natural flood buffers	% land in wetlands ÷ SV	(Beatley and Newman 2013)	P	1	S
-Pervious surfaces	Average percent perviousness	(Brody et al. 2012)	P	1	S
-Soil quality	% land area that does not contain erodible soils	(Bradley and Grainger 2004)	P	1	S
2-4- Biodiversity				1	

-Living species	% species susceptible to extinction		N	2	S
2-5- Biomass (Vegetation)				**2**	
-Total mass of organisms	Harvest index (HI) the ratio between root weight and total biomass		P	2	S
-Density of green vegetation across an area	Normalized difference vegetation index (NDVI)	(Cimellaro et al. 2016)	P	2	D
2-6- Sustainability				**3**	
-Undeveloped forest	% land area that is undeveloped forest ÷ SV	(Cutter et al. 2008)	P	2	S
-Wetland variation	% land area with no wetland decline	(Cutter et al. 2008)	P	2	S
-Land use stability	% land area with no land-use change ÷ SV	(UNDE 2007)	P	1	S
-Protected land	% land area under protected status ÷ SV	(Rubinoff and Courtney 2008)	P	2	S
-Arable cultivated land	% land area that is arable cultivated land ÷ SV	(UNDE 2007)	P	2	S
3- Organized governmental services				**3**	
3-1-Executive/ Administrative				**3**	
-Health insurance	% population under age 65 with health insurance	(Chandra et al. 2011)	P	3	S
-Disaster aid experience	Presidential disaster declarations divided by number of loss-causing hazard events ÷ SV	(Tierney and Bruneau 2007)	P	3	S
-Local disaster training	% population in communities with Citizen Corps program	(Godschalk 2003)	P	2	S
-Emergency response services	% workforce employed in emergency services (fire-fighting, law enforcement, protection) ÷ SV	(Cutter et al. 2008b)	P	3	S
-Schools	Number of schools per 1000 students ÷ SV		P	3	S
3-2- Judicial				**1**	
-Jurisdictional coordination	Governments and special districts per 10,000 persons ÷ SV	(Murphy 2007)	P	2	S
3-3- Legal/ Security				**2**	
-Performance regimes-state capital	Proximity of county seat to state capital ÷ SV	(Bowman and Parsons 2009)	P	2	S
-Performance regimes-nearest metro area	Proximity of county seat to nearest county seat within a Metropolitan Statistical Area ÷ SV	(Bowman and Parsons 2009)	P	2	S
3-4- Mitigation/ Preparedness				**3**	
-Mitigation spending	Ten year average per capita spending for mitigation projects ÷ SV	(Rose 2007)	P	3	S
-Nuclear plant accident planning	% population within 10 miles of nuclear power plant	(Cutter et al. 2014)	N	2	S
-Effective mitigation plans	% population covered by a recent hazard mitigation plan	(Cutter et al. 2010)	P	3	S
-Exposure to hazards	% building infrastructure not in high hazard zones		P	3	S
-Protective resources	% land area that consists of windbreaks and environmental plantings	(Cutter et al. 2008a)	P	2	S
-Financed activities for risk reduction	% governmental financial resources to carry out risk reduction activities ÷ SV	(UNISDR 2012)	P	2	S
-Essential infrastructure robustness	% of local schools, hospitals and health facilities that remained operational during emergencies in past events	(UNISDR 2012)	P	3	S

-Essential infrastructure assessment	% essential infrastructures that are under regular assessment programs		P	3	S
-Accuracy of building codes	% designed structural damage – % actual structural damage (from past events)		P	3	S
-Training programs for officials	% of officials and leaders who are under regular training programs		P	2	S
-Availability of early warning centers	Average number of early warning centers per each independent zone ÷ SV		P	3	S
-Citizen disaster preparedness and response skills	Red cross training workshop participants per 10,000 persons ÷ SV	(Cutter et al. 2014)	P	3	S
3-5- Recovery/ Response				**3**	
-Money dedicated to supporting the restoration	Micro financing, cash aid, soft loans, loan guarantees available to affected households after disasters to restart livelihoods ÷ SV	(UNISDR 2012)	P	3	S
-Ecosystem support plans	Local government plan to support the restoration, protection and sustainable management of ecosystems services (0 or 1)	(UNISDR 2012)	P	2	S
-Local institutions access to financial reserves to support effective disaster response and early recovery	1 (there is access), 0 (no access)		P	3	S
-Local government access to resources and expertise to assist victims of psycho-social impacts of disasters	1 (there is access), 0 (no access)		P	3	S
-Disaster risk reduction measures integrated into post-disaster recovery and rehabilitation activities	1 (if there is), 0 (otherwise)		P	3	S
-Contingency plan degree including an outline strategy for post-disaster recovery and reconstruction	1 (if there is), 0 (otherwise)		P	3	S
4- Physical infrastructure				**3**	
4-1- Facilities				**3**	
-Sturdier housing types	% housing units not manufactured homes	(Tierney 2009)	P	3	S
-Temporary housing availability	% vacant units that are for rent	(Félix et al. 2013)	P	3	D
-Housing stock construction quality	% housing units built prior to 1970	(Cutter et al. 2014)	N	3	S
-Community services	Area of community services (recreational facilities, parks, historic sites, libraries, museums) per population ÷ SV	(Burton 2015)	P	1	S
-Economic infrastructure exposure	% commercial establishments outside of high hazard zones ÷ total commercial establishment	(Rubinoff and Courtney 2008)	P	3	S
-Distribution commercial facilities	Commercial infrastructure area per area ÷ SV		P	2	S
-Hotels and accommodations	Number of hotels per total area ÷ SV	(Cutter et al. 2010)	P	3	S
-Schools	Schools area (primary and secondary education) per population ÷ SV		P	3	S
4-2- Lifelines				**3**	

-Telecommunication	Average number of Internet, television, radio, telephone, and telecommunications broadcasters per household ÷ SV	(Pietrzak et al. 2012)	P	3	D
-Mental health support	Psychosocial support facilities per population ÷ SV	(Chandra et al. 2011)	P	1	S
-Physician access	Number of physicians per population ÷ SV	(Cutter et al. 2014)	P	2	S
-Medical care capacity	Number of hospital beds per population ÷ SV	(Cutter et al. 2014)	P	3	D
-Evacuation routes	Major road egress points per population ÷ SV	(Cutter et al. 2014)	P	3	S
-Industrial re-supply potential	Rail miles per total area ÷ SV	(Cutter et al. 2014)	P	3	S
-High-speed internet infrastructure	% population with access to broadband internet service	(Cutter et al. 2014)	P	3	D
-Efficient energy use	Ratio of Megawatt power availability to demand		P	3	D
-Efficient Water Use	Inverted water supply stress index ÷ SV	(Cimellaro et al. 2016)	P	3	D
-Gas	Ratio of gas production to gas demand		P	3	D
-Access and evacuation	Principal arterial miles per total area ÷ SV	(Cutter et al. 2010)	P	3	S
-Transportation	Number of rail miles per area ÷ SV	(Cutter et al. 2008b)	P	3	S
-Waste water treatment	Number of WWT units per population ÷ SV				S

5- Lifestyle and community competence				**1**	
5-1- Collective Action and Decision Making				**3**	
-Authorities interdependency	Less than 3 parties are involved in the decision-making process (1), otherwise (0)		P	2	S
5-2- Collective Efficacy and Empowerment				**3**	
-Creative class	% workforce employed in professional occupations ÷ SV	(Cumming et al. 2005)	P	2	S
-Scientific services	Professional, scientific, and technical hour services per population ÷ SV	(Cumming et al. 2005)	P	1	S
5-3- Quality of Life				**2**	
-Means of transport	% households with at least one vehicle	(Peacock et al. 2010)	P	2	S
-Safety	Crime rate	(Sherrieb et al. 2010)	N	2	D
-Quality of homes	Sustainability rating systems (LEED, BREEAM) ÷ maximum index number		P	2	S
-Quality of neighborhood	Sustainability rating systems (LEED, BREEAM) ÷ maximum index number		P	2	S

6- Economic development				**3**	
6-1- Financial Services				**3**	
-Hazard insurance coverage	% housing units covered by National Insurance Program	(Cutter et al. 2014)	P	3	S
-Crop insurance coverage	Lands areas which are covered by Crop insurance program ÷ total area of cultivated lands	(Cutter et al. 2014)	P	3	S
-Financial resource equity	Number of lending institutions per population ÷ SV	(Birkmann 2006)	P	3	S
-Tax revenues	Corporate tax revenues per 1,000 population ÷ SV	(Sherrieb et al. 2010)	P	2	S
6-2- Industry- Employment Services				**3**	
-Employment rate	% labor force employed ÷ SV	(Sherrieb et al. 2010)	P	2	S
-Business size	% large businesses	(Rose and	P	2	S

Indicator	Metric	Reference			
		(Krausmann 2013)			
-Professional and business services	% population that is not institutionalized or infirmed	(Rubinoff and Courtney 2008)	N	1	D
-Economic stability	% employment rate	(Burton 2015)	P	3	D
-Economic diversity	% population not employed in primary industries ÷ total employed population	(Cutter et al. 2010)	P	1	S
-Households insurance	% households covered by National Insurance Program policies		P	3	S
-Research and development firms	Number of research and development firms ÷ SV	(Cumming et al. 2005)	P	1	S
-Business development rate	Business gain /total business	(Sherrieb et al. 2010)	P	3	S

6-3- Industry- Production   **2**

Indicator	Metric	Reference			
-Food provisioning capacity	Food security rate	(Pingali et al. 2005)	P	3	D
-Large retail-regional/national geographic distribution	Large retail stores ÷ total number of stores	(Rose and Krausmann 2013)	P	2	S
-Local food suppliers	Farms marketing products through Community supported Agriculture per 10,000 persons ÷ SV	(Berardi et al. 2011)	P	2	S
-Manufacturing	Mean sales volume of businesses ÷ SV	(Rose 2007)	P	2	S

7- Social-cultural capital   **2**

7-1- Child and Elderly Services   **3**

Indicator	Metric	Reference			
-Child and elderly care programs	1 (if there is a program), 0 (if no)		P	3	S

7-2- Commercial Centers   **2**

Indicator	Metric	Reference			
-Social capital-civic organizations	Number of civic organizations per population ÷ SV	(Sherrieb et al. 2010)	P	3	S
-Commercial establishments	Area of commercial establishments per population ÷ SV	(Rubinoff and Courtney 2008)	P	1	S

7-3- Community Participation   **3**

Indicator	Metric	Reference			
-Pre-retirement age	% population below 65 years of age	(Morrow B. 2008)	P	3	S
-Non-special needs	% population without sensory, physical, or mental disability	(Davis and Phillips 2009)	P	3	D
-Political engagement	% voting age population participating in presidential election	(Sherrieb et al. 2010)	P	2	S
-Female labor force participation	% female labor force participation	(Cutter et al. 2010)	P	2	S
-Population participating in community Rating System	% population participating in Community Rating System (CRS)	(Cutter et al. 2010)	P	2	D
-Emergency community participation	% community participation in case of warning systems	(UNISDR 2012)	P	3	D

7-4- Cultural and Heritage Services   **1**

Indicator	Metric	Reference			
-Cultural resources	National Historic Registry sites area per population ÷ SV	(Rubinoff and Courtney 2008)	P	1	S

7-5- Education Services/ Disaster Awareness   **3**

Indicator	Metric	Reference			
-English language competency	% population proficient English Speakers	(Hilfinger Messias et al. 2012)	P	1	S
-Adult education and training programs	Number of yearly adult education and training programs per population ÷ SV	(Burton 2015)	P	3	S

-Education programs on DRR and disaster preparedness for local communities	Number of education programs on DRR and disaster preparedness per each local community by local government per year ÷ SV	(UNISDR 2012)	P	3	S
-Integration of disaster risk reduction in educational curriculum	Number of courses in disaster risk reduction as part of the educational curriculum per schools and colleges ÷ SV	(UNISDR 2012)	P	3	S
-Citizens awareness of evacuation plans or drills for evacuations	Average number of maneuver per institution ÷ SV		P	2	S
7-6- Non-Profit Organization				**3**	
-Social capital-disaster volunteerism	Red cross volunteers per 10,000 persons ÷ SV	(Cutter et al. 2014)	P	2	D
7-7- Place Attachment				**2**	
-Social capital-religious organizations	Persons affiliated with a religious organization per 10,000 persons ÷ SV	(Sherrieb et al. 2010)	P	1	S